Contents

A brief overview about the current opinions in cell motility

Introduction

Following the motto: "It moves-it's alive" motility is one of the most obvious implementations of life. On the level of the single eukaryotic cell movement on a solid substrate is established by a common crawling, or amoeboid, mechanism (Abercrombie et al., 1970b). This is what I will refer to as cell motility. Some single cells, for example Dictyostelium discoideum follow a gradient of a chemoattractant, which the cells secret, to form aggregates under unfavourable conditions (Gerisch, 1982). This seemingly simple mechanism can lead to complex patterns. The direction of movement is often determined by gradients of a signal, which can be chemical substances, temperature, light, the rigidity of the substrate or adhesion sites and is then called chemotaxis, thermotaxis, phototaxis, durotaxis or haptotaxis, respectively. Some movements take place along magnetic field lines (magnetotaxis), in the direction of gravitational force (gravitaxis) or in an electric field (galvanotaxis). In the absence of an external signal cells may be stationary or move in a random fashion. During development of multicellular organisms movement of single cells and cell layers defines the morphology of the future body. When the connections between cells are destroyed, a wound is created, and the cells start to move towards each other in order to re-establish the integrity of the tissue. Immune cells patrol inside our bodies and are recruited to sites of infection to eliminate intruders like bacteria. Growth cones of neurons dynamically wire our brains to create our thoughts and minds. Misregulation can lead to diseases and to malignant cells that move out of a primary tumor to distribute within the whole organism to form new, possibly lethal, tumors in a process called metastasis (Bray, 1992; Trinkaus, 1984).

The motile machinery is not only used for the translocation of the whole cell, but also to establish transport of vesicles inside the cell, and pathogens like Listeria, Vaccinia and Ricketsia capture the cell´s motile machinery to spread from one cell to the next, thereby escaping the immune system (Gouin et al., 2005).

Visualising motility.

Cell motility is a dynamic process, detected by the early practitioners of light microscopy (Dunn and Jones, 2004). Using time lapse microscopy the movement of processes that lie beyond the time scale of the perception of our visual system, be it milliseconds or several hours, can be analysed. Major advances in microscopy have been facilitated by the development of sensitive detection systems (CCD cameras-(Inoue, 1986)) allowing the long term recording of cell behaviour under conditions of low radiation intensities. Traditional bright Phase Contrast or Differential Interference Contrast (DIC) Microscopy have been supplemented by fluorescence microscopy, a trend accelerated by the discovery of fluorescent proteins, like green fluorescent protein (GFP), that can be genetically engineered as tags on a molecule of choice (Shaner et al., 2005). Using different fluorophores the localisations of several proteins can be determined simultaneously by epifluorescence microscopy. And techniques like fluorescence recovery after photobleaching (FRAP) (Axelrod et al., 1976), photoactivation of fluorescence (PAF) (Patterson and Lippincott-Schwartz, 2002), fluorescence localization after photobleaching (FLAP) (Dunn et al., 2002), fluorescence loss in photobleaching (FLIP)(Cole et al., 1996), Fluorescent Speckle Microscopy (FSM)(Waterman-Storer and Salmon, 1997) or Fluorescence Resonance Energy Transfer (FRET) (Miki et al., 1986) have been developed to analyse the dynamics of proteins in living cells. Confocal and Multiphoton microscopy microscopy enable optical sectioning of thicker cell parts or tissues, whereas Internal Reflection Microscopy (IRM) (Curtis, 1964) and Total Internal Reflection Fluorescence (TIRF) (Lanni et al., 1985) microscopy is used to visualize structures close to the substrate like adhesion sites. With DRIMAPS (Digitally Recorded Interference Microscopy with Automatic Phase Shifting) the dry mass distribution within a cell can be determined in real time (Peckham et al., 1999). Advances in light microscopy are currently so rapid that new technologies are emerging each year. In particular, recent developments are pushing the Rayleigh limit down to the nanometers scale (Gustafsson, 2008; Shroff et al., 2008). Sophisticated data analysis is here being applied increase the information that can be gained. By the addtition or microinjection of chemical compounds or specific proteins or protein-domains (or overexpression), or by the use of knock-down with small interfering RNAs (siRNA) and knock-out cell lines the local and global role of proteins and their interplay can be deciphered.

By the use of electrons instead of light the resolution can be directly increased to the nanometer scale. This technique, however, requires the observation of cells in vacuum and therefore they have to be accordingly prepared. There exist a variety of techniques for immobilising cells and it is an art of its own to fix the cells and their underlying structures in their native state and to contrast them without introducing artefacts, especially for the fragile actin network, which is of main interest for the scientist interested in cell motility. A (formerly) prominent example of an artefact that was accepted as a fact for a decade and then disappeared is the "microtrabecular lattice", proposed by Porter, a story that was revisited in subsequent reviews (Heuser, 2002; Small, 1988). Specifc criteria for preserving the actin cytoskeleton for electron microscopy is further discussed by Small et al., (Small et al., 2008). Both light microscopy and electron microscopy techniques have their drawbacks: either the dynamics are observed at a low resolution or a static (dead) cell is observed at high resolution. In combination, however, the two techniques have the potential to give us the information about the ultrastructure at a known dynamic state. An example of using this combination is presented in paper 2.

Push and pull.

During movement a protrusion is first established at the cell front, followed by retraction of the rear (Figure 1). Actin filaments, which are arranged in a criss-cross network in the lamellipodium, a flat sheet of 100 – 200 nm thickness and 1 – 5 µm breadth at the cell front, grow and push the membrane forward. Parallel bundles of actin filaments can transect lamellipodia, pushing finger-like "filopodia" beyond the lamellipodium front. The nomenclature in this field is not clearly defined. Here I use the o-declination for the neutral lamellipodium and the filopodium and the a-declination for the feminine lamella and their corresponding plural –a and –ae, respectively. The lamella, according to the traditional concept first described by Abercrombie (Abercrombie et al., 1970b), is the region behind the lamellipodium where actin-myosin arrays form, and contraction of these arrays leads to translocation of the cell body. More recently it has been suggested that the lamella extends up to the front of the cell edge, underneath the lamellipodium, and directly drives protrusion, and that the lamellipodium is dispensable for motility (Giannone et

al., 2007; Ponti et al., 2004) This dispute will be treated in more detail in the discussion.

Filopodia, consist of bundles of about 20-50 actin filaments (our own obsrvations) with their growing ends at the tip and can become up to 70 µm long (Jacinto and Wolpert, 2001). They can be highly dynamic extending and retracting at a rate of approximately 10 µm/min, which can double during periods of intense activity. They are thought to probe the environment for signals and to establish cell-cell contacts and contribute to the construction of contractile bundles in the lamella (Jacinto and Wolpert, 2001; Nemethova et al., 2008; Wood and Martin, 2002). Since they frequently emanate from lamellipodia it has been suggested they arise through bundling of lamellipodial actin filaments (Svitkina et al., 2003)(Small et al., 1981, 1982). On the other hand it has been shown that they can form independently of lamellipodia (Steffen et al., 2006) so there might exist independent mechanisms that contribute to filopodia formation. Microspikes are similar to filopodia, and often act as their precursers, but they are embedded in and do not project beyond the lamellipodium edge.

Traction is developed against adhesions, which connect the actin cytoskeleton to the substrate. They are initiated as focal complexes close to the lamellipodium rear, and can mature into focal adhesions, which dissolve at the rear as the cell progresses (Kaverina et al., 2002). Lamellipodia can be observed to lose contact to the substrate and to fold up- and backwards to form "ruffles" (Abercrombie et al., 1970c). Ruffles can be thus be defined as lamellipodia-like structures that do not directly contribute to cell motility, but possibly indirectly through the potentiation of adhesion formation during retraction (Rinnerthaler et al., 1988) and the delivery of actin filaments to the rear (Small and Resch, 2005). Dorsal ruffles have been implicated in macropinocytosis (Abercrombie et al., 1970a) act in internalization of receptors (Chhabra and Higgs, 2007; Ladwein and Rottner, 2008) and in phagocytosis (Kaverina et al., 2002; Swanson and Baer, 1995).

Retraction of the cell rear and translocation of the cell body is established by contractile assemblies (Chen, 1981; Dunn, 1980) which consist of actin-myosin arrays interconnected through the cell and to focal adhesions.
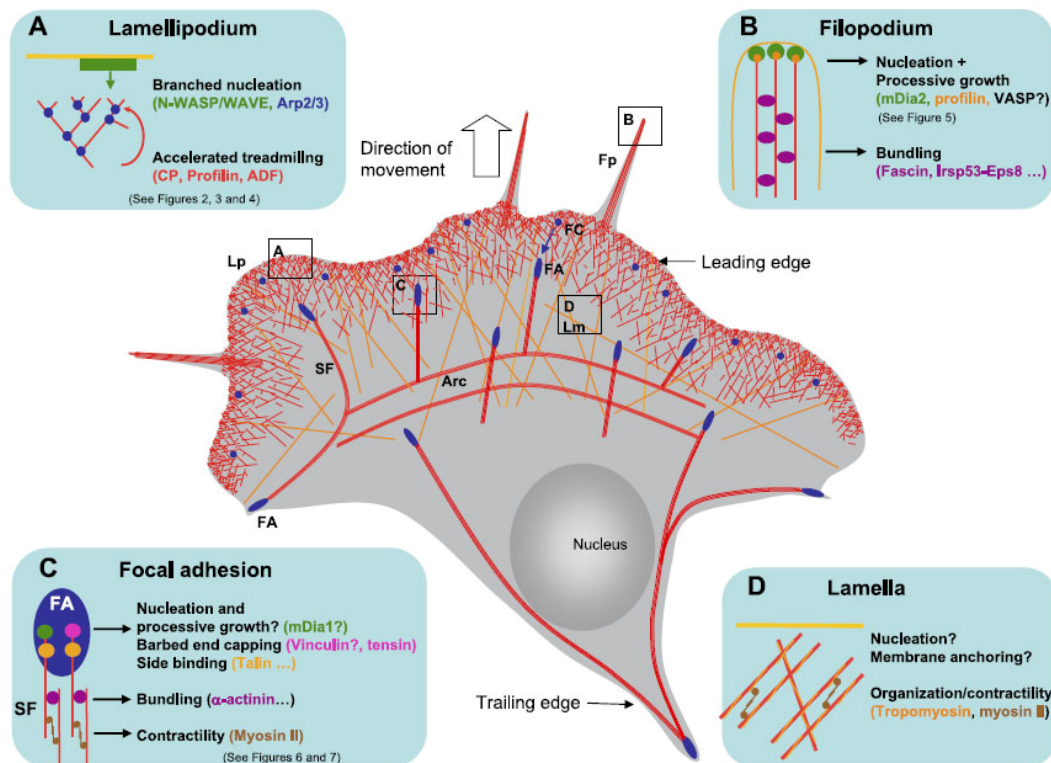
Figure 1: Schematic illustration of the actin cytoskeleton in a migrating cell. Lp, lamellipodium; Fp, filopodium; Lm, lamella; SF, stress fiber; FA, focal adhesion; FC, focal complex. From (Le Clainche and Carlier, 2007).

The main player: actin.

The main molecule responsible for protrusion is actin. Actin is a globular molecule consisting of 375 amino acids and has a molecular weight of 42 kD. It is highly conserved among eukaryotes and in humans comprises 6 subfamilies. Recently, even in prokaryotes a homologue with similar activities was found: MreB. Actin is polar and has four domains which form a cleft that binds ATP or ADP and a divalent cation (Mg2+). The monomer (globular or G-actin) can polymerize to produce helical filaments (F-actin), which constitute part of the cytoskeleton and give cells their shape. The structure of the filaments is not static but constantly changes between different states concerning rotation and tilt, so called breathing (Reisler and Egelman, 2007). Actin filaments function during mitosis and cytokinesis, they serve as scaffolds for muscle contraction with myosin and as transport tracks for unconventional myosins. More recently actin has also been implicated in the control of gene expression (Posern and Treisman, 2006).
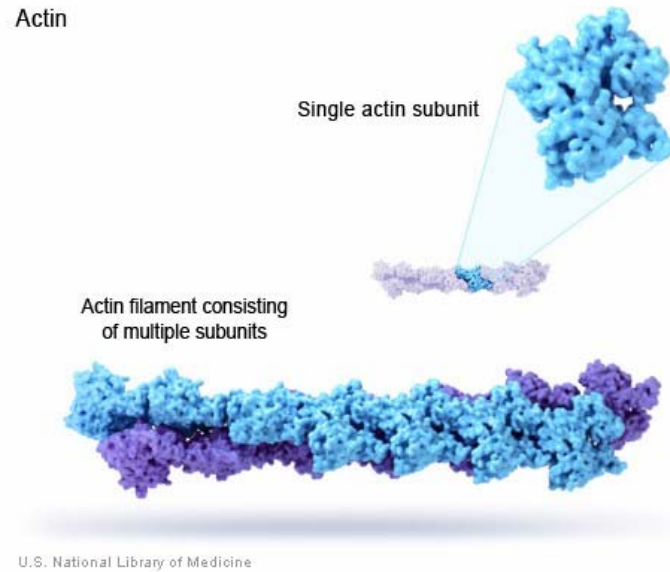
Figure 2: Structures of the Actin mono- and polymer. From the U.S. National Library of Medicine (http://ghr.nlm.nih.gov/handbook/illustrations/actin).

Back to the front: Actin treadmilling provides the basic mechanism for cell motility

The two ends of actin filaments, which have been called barbed and pointed due to their appearance after decoration with myosin heads, exhibit different critical concentrations for the predominant and more reactive ATP-actin: 0.1 μM at the barbed end and 0.7 μM at the pointed end (Pollard et al., 2000). Actin filaments preferentially incorporate ATP-actin at their barbed end which hydrolyses to ADP.Pi followed by Pi release, thereby decreasing the stability of the filament towards the pointed end. At G-actin concentrations between the critical concentrations at the two ends, a fascinating effect is observed: the filament polymerizes and depolymerises at the same time, on opposite ends, keeping the filament length as well as the F- and G- actin concentrations constant, in a process termed treadmilling. Analysis of actin dynamics in cells using different techniques have shown that protrusion in lamellipodia is based on a treadmilling mechanism, whereby filaments grow at the front and depolymerise at the rear (Lai et al., 2008; Wang, 1985; Waterman-Storer and Salmon, 1997). This phenomenon might have been the starting point for the evolution of cell motility, but with actin alone in solution it is very slow (Pollard, 2007). Other proteins assist to increase this intrinsic effect to higher rates (about 100x), which we observe in living cells, mainly by increasing the depolymerisation rate at the

pointed end. Inefficient translation of the filament growth into protrusion results in retrograde flow (Small and Resch, 2005; Theriot and Mitchison, 1991; Wang, 1985).

Rising to higher rates with actin binding proteins.

In a landmark paper, Carlier and colleagues (Loisel et al., 1999) were able to reproduce treadmilling in an in vitro motility assay that mimicked the movement of pathogens in cytoplasm. They determined a minimum set of proteins required to increase the treadmilling rates up to those observed inside cells. It comprises a filament nucleator, a barbed end capper, a depolymerizer and a shuttler of monomers from the depolymerising pointed to the barbed end. I will now discuss these different players in the life of the actin filament. The list is certainly not complete: since the basic process is ancient there exist several homologues in different species, which sometimes have evolved varying activities and ways of regulation, and additional players continue to be discovered.

Natural born filaments (are rare) – actin filament nucleating proteins.

The rate-limiting step of actin polymerization in vitro is the assembly of a trimer (Pollard and Borisy, 2003). Nucleation is however a slow process and in the cell is promoted by specific nucleating proteins (Pollard, 2007). Among these, the Arp2/3 complex and formins are the best characterised (Pollard, 2007). Also, in the cell, nucleation is spatially and temporally restricted and free monomers are bound to proteins to avoid spontaneous polymerization (see below). For the assembly of lamellipodial filaments the Arp2/3 complex has been shown to be the principal player (Machesky and Insall, 1999; Pollard, 2007). It is localized throughout the lamellipodium (Welch et al., 1997) but is incorporated only at the lamellipodium tip (Lai et al., 2008). Knock-down of Arp2/3 complex activators (see further below) abolishes lamellipodia formation (Steffen et al., 2006). The actin related proteins (Arps) 2 and 3 have similar structures to actin and form the first dimer of a new filament and, together with five additional proteins and a nucleation promoting factor, recruit the first actin monomer of a filament. In this way the Arp2/3 complex forms the pointed end of a filament (Mullins et al., 1998). In vitro, the nucleation of actin by

Arp2/3 is promoted by binding to the sides of preformed actin filaments (at a preferred 70° angle), which in turn results in the formation of branched filament arrays. The same types of arrays have been described in lamellipodia prepared for electron microscopy and it has accordingly been concluded that dendritic branching of actin forms the basis of lamellipodia protrusion. We will return to this idea below.

The Arp2/3 complex is activated by the WASP family of proteins (Takenawa and Miki, 2001). WASP and N-WASP are implicated in regulating actin-based vesicular trafficking (Ridley, 2006). Arp2/3 activity at the leading edge is regulated by WASP family Verprolin homologous (WAVE) proteins. The tripartite unit with Arp2/3 and G-actin leads to nucleation (Pantaloni et al., 2001). The WASP family members share a similar structure: At the C-terminal region is the VCA module, which stands for Verprolin homology (also WASP homology (WH) 2), Cofilin homology and acidic domains. The WH2 domain recruits an actin monomer to the Arp2/3 complex, which is connected to the acidic domain, and brought together through the c-region (Takenawa and Suetsugu, 2007). They all share a basic region, which binds F-actin and the proline rich region has been implicated in profilin binding. WASP and N-WASP share the WH1 domain which binds diverse regulatory proteins (Takenawa and Suetsugu, 2007). Without stimulation these two proteins are in an autoinhibited conformation, which is released by binding of Cdc42 to the GTPase binding domain (GBD) followed by recruitment to the plasma membrane (Kim et al., 2000; Prehoda et al., 2000). In contrast, WAVE proteins are in an active conformation and lack a GBD domain and instead of a WH1 domain they have a WAVE homology domain (WHD). The WAVE complex, consisting of Abi1, Nap1, HSPC300 and Sra1, is localized to the plasma membrane upon activation by Rac1 (Stradal et al., 2004; Takenawa and Miki, 2001).

A second group of nucleators are the formins. They display a diverse family of ubiquitous, highly conserved multidomain proteins involved in motility, cell adhesion, filopodia and stress fibre formation, regulation of transcription and more (Faix and Grosse, 2006). They consist of formin-homology 2 (FH2) domains, by which they dimerize and which are sufficient for nucleation in-vitro (Kovar, 2006). In-vivo also the formin homology 1 domain is required, probably for its profilin-actin binding domain to recruit monomers (Kovar et al., 2003; Pruyne et al., 2002). After nucleation formins remain bound to the barbed end of the new filament without blocking

polymerization (except fission yeast cdc12 (Kovar et al., 2003)), and are therefore called "leaky cappers" (Zigmond et al., 2003). Actin monomers are inserted between the FH2 domain and the barbed end, with formins acting as processive motors (Goode and Eck, 2007). The subfamily of Diaphanous-related formins (DRFs) in their basal state are autoinhibited and only activated upon binding of Rho family GTPases (Alberts, 2001; Li and Higgs, 2003). Of this family mDia1 is thought to be responsible for nucleating stress fibres (Hotulainen and Lappalainen, 2006; Watanabe et al., 1999), but has not been localised at their ends and mDia2 has been found at the tips of filopodia and has been implicated in their formation (Faix and Rottner, 2006; Pellegrin and Mellor, 2005).

A third nucleator, Spire, has recently been reported. It contains four WH2 domains by which the actin monomers are recruited and caps the pointed end after nucleation. Spire thought to be involved in intracellular membrane transport processes and the coordination of cortical microtubules and actin filaments (Kerkhoff, 2006).

Need for speed - Ena/VASP proteins increase the protrusion rate.

Ena/VASP family proteins are a structurally conserved family in vertebrates, invertebrates and Dictyostelium discoideum and contain an N-terminal EVH1 domain required for localization, a proline rich domain and a C-terminal EVH2 domain for binding G- and F-actin and for the formation of multimers. Vertebrates express three isoforms called Mena, EVL and VASP. They are localized to sites of actin assembly like focal adhesions, stress fibres, lamellipodia and filopodia tips (Reinhard et al., 1992; Rottner et al., 1999), play a central role in filopodia formation (Gupton and Gertler, 2007) and are recruited by intracellular pathogens (Laurent et al., 1999). The polymerization rate of actin in-vitro and the protrusion rate in-vivo are increased by the ability of Ena/VASP to bind to the side of an actin filament, recruit profilin-actin and insert a monomer in a processive manner (Drees and Gertler, 2008; Rottner et al., 1999). Clustering leads to cooperative polymerization and additionally to the exclusion of capping protein in a non-competitive way (Breitsprecher et al., unpublished).

Keep it short – Filament severing and depolymerization at the pointed end.

ADF/Cofilin binds to the pointed end of an actin filament, which leads to depolymerization, thereby replenishing the monomer pool. ADF/cofilin increases the rate of treadmilling in-vitro and is localized throughout the lamellipodium (Aizawa et al., 1997; Carlier et al., 1997; Svitkina and Borisy, 1999). ADF/Cofilin also severs actin filaments in-vitro, thereby increasing the number of pointed ends leading on one hand to even faster degradation of filaments, but also to an increasing number of barbed ends. It has been proposed that these free barbed ends can serve as nucleation sites for actin polymerization (Condeelis, 2001; DesMarais et al., 2005; Ghosh et al., 2004). If and how this could contribute to motility in an established lamellipodium remains obscure. At least in B16 cells no significant effect of ADF/cofilin depletion on the number of barbed ends could be detected (Hotulainen et al., 2005). Cofilin is found in all eukaryotic species so far studied (Ono, 2007). Gelsolin was the first actin severing protein discovered and is widely distributed among metazoan species. Gelsolin related proteins include villin, severin and brevin. When activated by Ca^{++}, gelsolin binds to and severs an actin filament, preferentially ADP-actin and caps the (+) end, blocking filament regrowth (Laham et al., 1995; Pantaloni et al., 2001). F-actin is protected from Gelsolin by tropomyosin binding (Fattoum et al., 1983).

The pick-up – G-actin sequestering proteins.

If G-actin were free in the lamellipodium spontaneous polymerization would occur down to the critical concentration. As discussed later, monomeric actin exists in cells at concentrations far above the critical concentration for growth at the barbed end. Actin must therefore be taken out of the polymerisation pool by sequestering proteins: thymosin β4 competes with ADF/cofilin (Dedova et al., 2006) as well as with profilin for G-actin (Goldschmidt-Clermont et al., 1992; Pantaloni and Carlier, 1993). The competition between thymosin β4 and profilin is important for directing actin monomers to polymerization at the plus end and The competition between thymosin β4 and ADF/cofilin might be important for shifting ADF/cofilin depolymerized actin to

the thymosin maintained actin monomer pool that can be readily utilized by profilin for polymerization (Ono, 2007).

The end-to-end Shuttle.

Binding to profilin promotes ATP/ADP exchange and inhibits nucleation and polymerization at the pointed, but drives elongation at the barbed ends of filaments (Pantaloni and Carlier, 1993; Pollard and Cooper, 1984; Pring et al., 1992; Tilney et al., 1983).

Terminators – Barbed-end capping proteins.

Nucleation is in equilibrium with termination of elongation to sustain a constant number of filaments. Filament growth can be terminated by "capping proteins". In-vitro capping protein (CP) caps actin filament barbed ends with high affinity thereby preventing the addition or loss of actin subunits (Isenberg et al., 1980; Wear et al., 2003). Also known as β actinin, CapZ in skeletal muscle and Cap32/34 in Dictyostelium, capping protein is present as a heterodimer in almost all eukaryotic cells. After nucleation filaments are thought to elongate until the barbed ends are bound by capping protein. In the current view this leads to a branched network of short filaments (Pollard, 2007). PIP2 and CARMIL bind directly to CP and inhibit binding to actin. PIP2 rapidly and reversely inhibits CP and uncaps barbed ends in vitro.

CARMIL (Capping protein ARp2/3 Myosin I Linker) binds CP and the Arp2/3 complex and a class I myosin with a Src homology SH3 domain. CP may also be regulated indirectly by proteins that bind the barbed end of the actin filament like Ena/VASP and formins (Uruno et al., 2006; Wear et al., 2003).

Ready, steady, go! – Integrating external signals.

Regulation of motility involves the family of small Rho GTPases (Hall, 1998; Ridley, 2001) Rho proteins are activated by guanine nucleotide exchange factors (GEFs)

that replace GDP by GTP, and de-activated by hydrolysis of GTP by GTPase activating proteins (GAPs). GEFs are activated by receptors (Takai et al., 2001). RhoA acts downstream on mDia and the myosin II phosphorylation pathway regulate stress-fibre formation and contractility, whereas Rac and cdc42 stimulate the formation of protrusions by de-novo actin polymerization. Both subfamilies have specific and overlapping functions in signalling to actin remodelling. Microinjection and overexpression of various constructs, including dominant negative versions, showed that Rac and, to a lesser extent, Cdc42 are responsible for the formation of lamellipodia and ruffles, while Cdc42 strongly induces filopodia (Aspenstrom et al., 2004). Despite their strong influence on migration and spreading the results of knock-out experiments have been taken to indicate that Rac GTPases are not essential for these processes (Vidali et al., 2006). Rac and Cdc42 act via nucleation promoting complexes or directly on nucleating proteins: Rac1 binds the WAVE complex component Sra-1 to activate actin filament assembly by Arp2/3. Cdc42 interacts directly with WASP and N-WASP and it also binds mDia2 to initiate filopodia formation (Ladwein and Rottner, 2008).

Rho proteins are activated by growth factors (Hall, 1998) and integrin receptors (Price et al., 1998), which can activate, upon ligand binding, Phosphoinositide 3-kinases (PI3K) to produce Phosphatidylinositol (3,4,5)-triphosphate (PIP3), which in turn activates GEFs (Scita et al., 2000).

Aims of the present study

Two basic questions were addressed in the present work:

1. What is the concentration of monomeric actin at active sites of protrusion, namely in lamellipodia?

2. How are actin filaments organised and reorganised during the different phases of lamellipodia activity: protrusion, pause and retraction?

The first question is addressed the first manuscript, Paper I
"F- and G-actin concentrations in lamellipodia of moving cells."

The second question is addressed in the now published Paper II
"Differentially oriented populations of actin filaments generated in lamellipodia collaborate in pushing and pausing at the cell front."

Papers

F- and G-actin concentrations in lamellipodia of moving cells.

Stefan A. Koestler, Klemens Rottner, Frank Lai, Jennifer Block, Marlene Vinzenz and J. Victor Small

Abstract

Cells protrude by polymerizing monomeric (G) into polymeric (F) actin at the tip of the lamellipodium. Actin filaments are depolymerized towards the rear of the lamellipodium in a treadmilling process, thereby supplementing a G-actin pool for a new round of polymerization. In this scenario the concentrations of F- and G-actin are principal parameters, but have hitherto not been directly determined. By comparing fluorescence intensities of bleached and unbleached regions of lamellipodia in B16-F1 mouse melanoma cells expressing GFP-actin, before and after extraction with Triton X-100, we show that the ratio of F- to G-actin is 3.1+/- 0.9. Using electron microscopy to determine the F-actin content, this ratio translates into F- and G-actin concentrations in lamellipodia of approximately 500 µM and 160 µM respectively. The excess of G-actin, at several orders of magnitude above the critical concentrations at filament ends shows that the polymerization rate is not limited by diffusion and is tightly controlled by polymerization/depolymerization modulators.

Introduction

Eukaryotic cells move by the extension of a leaf-like structure, the lamellipodium, at the cell front (Abercrombie et al., 1970b). Protrusion occurs by polymerization of actin filaments at the tip of the lamellipodium, thereby pushing the membrane forward (Wang, 1985). Actin filaments are polar, with the barbed, fast growing ends pointing towards the direction of protrusion (Small et al., 1978). Under steady state conditions the network of actin filaments in lamellipodia maintains a constant breadth by coordinated depolymerization from the filament pointed ends towards the rear, in a treadmilling regime (Lai et al., 2008; Wang, 1985; Waterman-Storer et al., 1998; Wegner, 1976) that is tightly regulated. Treadmilling relies in the first instance on inherent differences of critical concentration for growth at the two filament ends, measured in vitro as around 0.06 µM and 0.6 µM at the plus and minus ends respectively (Le Clainche and Carlier, 2007; Pollard et al., 2000). Regulation can take

place on several levels: actin filament nucleation, elongation and depolymerization, monomer sequestration and filament end capping (Le Clainche and Carlier, 2007; Pollard, 2007). For an understanding of the basic principles of actin turnover and for simulating the molecular scenarios underlying protrusion (Novak et al., 2008) the biochemical parameters in vivo and, not least, the concentrations of F- and G-actin in the lamellipodium need to be known.

Global estimates of F- and G-actin ratios obtained by the fractionation of cell extracts (Bray and Thomas, 1976; Fechheimer and Zigmond, 1983; Hartwig and Shevlin, 1986; Heacock et al., 1984; Mose-Larsen et al., 1982) and the use of the DNAse inhibition assay (Blikstad et al., 1978) showed that there are approximately equivalent amounts of polymerized and unpolymerised actin in non-muscle cells, with estimates of the monomeric actin concentration ranging widely, from 12-300 µM (Pollard et al., 2000). Only recently were techniques developed to directly quantitate the local concentrations of proteins in living cells, namely in fission yeast. In a careful, fluorescence-based approach (Wu and Pollard, 2005) obtained global concentrations by quantitative immunoblotting and local concentrations from the relative fluorescence intensity. The relative concentrations of F- and G-actin were not however addressed. Estimates of actin filament concentrations in lamellipodia range from 700 µM, based on filament counts from electron microscopy (Hoglund et al., 1980) to 1600 µM, from the comparison of the phalloidin label intensities of single filaments and lamellipodia of fixed cells (Abraham et al., 1999). The latter authors supposed that the G-actin concentration at the lamellipodium tip was in the range of 8 µM (Abraham et al., 1999).

In this work we established a method to determine the F- and G-actin concentrations in the lamellipodium. Our measurements demonstrate a local concentration of G-actin in lamellipodia of around 160 µM, several orders of magnitude higher than the critical concentration for polymerization.

Results and discussion

Concentration of F-actin in lamellipodia

Our estimates of F–actin concentration are based on counts of filament numbers in aldehyde/Triton fixed and negatively-stained lamellipodia (Koestler et al., 2008) (Koestler et al., 2008). By monitoring the extraction/fixation process during the preparation of cells for electron microscopy in the light microscope we have shown that the gradient of intensity of GFP-actin across lamellipodia can be preserved by our fixation protocol (Koestler et al., 2008). This gradient correlates with a progressive drop in filament number away from the front of the lamellipodium that we suppose reflects a graded length of filaments with all plus ends located at the tip. The location of filament plus ends at the tip is consistent with the restriction of the WAVE nucleation complex to the actin-membrane interface ((Stradal et al., 2001); Supplementary figure 1).

Correlated light and electron microscopy of protruding lamellipodia showed that the filament density did not correlate linearly with the protrusion rate. This suggests that a critical filament density must be required for maintaining the structural integrity of a cytoplasmic leaflet. We conclude that protrusion rate is rather a function of several other factors, encompassing polymerization rates, filament arrangements and retrograde flow. Extending previous measurements (Koestler et al., 2008), filament counts close to the front edge of the lamellipodium yielded a value of 103 per μm filaments (sd = 17; 20 measurements in 5 cells) in constantly protruding lamellipodia segments. Calculation of the concentration of F-actin requires a value for the thickness of the lamellipodium. Various methods have been used to estimate the thickness of lamellipodia, including thin section electron microscopy (Abercrombie et al., 1970b), standing wave fluorescence microscopy (Abraham et al., 1999), stereo microscopy of negatively stained preparations (Hoglund et al., 1980) and atomic force microscopy, with values ranging from around 70 - 180 nm. Plastic cross sections of B16 cell lamellipodia showed a constant thickness across their breadth between 70 and 100 nm (not shown). Taking into account some shrinkage during embedding and other published estimates, we assume here a lamellipodia thickness in B16 cells of 120 nm. Future measurements by cryo electron tomography will lead to a more accurate estimate of this value. Taking this thickness and a density of 103

filaments/µm at the front of the lamellipodium the concentration of F-actin was estimated as around 500 µM (488 µM; for the calculation see materials and methods).
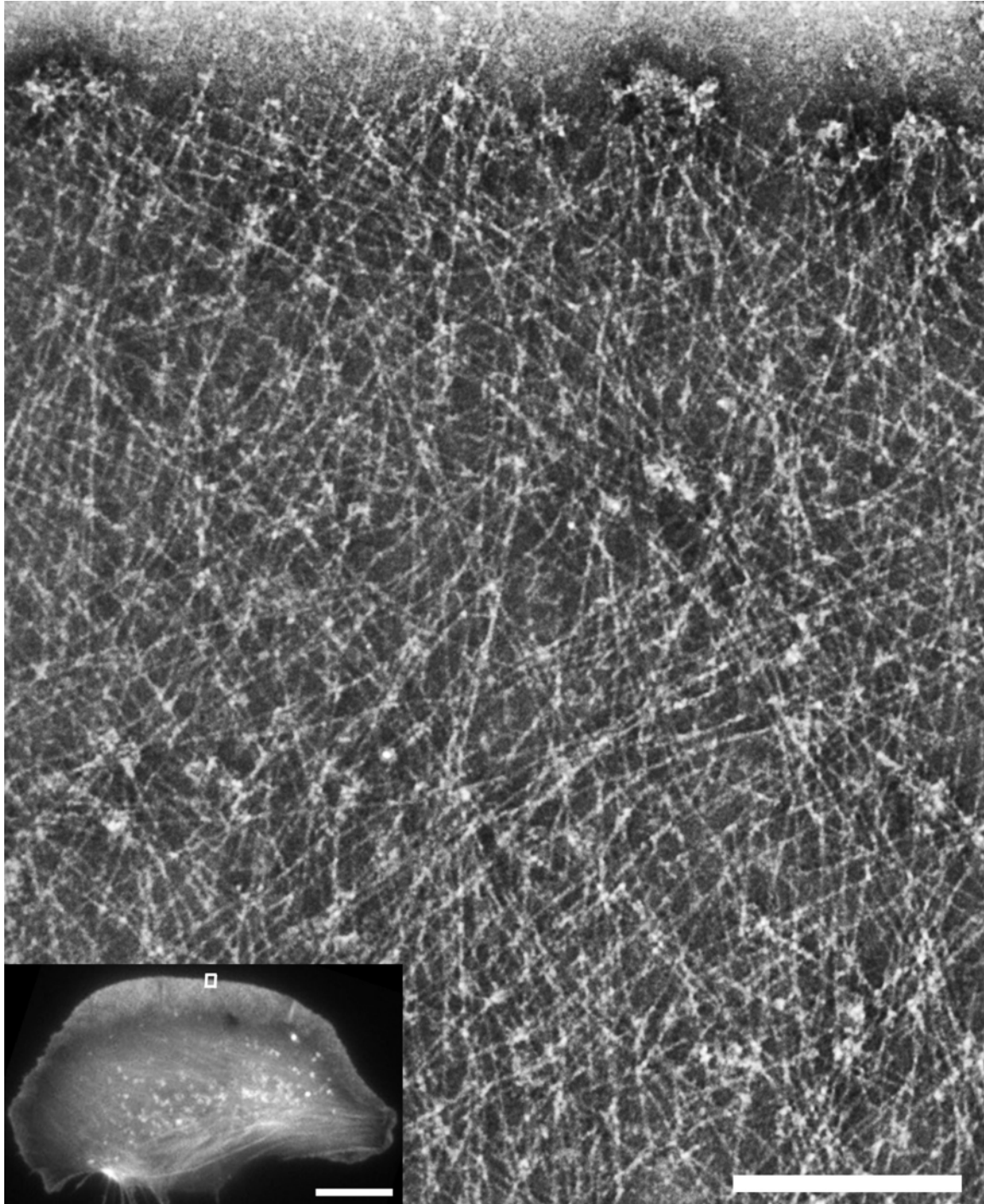

Figure 1: Correlative light- and electron microscopy of the lamellipodium of a GFP-actin expressing B16 cell. The single filaments are well defined. Bar, 200 nm. Inset shows the living cell just before fixation. The rectangle indicates the region of the electron micrograph. Bar, 10 µm.

Monomeric GFP-actin saturates rapidly in bleached lamellipodia

To measure the G-actin component in lamellipodia we took advantage of the spatial features of recovery of GFP-actin fluorescence after photobleaching (Figure 2). During the early phase of recovery of F-actin fluorescence at the lamellipodium front, the rest of the bleached zone is populated by monomeric GFP-actin. The fluorescence signal in this zone should then reflect the G-actin concentration, if it saturates before recovery of F-actin from the front. To estimate the rate of recovery of the G-actin component in the body of the lamellipodium, we performed a double bleach experiment, in which bleaching of the lamellipodium was followed by selective bleaching at the tip (Figure 2). In this way we were able to determine the GFP-actin signal in the lamellipodium without a contribution from GFP-F-actin at the tip. Within the limits of sensitivity of the dual head confocal microscope system used, the GFP fluorescence intensity in the lamellipodium was already saturated by the time of the first image acquisition after the initial photobleach (within 6 secs). The GFP fluorescence intensity in the bleached zone in the early recovery after photobleach could then be taken as a concentration indicator.
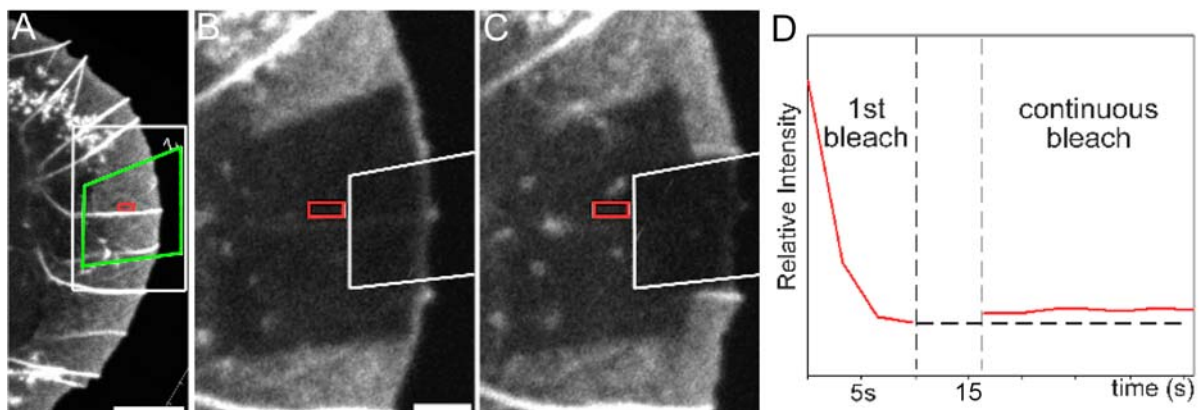

Figure 2: Dual bleach experiments demonstrate that monomeric actin saturates in the lamellipodium within 6 sec after photobleach and is incorporated into F-actin only at the tip. A shows the overview before bleach. Bar, 5 µm. Enlarged images of the region indicated with the white box in A show the bleached region immediately (B) and 20 s after bleach (C). Bar, 3µm. Following the first bleach of the lamellipodium (green box in A), bleaching was continued in the region outlined by the box in B and C. Graph (D) shows the average intensity, measured in the red rectangular region, over time. The empty frame between initial bleach and recovery is indicated by two

vertical dashed lines. Note, that the intensity in the region marked by the red square stays constant after bleach (shown are 22 s) when bleaching the more distal region.

Selective extraction of the G-actin component

In principle, the GFP signal in the bleached region of lamellipodia could contain a contribution from unbleached F-actin. In order to correct for this, we extracted cells with Triton X-100 during the early phase of recovery after photobleach and took the drop in fluorescence in the bleached zone as a measure of G-actin (Figure 3). The extraction conditions had then to satisfy two criteria to justify attribution of the loss of fluorescence to momeric GFP-actin: 1, F-actin should be retained in the cytoskeleton; and 2, the change in conditions (pre- versus post-extraction) should not affect the fluorescence characteristics of GFP (or the magnitude of the change should be known). Experiments showed that while the Triton/glutaraldehyde mixture used for electron microscopy satisfied the first criterion, the presence of glutaraldehyde caused a gradual quenching of the GFP signal. Other extraction conditions were therefore investigated. By using polyethylene glycol in the extraction mixture (see Materials and Methods) without glutaraldehyde, both conditions could be closely satisfied. First, the gradient of GFP-actin fluorescence in the unbleached regions of the lamellipodium could be preserved, indicating retention of the main component of F-actin (Figure 3). Second, the fluorescence intensity of single microtubules in B16 cells transfected with GFP tubulin, measured by TIRF microscopy, before and after applying the extraction protocol, was essentially unchanged (Supplementary figure 2).
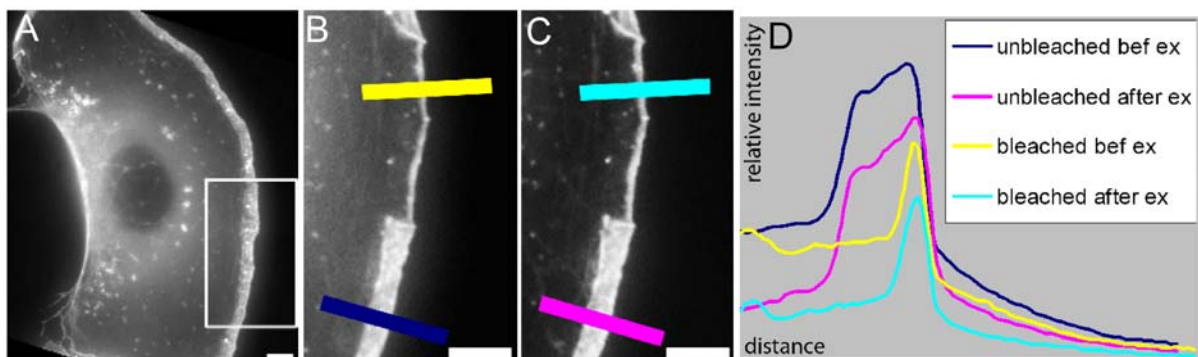

Figure 3: Selective extraction of G-actin after photobleaching. A) Overview of a GFP-actin expressing cell just before photobleach. B, C: Enlarged region indicated in A) about 2 s after bleach (B) and after extraction (C). Bars, 5 μm. Graph shows intensity scans along the lines indicated in B and C. Dark blue line: unbleached region before

extraction; yellow: bleached region before extraction; pink: unbleached region after extraction; light blue: bleached region after extraction. Note also the preservation of the gradient in the unbleached region before and after extraction.

In the representative extraction experiment shown in Fig.3 bleaching was performed using a confocal scanning head and image acquisition pre- and post-extraction with a CCD camera for optimal sensitivity (see Materials and Methods; Lai et al., 2008). Taking the fluorescence intensity at the unbleached lamellipodium tip before extraction as F- + G-actin we obtained an average F- to G-actin ratio of 3.1:1 (SDM=0.88, SEM=0.25, n=12). For a concentration of 488 µM F-actin (see above) calculated from the filament counts, this gave a G-actin concentration of 156 µM. Here we assumed that the G-actin concentration at the tip of the lamellipodium is similar to that a few µm behind (between 1 and 3 µm), as suggested by the more or less constant thickness of the lamellipodium and the level drop of fluorescence intensity across the lamellipodium upon lysis (Figure 2).

Given extraction conditions that result in a selective loss of only the G-actin component, there should in principle be no need to resort to photobleaching; the fluorescence loss in the lamellipodium should then yield the G-actin fraction. In practice, we found that the fluorescence loss on Triton extraction in the unbleached lamellipodium was more variable than in the bleached region. Higher losses than 20 % correlated with a flattening of the gradient of actin fluorescence, suggesting the removal of a fraction of filaments from the lamellipodium in these cases. In the bleached region a fractional loss of F-actin would have no significant effect on the drop in the fluorescence signal on extraction. In examples such as figure3 the loss of fluorescence in the bleached and unbleached regions was comparable, indicating retention of F-actin.

Actin under control
Our estimates indicate that the G-actin concentration in the lamellipodium is about 1000 times higher than the critical concentration for elongation at the barbed end. Based on in vitro rate constants (Pollard et al., 2000) this concentration would support polymerization rates up to 200 µm/min! Therefore the concentration of actin in lamellipodia is itself not a limiting factor for protrusion. This is not in line with the

funneling hypothesis, which assumes that G-actin is limiting and that capping protein blocks a subpopulation of barbed filament ends so that the remaining uncapped filaments can grow faster (Le Clainche and Carlier, 2007) . We conclude that spontaneous nucleation/polymerization is inhibited by sequestration of G-actin with profilin and thymosin β4, and by capping of filament barbed and pointed ends by capping protein and Arp2/3 complex, respectively (Pollard et al., 2000). Nucleation and polymerization promoting factors therefore regulate polymerization by releasing inhibition in a controlled way. The role of proteins in regulating the actin pools in lamellipodia could be analyzed in future experiments by the use of the method presented here.

How is the high G-actin concentration within the lamellipodium maintained? Diffusion of depolymerized actin from the lamellipodium into the cytoplasm could lead to a depletion of the G-actin pool within the lamellipodium. Depending on the volume that is available for diffusion away from the lamellipodium active transport might be required to counteract this effect. In the fish keratocyte, which mainly consists of a broad lamellipodium and the nucleus, which is impermeable to G-actin by diffusion, no additional transport would be required, in contrast to cells, where the cytoplasmic volume is high compared to the lamellipodium. Observations by Zicha et al. (Zicha et al., 2003) in T15 rat fibroblasts suggested that the transport of G-actin into lamellipodia occurred faster than could be explained by diffusion. They therefore concluded that G-actin diffusion may be supplemented by myosin dependent contraction of the cell body. In B16 cells, however, inhibition of myosin leads to an increase of the protrusion rate and an uncoupling of the lamellipodium from the cell body for several minutes, indicating a myosin independent transport in these cells (Koestler et al., 2008). Whether or not there is a G-actin gradient inside cells could be measured by using fluorescent dextran or GFP/RFP as indicator for the thickness of the cell in combination with an extraction protocol like that used for lamellipodia.

In conclusion, we have provided the first estimates the F- and G-actin concentrations in lamellipodia of living cells. The concentrations obtained provide a basis for the further development of ideas about the mode of protrusion and the regulation of actin polymerization and depolymerisation during cell migration.

Supplementary figures:
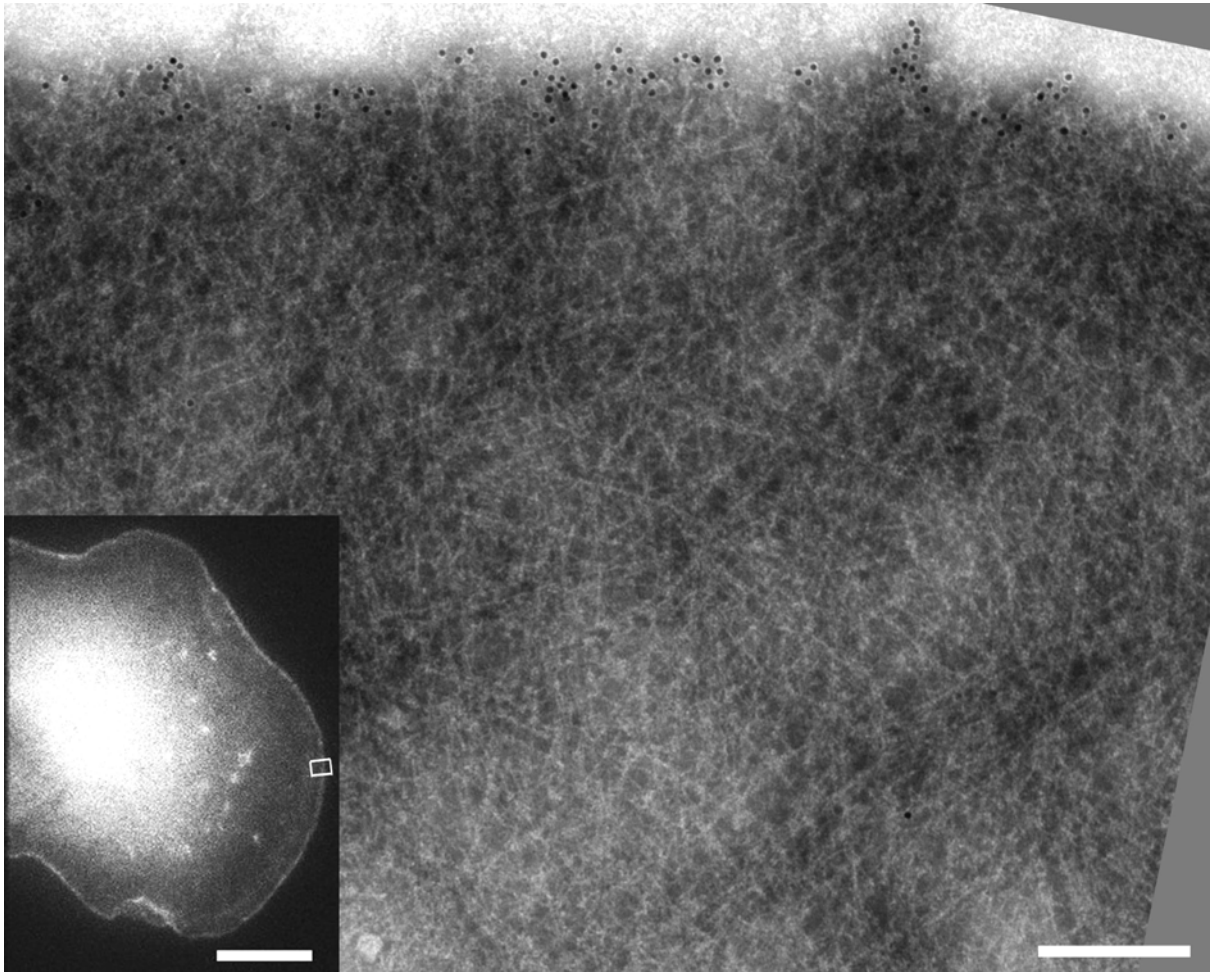
Supplementary figure 1: Correlative light- and electron microscopy and immunogold labeling of Abi1-GFP. Note localization of 10 nm gold label (black dots) at the tip of the cell edge. The definition of the filaments is reduced compared to Figure 1 because of the treatment for immunogold labeling. Bar 200 nm. Inset shows the living Abi1-GFP expressing cell in the light microscope just before fixation. The rectangle indicates the region of the electron micrograph. Bar 10 µm.
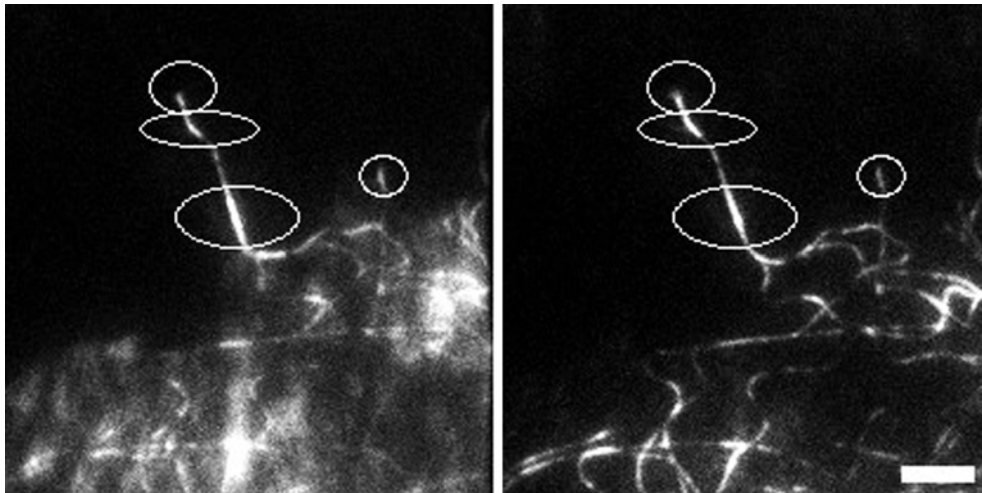
Supplementary figure 2: The fluorescence intensity of GFP does not change upon cell-lysis. In order to be able to correlate the GFP-intensities in the living and the lysed cell intensity measurements of GFP-α-Tubulin (mouse) in B16 cells were carried out before (left) and after (right) addition of detergent. In contrast to actin filaments microtubules can be imaged as single polymers by fluorescence microscopy, thereby making it feasible to visually control the maintenance of polymer. To reduce the influence of the soluble fraction of GFP-Tubulin on the intensity measurements microtubules in the periphery and close to the substrate were chosen and imaged by TIRF microscopy. To avoid chemical fixatives PEG was used to stabilize the cytoskeleton. The difference in the maximum fluorescence values of Microtubules before and after extraction was around 3.9 % (mean, standard deviation = 3.0 %, 33 measurements in 14 cells). This difference is negligible and therefore no correction was applied to the experimental data for actin.

Materials and Methods

B16F1 cells were maintained and transfected and observed in a heating chamber as described before (Koestler et al., 2008).

FRAP experiments were performed with a LSM 510 Meta (Zeiss, Jena, Germany), which was equipped with a 100× 1.45NA αPlan-FLUAR TIRF objective (Zeiss) and an interline transfer, progressive scan CCD camera (Coolsnap$_{HQ}$; Photometrics, Tucson, AZ, USA; or Cascade II, Roper Scientific) driven by Metamorph software (Molecular Devices Corp., Downingtown, PA, USA). Selected cellular areas covering parts of protruding lamellipodia were bleached (20-30 iterations at full laser power at 488 nm, 30 mW argon laser) immediately after one full-frame scan of respective fields, which was followed by switching to epi-fluorescence imaging using a mercury lamp (100 W) as light source. Switching time was approximately 2 s.

Dual-bleach experiments were performed using a double-scan-headed confocal microscope (Fluoview1000, Olympus), allowing simultaneous imaging (with 30 mW 488 nm multiline argon at laser powers of approximately 1–5 %) and photobleaching using a 20 mW 405 nm diode laser. Output laser powers were approximately 5–10% for photobleaching. A 100 × /1.45NA PlanApo TIRF objective (Olympus Inc.) was used in all experiments. Movies were acquired at a scanning rate of 2.711 or 3.264 s per frame. The initial photobleach of the region covering the whole breadth of the lamellipodium was followed by an empty frame and continuous bleaching near the edge. Image analysis was carried out on a PC using FV10-ASW 1.6 viewer (Olympus Inc., Olympus, Hamburg, Germany) and Metamorph (Molecular Devices Corp.) software.

For lysis, cells were observed in 4 % polyethylene glycol (20.000 g/mol) in cytoskeleton buffer (see e.g. (Koestler et al., 2008)) (without EGTA) and prepared with pipes (pH 7.0). Triton X-100 was added to a final concentration of 1 % within 5 s after photobleaching (in most experiments).

EGFP-alpha-mouse-tubulin expressing cells were observed with a Zeiss Axiovert 200 equipped for TIRF microscopy (Zeiss/Visitron) equipped with a 100× 1.45NA αPlan-FLUAR TIRF objective (Zeiss), solid state 488 nm laser, and a Cascade camera

(Roper Scientific) and lysed as above. Analysis was performed on a Windows PC with Metamorph Software.

Correlative light- and electron-microscopy was performed as described (Koestler et al., 2008) on GFP-Abi1 (kindly provided by Klemens Rottner) and mCherry-Actin transfected B16 cells, treated for 15 – 30 min with AIF, except for immunogold labelling: after fixation under the light microscope the cells were incubated with anti-GFP-antibodies (rabbit; kindly provided by Jan Faix) in PBS containing 1 µg/ml Phalloidin, for two days followed by incubation with gold-conjugated anti-rabbit-antibody for two days.

The actin concentrations were calculated from the mean value of the actin filament number, 103, and the F:G-actin ratio of 3.1:1: The total length of filaments in a 1 x 1 µm sheet is 103×10^3 nm. The volume in 1 µm² of Lamellipodium with 120 nm thickness corresponds to.1.2×10^{-10} µl. Taking 13 subunits per 38 nm of filament length, the number of actin molecules in a 1x1 µm sheet gives 35.24×10^3 molecules in 1.2×10^{-10} µl. This makes 2.94×10^{20} molecules per litre, corresponding to an F-actin concentration of 488 µM.

References

Abercrombie, M., J.E. Heaysman, and S.M. Pegrum. 1970. The locomotion of fibroblasts in culture. I. Movements of the leading edge. *Exp Cell Res.* 59:393-8.

Abraham, V.C., V. Krishnamurthi, D.L. Taylor, and F. Lanni. 1999. The actin-based nanomachine at the leading edge of migrating cells. *Biophys J.* 77:1721-32.

Blikstad, I., F. Markey, L. Carlsson, T. Persson, and U. Lindberg. 1978. Selective assay of monomeric and filamentous actin in cell extracts, using inhibition of deoxyribonuclease I. *Cell.* 15:935-43.

Bray, D., and C. Thomas. 1976. Unpolymerized actin in fibroblasts and brain. *J Mol Biol.* 105:527-44.

Fechheimer, M., and S.H. Zigmond. 1983. Changes in cytoskeletal proteins of polymorphonuclear leukocytes induced by chemotactic peptides. *Cell Motil.* 3:349-61.

Hartwig, J.H., and P. Shevlin. 1986. The architecture of actin filaments and the ultrastructural location of actin-binding protein in the periphery of lung macrophages. *J Cell Biol.* 103:1007-20.

Heacock, C.S., K.E. Eidsvoog, and J.R. Bamburg. 1984. The influence of contact-inhibited growth and of agents which alter cell morphology on the levels of G- and F-actin in cultured cells. *Exp Cell Res.* 153:402-12.

Hoglund, A.S., R. Karlsson, E. Arro, B.A. Fredriksson, and U. Lindberg. 1980. Visualization of the peripheral weave of microfilaments in glia cells. *J Muscle Res Cell Motil.* 1:127-46.

Koestler, S.A., S. Auinger, M. Vinzenz, K. Rottner, and J.V. Small. 2008. Differentially oriented populations of actin filaments generated in lamellipodia collaborate in pushing and pausing at the cell front. *Nat Cell Biol.* 10:306-13.

Lai, F.P., M. Szczodrak, J. Block, J. Faix, D. Breitsprecher, H.G. Mannherz, T.E. Stradal, G.A. Dunn, J.V. Small, and K. Rottner. 2008. Arp2/3 complex interactions and actin network turnover in lamellipodia. *Embo J.* 27:982-92.

Le Clainche, C., and M.F. Carlier. 2007. Regulation of Actin Assembly Associated With Protrusion

and Adhesion in Cell Migration. *Physiol Rev : , 2008;*

doi:10.1152/physrev.00021.2007. 88:489-513.

Mose-Larsen, P., R. Bravo, S.J. Fey, J.V. Small, and J.E. Celis. 1982. Putative association of mitochondria with a subpopulation of intermediate-sized filaments in cultured human skin fibroblasts. *Cell*. 31:681-92.

Novak, I.L., B.M. Slepchenko, and A. Mogilner. 2008. Quantitative analysis of G-actin transport in motile cells. *Biophys J*. 95:1627-38.

Pollard, T.D. 2007. Regulation of actin filament assembly by Arp2/3 complex and formins. *Annu Rev Biophys Biomol Struct*. 36:451-77.

Pollard, T.D., L. Blanchoin, and R.D. Mullins. 2000. Molecular mechanisms controlling actin filament dynamics in nonmuscle cells. *Annu Rev Biophys Biomol Struct*. 29:545-76.

Small, J.V., G. Isenberg, and J.E. Celis. 1978. Polarity of actin at the leading edge of cultured cells. *Nature*. 272:638-9.

Stradal, T., K.D. Courtney, K. Rottner, P. Hahne, J.V. Small, and A.M. Pendergast. 2001. The Abl interactor proteins localize to sites of actin polymerization at the tips of lamellipodia and filopodia. *Curr Biol*. 11:891-5.

Wang, Y.L. 1985. Exchange of actin subunits at the leading edge of living fibroblasts: possible role of treadmilling. *J Cell Biol*. 101:597-602.

Waterman-Storer, C.M., A. Desai, J.C. Bulinski, and E.D. Salmon. 1998. Fluorescent speckle microscopy, a method to visualize the dynamics of protein assemblies in living cells. *Curr Biol*. 8:1227-30.

Wegner, A. 1976. Head to tail polymerization of actin. *J Mol Biol*. 108:139-50.

Wu, J.Q., and T.D. Pollard. 2005. Counting cytokinesis proteins globally and locally in fission yeast. *Science*. 310:310-4.

Zicha, D., I.M. Dobbie, M.R. Holt, J. Monypenny, D.Y. Soong, C. Gray, and G.A. Dunn. 2003. Rapid actin transport during cell protrusion. *Science*. 300:142-5.

LETTERS

Differentially oriented populations of actin filaments generated in lamellipodia collaborate in pushing and pausing at the cell front

Stefan A. Koestler[1], Sonja Auinger[1], Marlene Vinzenz[1], Klemens Rottner[2] and J. Victor Small[1,3]

Eukaryotic cells advance in phases of protrusion, pause and withdrawal[1]. Protrusion occurs in lamellipodia, which are composed of diagonal networks of actin filaments, and withdrawal terminates with the formation of actin bundles parallel to the cell edge. Using correlated live-cell imaging and electron microscopy, we have shown that actin filaments in protruding lamellipodia subtend angles from 15–90° to the front, and that transitions from protrusion to pause are associated with a proportional increase in filaments oriented more parallel to the cell edge. Microspike bundles of actin filaments also showed a wide angular distribution and correspondingly variable bilateral polymerization rates along the cell front. We propose that the angular shift of filaments in lamellipodia serves in adapting to slower protrusion rates while maintaining the filament densities required for structural support; further, we suggest that single filaments and microspike bundles contribute to the construction of the lamella behind and to the formation of the cell edge when protrusion ceases. Our findings provide an explanation for the variable turnover dynamics of actin filaments in lamellipodia observed by fluorescence speckle microscopy[2] and are inconsistent with a current model of lamellipodia structure that features actin filaments branching at 70° in a dendritic array[3].

Migrating cells exploit two properties of actin filaments to move: the property to polymerize and push (to effect protrusion) and the ability to slide with myosin II (to drive retraction). Protrusion is effected by lamellipodia[1,4], thin sheets of cytoplasm containing networks of actin filaments that have their fast growing plus-ends abutting the leading membrane[5]. Current ideas of how protruding lamellipodia are organized have come mainly from electron microscopic analysis of cells that show constant motility, in particular, the epidermal keratocyte[3,6]. From images obtained using a critical-point drying procedure for specimen preparation, a model of lamellipodium organization has been proposed

that features a dendritic network of actin filaments with the Arp2/3 complex situated at 70° branch points[3,7,8].

In migrating cells, lamellipodia not only protrude, they undergo phases of protrusion, pause and withdrawal, the latter often associated with ruffling[1]. Filopodia and related bundles embedded in the lamellipodia mesh, also referred to as microspikes[4], contribute to these activities. To gain insight into the structural basis of changes in protrusive activity, we have developed procedures for correlating the local movements of lamellipodia (monitored by live-cell imaging) with their organization after negative-stain electron microscopy. Results obtained using this approach reveal filament arrangements and rearrangements in lamellipodia that are difficult to reconcile with the dendritic model. They also show how filament remodelling in lamellipodia may contribute to the construction of stationary cell edges and to the assembly of the cytoskeleton of the lamella region behind the lamellipodium[9].

Figure 1 shows the final frames of a video sequence (Supplementary Information, Movie 1) of a fast and steadily protruding B16 melanoma cell expressing green fluorescent protein (GFP)–actin and mCherry–VASP, before and after fixation on the light microscope (Fig. 1a, b) and an overview of the cell in the electron microscope (Fig. 1d). VASP (vasodilator-stimulated phosphoprotein) is a useful indicator of protrusion, as the intensity of lamellipodia-tip labelling is proportional to the protrusion rate[10]. The time between the final video frame and the fixation event was approximately 3 s. Scans of the GFP intensity across the lamellipodium (Fig. 1b, inset) in the main protruding zone (Fig. 1b, box) demonstrated that the gradient of actin fluorescence in the lamellipodium of the living cell was preserved by the fixation process. Frames of the video sequence in the boxed area in Fig. 1b are shown in Fig. 1c (upper panels), together with the velocity profile in this position (Fig. 1c, bottom panel). The mean protrusion rate over the terminal 60 s was 3.5 μm min⁻¹. Electron micrographs of the same region close to and 5 μm behind the lamellipodium front (Fig. 1d, small boxed regions) are shown in Fig. 2a and b (for an overview, see Supplementary Information, Fig. S1). The number of filaments crossing 1 μm lines drawn 0.2 μm
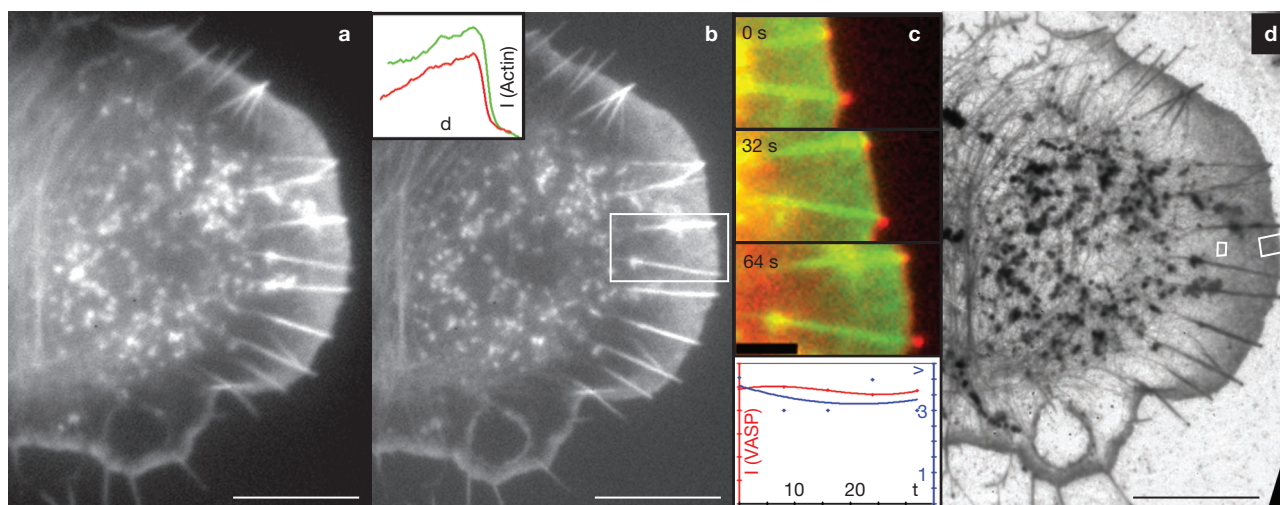
Figure 1 Arrest of a steadily protruding lamellipodium and preservation of the actin gradient. (**a**) Final frame (GFP channel) of a video sequence showing a B16 melanoma cell expressing GFP–actin and mCherry–VASP. (**b**) Actin–GFP image of a cell fixed within 3 s after the last video frame shown in **a**. The inset shows intensity scans (I (Actin)) across the lamellipodium (boxed region) before (green line) and after (red line) fixation; d in the inset is the distance.

(**c**) Upper panels: video sequence leading to fixation of boxed region in **b** (green, GFP–actin; red, mCherry–VASP). Lower panel: protrusion rate over the terminal period (v, µm min^{-1}; blue) and the relative mCherry–VASP intensity at the front edge of the lamellipodium (I (VASP); red). (**d**) Overview electron micrograph of the cell after negative staining. Bars are 10 µm (**a**, **b**, **d**) and 3 µm (**c**). See also Supplementary Information, Movie 1.

behind the cell front in this advancing lamellipodium averaged 90 ± 10. Particularly noteworthy was the wide angular distribution of filaments, from 15–90°, with respect to the cell edge (Fig. 2a, left inset). In a region 5 µm behind the front of the same lamellipodium (Fig. 1d, Fig. 2b, small box inset; Supplementary Information, Fig. S1), the filament density was lower (59 ±15 filaments µm^{-1}). In addition, there was an increase in the proportion of filaments at low angles to the cell front (Fig. 2b, inset). The gradient of filament density across the lamellipodium back to 3.5 µm from the front correlated with the gradient of actin–GFP intensity in the same position of the living and fixed cell (Fig. 2a, right inset) and revealed a drop in filament number of 11% over the first micron.

Figure 3a–e (Supplementary Information, Movie 2) shows a cell for which three regions of different protrusive activity are highlighted (Fig. 3b), with enlarged video frames in Fig. 3c–e. At position C (Fig. 3b), the protrusion rate (approximately 2 µm min^{-1}) and VASP intensity were more or less constant over the terminal 2 min (Fig. 3c, middle panel). Figure 3f shows the organization of actin filaments at the front of the lamellipodium in the same region of the cell. Further analysis (Fig. 3c, histogram, lower panel) showed an angular distribution of filaments in a region 0.2 µm from the cell front; notably, there was a wide distribution of angles down to 15°, as well as the presence of a small population of filaments subtending angles below 20° to the cell edge (Fig. 3f), which also extended up to the tip of the lamellipodium (arrow). The cell in Fig. 3 moved throughout the video sequence without a significant change in overall shape. Consequently, the radial protrusion rate decreased steadily from the advancing shoulders out to the lateral flanks. In position D (Fig. 3b), the rate of protrusion just prior to fixation was 1 µm min^{-1} and the VASP label declined steadily over the terminal 2 min (Fig. 3d, middle panel). In this position, a large proportion of filaments was oriented at lower angles to the cell edge (Fig. 4a; see also histogram in Fig. 3d) and could be seen to originate from foci at the lamellipodium front. The same reorganization of filaments from the peak towards the flank was seen in equivalent positions of the lamellipodium on the opposite half

of the cell (data not shown). At the extreme lateral flank of the same cell (position E, Fig. 3b, e) there was no net protrusion, but small fluctuations of the cell edge that ended in a minor retraction and complete loss of VASP label (Fig. 3E). Electron microscopy (Fig. 4b) showed that the lamellipodium at this position was approximately 0.5 µm wide and contained a major component of filaments oriented parallel to the cell edge, superimposed on a narrow band (0.2 µm wide) of divergent filament arrays and characteristic of early protrusions. Analysis of MTLn3 carcinoma cells, which migrate actively in vitro and in vivo[11], revealed essentially the same changes in filament organization between regions of protrusion and pause; namely, a shift in orientation of filaments to lower angles (some to below 15°) and, in addition, the appearance in pausing zones of a noticeable proportion of filaments with curved trajectories (Supplementary Information, Fig. S2). Slowing and pause were associated with a 30% reduction in filament numbers at the front (Fig. 3, positions C and D) of the B16 melanoma cell (Fig. 3f, inset).

According to their varied orientation to the cell front, actin filament tips must move laterally along the cell edge as they grow[12]. This lateral flow was reflected in the movement of microspike bundles, commonly embedded in protruding lamellipodia, of B16 melanoma cells (Supplementary Information, Fig. S3a–g and Movie 3). The angle that such bundles subtended with the cell front varied, ranging from 90° to below 10° (Supplementary Information, Fig. S3h), in the same range as observed for individual filaments. In addition, the proportion of microspikes at lower angles was higher in slowing and pausing lamellipodia when compared with continuously protruding ones (Supplementary Information, Fig. S3h). A direct consequence of this angular distribution was variation in the velocity of lateral movement of microspike tips along the cell edge and in the length of the bundles. Using photo-activatable-GFP (PA-GFP; Supplementary Information, Fig. S3e and Movie 3e), we showed that the polymerization rate in microspikes increased up to 15 µm min^{-1} for those oriented at approximately 15° to the cell edge (Supplementary Information, Fig. S3i). Microspike bundles moved laterally in opposite directions and
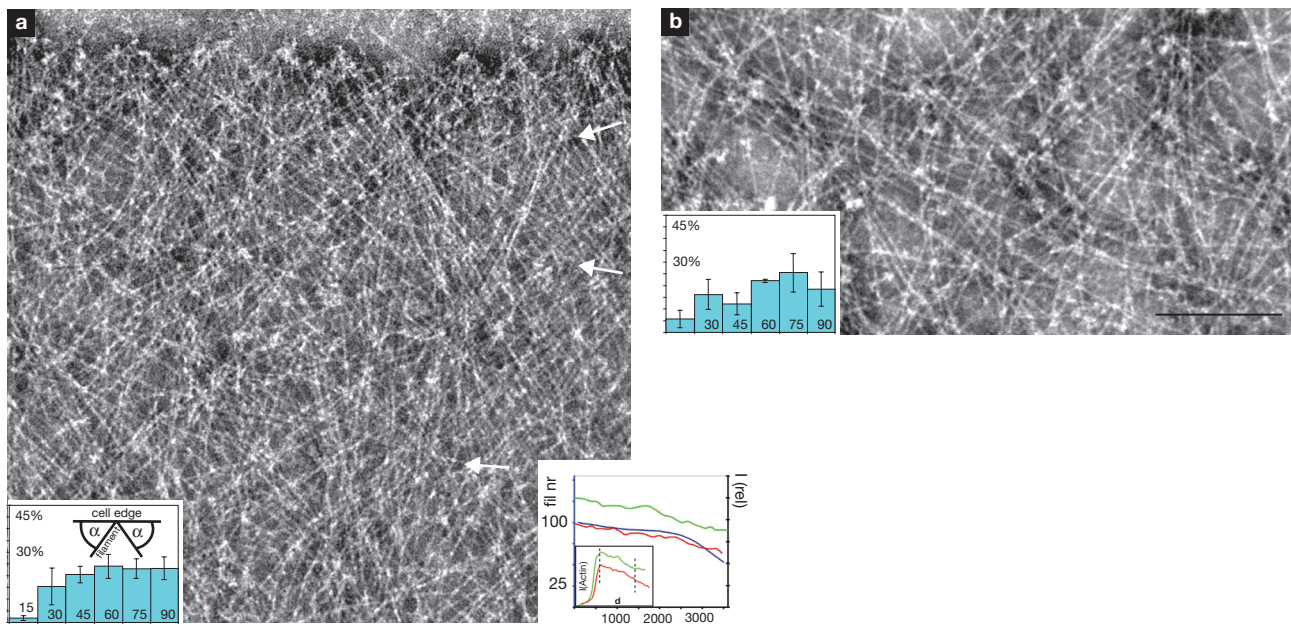
Figure 2 Actin filaments are variably orientated in protruding lamellipodia. (**a**) Electron micrograph of the front region of the lamellipodium shown in Fig. 1b–d (peripheral zone boxed in Fig. 1d and Supplementary Information, Fig. S1). The histogram shows the angular distribution of filaments crossing a line (1 μm) drawn parallel to and 100 nm behind the front edge of the lamellipodium (mean of five adjacent regions; total of 451 filaments). Filaments diverged at variable angles from foci at the cell front. Arrows indicate some examples of filaments at low angles. (**b**) The region in the same lamellipodium, 5 μm behind the cell edge (inner region boxed in Fig. 1d and Supplementary Information, Fig. S1); histogram shows the angular distribution of filaments crossing a line (1 μm) parallel to the cell front (mean of four adjacent regions 5 μm from front edge; total of 236 filaments). Note the decrease in filament density and increase in the number of filaments at lower angles to the cell edge. Inset right in **a**: comparison of the fluorescence signal across the lamellipodium (Fig.1b) with the actin filament density (per 1 μm of lamellipodium width) determined from electron micrographs taken from the region including Figs. 2a, b. The filament counts at 200 nm from the front were normalized to the peak of the fluorescence scan of the fixed cell (red). The fluorescence traces correspond to the signal between the dotted lines shown in the inset. Scale bar is 200 nm.

could be observed to cross each other (Supplementary Information, Fig. S3b and Movie 3b) or to fuse. One consequence of these bilateral movements was the generation of antiparallel arrays of actin filaments that formed bundles at the base of the lamellipodium, from where they entered the lamella and accumulated myosin (Supplementary Information, Fig. S3f and Movie 3f). Other microspikes contributed directly to the formation of retracting edges (Supplementary Information, Fig. S3a and Movie 3a). Although the lateral flow of microspikes could lead to their integration into the lamella with myosin, it was not dependent on myosin II, as shown by its persistence in the presence of the myosin II inhibitor blebbistatin (Supplementary Information, Fig. S3g and Movie 3g). In the short term (within 2–10 min), blebbistatin (50–100 μM) induced an increase in the rate of lamellipodia protrusion by a factor of 1.5–3 and an increase in the lamellipodium width (Supplementary Information, Fig. S3j, k), analogous to observations on immobilized *Aplysia californica* growth cones[13].

The negative staining method, as used here and in earlier studies (reviewed in ref. 14), has the advantage that linearity of filaments within the delicate meshwork of the lamellipodium is maintained and the dorsal and ventral arrays of actin are included in the electron microscope images. For the first time, we were thus able to relate the angular distributions of filaments and filament densities to the history of protrusion. Our direct measurements indicate that around 100 filaments per micron are utilized during protrusion. This value is approximately half that estimated indirectly by comparison of the fluorescence intensity of phalloidin-labelled single actin filaments with that of phalloidin-labelled lamellipodia of fixed 3T3 fibroblasts[15]. From the present and earlier

studies, it is clear that the filament density in lamellipodia does not determine the protrusion rate, as it differs little between keratocytes that can move at 15 μm min⁻¹ (ref. 6) and B16 melanoma and MTLn3 adenocarcinoma cells protruding five times more slowly. Correspondingly, we found that slowing of the cell edge was not accompanied by a significant decrease in filament density. Instead, there was a consistent increase in the number of filaments oriented at a low angle to the cell edge. The wide angular distribution of filaments, all with their plus-ends forward, indicate that there is a spread of polymerization rates, with filaments at low angles growing fastest to keep up with the front. The factors determining this variation in rate are unknown, but may be influenced by a type of force-dependent feedback mechanism[16], caused by progressively lower resistance to filament growth at lower angles. We suggest that the transition from protrusion to pause is signalled by the net local downregulation of actin plus-end polymerization complexes, but with some polymerization complexes being downregulated more than others. In this model, actin filaments polymerizing slowest act as a brake on protrusion through tethering with the leading membrane, analogous to the tethering of actin filaments to beads in mimetic models of cell motility[17,18]. Other, faster growing filaments must re-orient their trajectory, relative to the front edge, to grow. This causes an increase in the population of filaments at lower angles (Supplementary Information, Movie 4). If pause persists, more filaments become parallel to the cell front; some may also detach and move backwards with retrograde flow to the base of the lamellipodium, as observed with microspike bundles (Supplementary Information, Fig. S3c, Movie 3c; ref. 19).
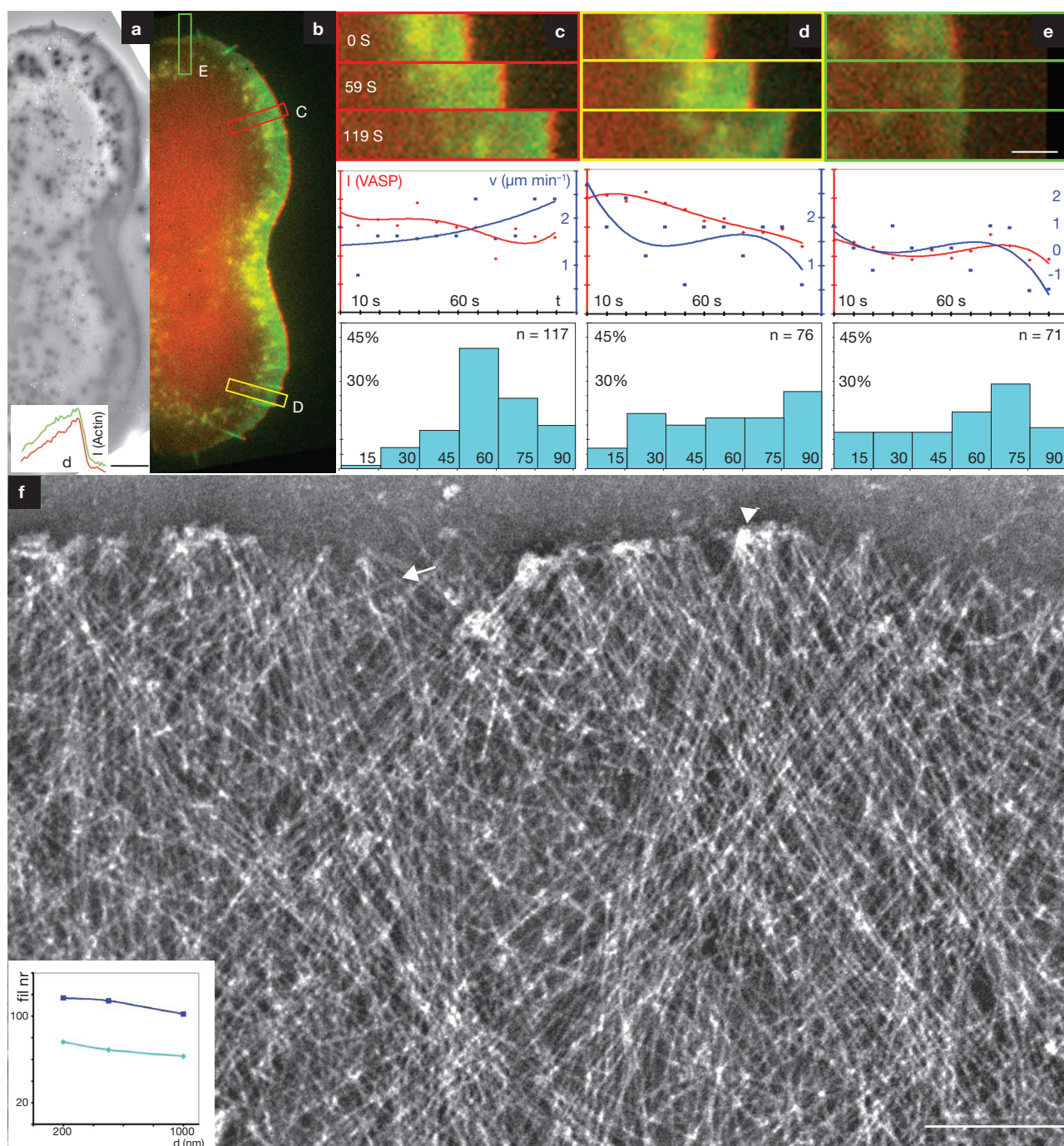
Figure 3 Actin filaments reorganize during the transition from protrusion to retraction. (**a**, **b**) Overview electron micrograph (**a**) and terminal video frame (**b**) of a B16 melanoma cell transfected with GFP–actin and mCherry–VASP (see Supplementary Information, Movie 2). Inset in **a**: intensity scans of GFP–actin fluorescence across the lamellipodium in a protruding region before (green) and after (red) fixation showing retention of actin-density gradient. (**c**–**e**) Upper panels show terminal video sequences of boxed regions **C**, **D** and **E** marked in **b** (green, GFP–actin; red, mCherry–VASP); Middle panels, protrusion rate (v, μm min^{-1}, blue) and relative VASP intensity at lamellipodium front (I (VASP), red) as a function of time (t, s); Lower panels, histograms of the angular distribution of filaments relative to the cell front for the corresponding electron micrographs (**f** and Fig. 4a, b), measured at 200 nm from cell edge across a line (1 μm). 'n' is the number of filaments measured; numbers in bars indicate the angle to the cell edge. (**f**) Electron micrograph of front region of protruding lamellipodium in boxed region **c**. Note partial grouping of filaments oriented at high angles to the front (arrowhead), as well as a subpopulation of individual filaments at shallow angles (arrow; see also histogram in **c**). Inset: comparison of filament counts back to 1 μm in this part of the lamellipodium (violet) with the pausing region shown in Fig. 4a (light blue). Scale bars are 5 μm (**a**), 2 μm (**c**–**e**) and 200 nm (**f**).

The advance of the lamellipodium depends on a balance between the rate of actin polymerization and the rate of retrograde flow. Recent findings on immobilized *Aplysia* growth cones indicate that a component of retrograde flow is driven by myosin II activity in the lamella[13], consistent with our observation of an increase in lamellipodia protrusion rate in B16 cells treated with blebbistatin. Pausing in lamellipodia may therefore
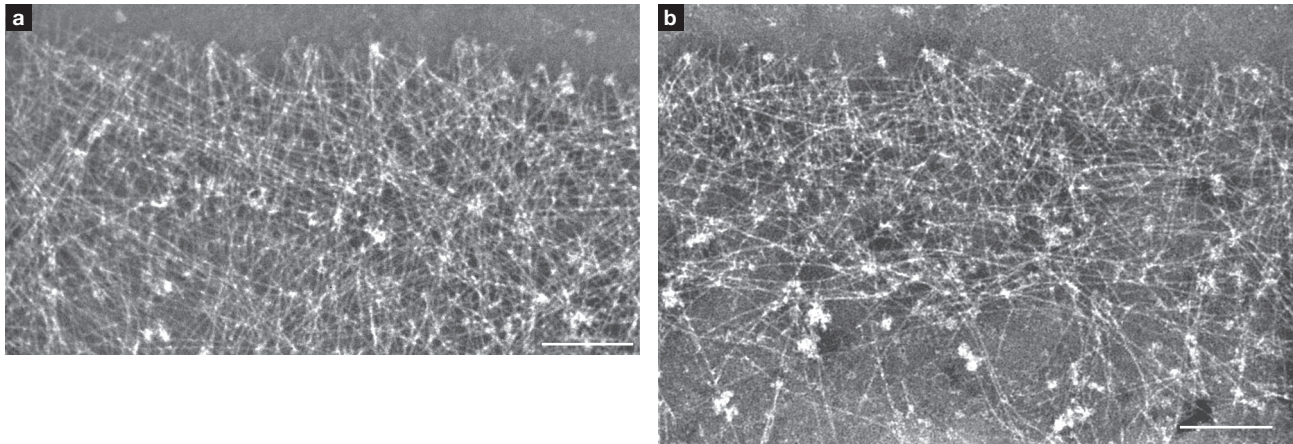
Figure 4 Slowing and pause is associated with an increase in the number of filaments at shallow angles to the lamellipodium front. (**a**) Electron micrograph of region D in Fig. 3b, where the protrusion rate had slowed down to 1 μm min^{-1} at the point of fixation (Fig. 3d, middle panel,). Note the prevalence of filaments at low angles to the cell edge (see also Fig. 3d histogram, lower panel) and that these filaments originate from foci at the lamellipodium front. (**b**) Electron micrograph of region E in Fig. 3b, on the lateral flank of the cell where protrusion had ceased (Fig. 3e, middle panel). Note the dominance of filaments parallel to the cell edge (see also Fig. 3e histogram, bottom panel). Scale bars are 200 nm.

be explained by a reduction in the net forward polymerization rate at filament plus-ends to the rate component of retrograde flow contributed by myosin–actin interactions at the base of the lamellipodium. An analogous situation is apparent in fish keratocyte lamellipodia, for which protrusion is maximal at the front and reduces to zero at the flanks. At the front there is minimal retrograde flow[20], whereas at the flanks, retrograde flow is maximal; this can be explained as the combined contributions of actin polymerization at the membrane and the myosin-dependent withdrawal of filaments into the cell body[20].

On the basis of this study, we propose a simple model in which different ramifications of filament reorganization in the lamellipodium lead to the contribution of anti-parallel filament arrays, including arcs[9,12,21], to the lamella during protrusion (Fig. 5a) and to the cell edge during retraction (Fig. 5b); in both cases filament arrays are produced to allow the formation of contractile assemblies with myosin. In this scheme, there is a gradation of filament lengths in lamellipodia according to the angular distribution and the drop in actin filament density away from the front. From elementary geometric considerations, filaments oriented at 15° to the cell edge that extend to the rear of the lamellipodium will be three times longer than those oriented at 55°. For a lamellipodium of 3 μm in width, this would correspond to maximum filament lengths of 11.6 μm and 3.7 μm, respectively (disregarding those that extend further into the lamella). During persistent pause, depolymerization from filament minus-ends will eliminate shorter filaments at higher angles to the cell edge first, leaving the longer filaments shorter, but still long enough to form a parallel bundle. We assume that the association of these latter filaments with tropomyosin protect them from further depolymerization[22] and promote their interaction with myosin to consolidate the cell edge. Rather than being static, filaments that enter the lamella continue to turnover (Supplementary Information, Fig. S3e, Movie 3e; ref. 2), so that their lamellipodia precursors can be viewed as seeds of the lamella cytoskeleton.

The currently popular dendritic network model of lamellipodium protrusion[7,8,23] features 70° Y-junctions within 20–50 nm of each other in the actin network[3] and branched filament segments behind the cell front that are capped at their plus ends. The model derives from analysis of electron micrographs of cytoskeletons prepared by the critical-point drying method[3] and extrapolation of data showing the ability of the Arp2/3-complex to induce the branching of actin filaments *in vitro*[24,25]. Definitive proof of whether or not branches exist at all in lamellipodia will need to come from cryo-electron tomography, to counter any arguments about artefacts induced by specimen preparation[26] and three-dimensional organization. The feasibility of visualizing actin filaments in vitreously frozen *Dictyostelium discoideum* amoebae has been shown previously[27] and the challenge now is to combine this methodology with information about the motile activity of the imaged regions. Nevertheless, we already show that there is no regular angle of 70° between filaments at the front of a protruding cell edge. And with a primary fixation stronger than that used previously[3], we found no evidence of actin-filament branches.

From analysis of actin-filament turnover by fluorescence speckle microscopy[2,28] and lamellipodia spreading dynamics[29], it has been concluded that the lamellipodium 'surfs' on top of the lamella underneath. Our results indicate, however, that all filaments in the lamellipodium originate from nucleation centres at the tip, with no superposition of the lamellipodium network on another array beneath; the lamellipodium and lamella are spatially and structurally distinct, although coupled at their boundaries[9], where myosin engagement begins. In addition, we provide an alternative explanation for the different populations of actin speckles observed in lamellipodia[2]. The longest-lived speckles can be explained as belonging to the long filaments that extend to the base of the lamellipodium and the short-lived speckles to those that terminate within the lamellipodium network. The possibility exists that a variable rate of treadmilling of individual filaments and bundles at different angles also contributes to the variability in retrograde flow rate. This idea could be tested by electron microscopy in conjunction with speckle microscopy[2] or spatiotemporal image correlation microscopy[30].

In conclusion, correlated live-cell imaging and electron microscopy has revealed a shift in the angular distribution of filaments in lamellipodia according to protrusive activity. These findings shed new light on the way actin is used to drive cell motility and also prompts a re-evaluation of current ideas about actin-filament organization in lamellipodia.
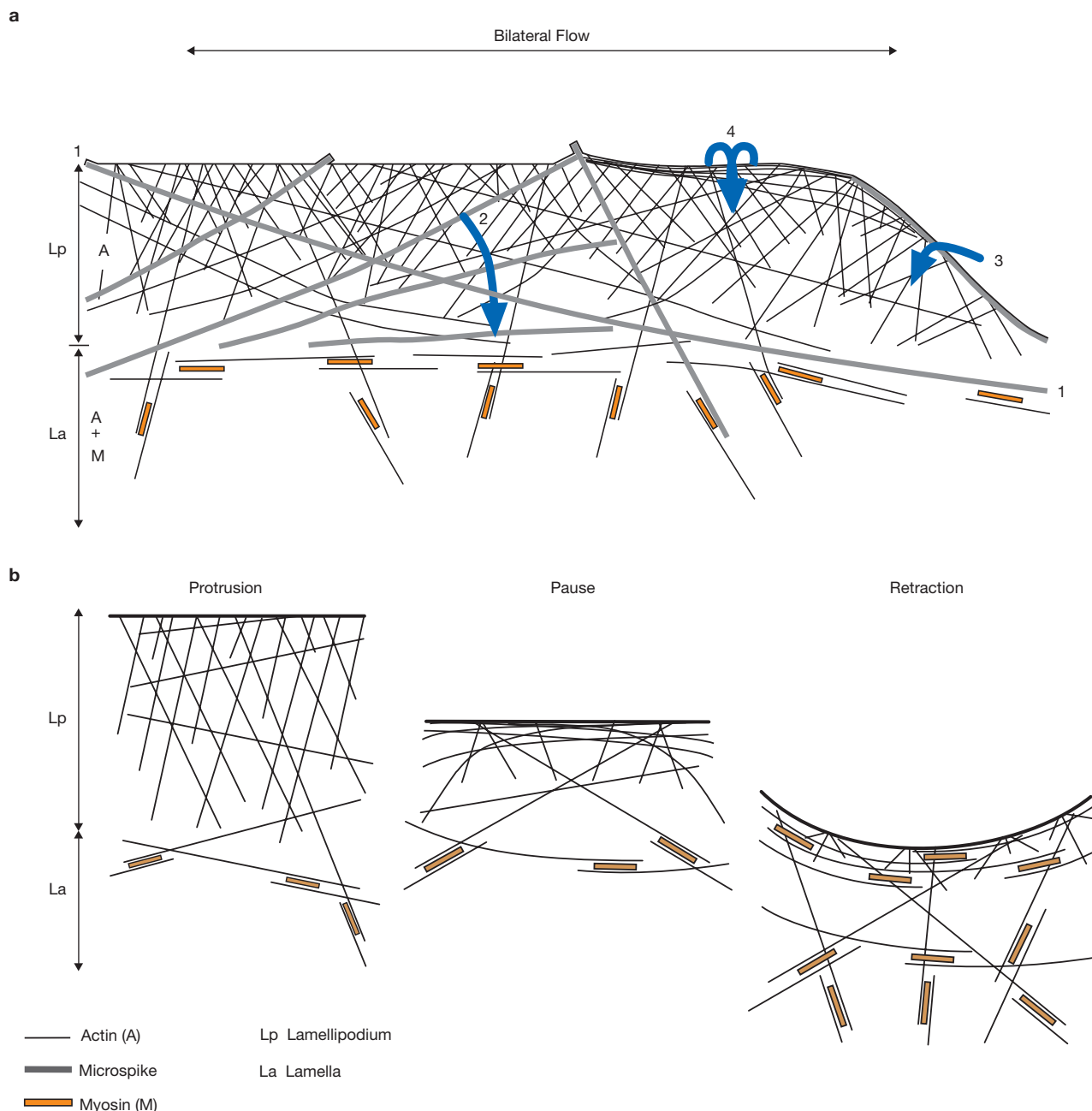
34

a

b

Figure 5 Filament reorganization during protrusion, pause and retraction. (**a**) Model of actin filament and microspike reorganization within the lamellipodium and their contribution to the lamella. Lp, lamellipodium, containing actin (A) and associated proteins; La, lamella, containing actin, associated proteins and myosin (A + M). Myosin filaments are depicted by orange bars. The variable orientation of individual filaments (black lines) and filament bundles (microspikes; thick, grey lines) results in a variable, bilateral component of polymerization of filament plus-ends along the front edge of the lamellipodium. Models: 1) marks the two ends of a long microspike bundle that contributes actin filaments directly to the lamella; 2) a microspike translating to the right is arrested by a more radial microspike — it dissociates from the cell edge and moves with retrograde flow into the lamella; 3) a microspike bundle can lead a ruffle that propagates laterally along the lamellipodium; 4) a ruffle folding rearwards from the front can generate bundles at the base of the lamellipodium. Myosin engages with the subpopulation of anti-parallel actin filaments generated through bilateral flow, which survives the depolymerization

activity of cofilin and other factors present in the lamellipodium. This filament population contributes to the construction of the lamella. (**b**) Scheme of transitions from protrusion to retraction. During persistent protrusion, the orientation of filaments is distributed preferably around higher angles to the cell front, with predominantly linear filaments. Slowing and pause are associated with a variable local reduction in actin polymerization rate at filament plus-ends and with depolymerization from the rear. The slowest-growing filaments retard protrusion and faster growing filaments turn more laterally, adopting curved trajectories. As pause persists, the longer filaments at low angles increase in proportion, due to the preferential loss of the shorter filaments at high angles by depolymerization. Retraction is associated with the recruitment of myosin into the peripheral actin bundle and through linkage of actin filaments into contractile assemblies of the lamella network. The contractile bundle is anchored at both ends into adhesion foci that developed during retraction (not shown). Microspikes also contribute filaments directly to retracting edges (Supplementary Information, Fig. S3a and Movie 3a).

METHODS

Correlated light and electron microscopy. The technique used for correlated light and electron microscopy is described in detail elswhere[1]. In brief, the procedure was as follows. Formvar films cast on a glass slide were floated on a water surface and coverslips (22 × 30 mm) were placed on the film, retrieved on Parafilm and dried. A grid pattern was then embossed on the film by evaporation of gold through tailor-made masks placed on the coverslips. The transfected cells were plated on coverslips coated with laminin (B16) or fibronectin (MTLn3). After video microscopy and fixation, the coverslips were transferred to a 9-cm Petri dish filled with cytoskeleton buffer (CB, 10 mM MES, 150 mM NaCl, 5 mM EGTA, 5 mM glucose, 5 mM $MgCl_2$; pH 6.1) and the film gently peeled off the coverslip with forceps. The film was then inverted and brought to the buffer surface to spread out under surface tension. Under a dissecting microscope, the film was floated on a stainless-steel ring platform and liquid removed until the film was immobilized, with the grid pattern centred. An electron microscopic grid (50 mesh hexagonal, copper) was then placed on the film with the central hole over the region containing the cell of interest. For this manipulation, the grid was mounted in forceps held in a modified Leica dual-pipette holder to allow controlled release, with the pipette holder mounted on a Narashige micromanipulator. The film was then floated off the stand by addition of buffer, recovered with a piece of parafilm, rinsed with negative stain solution and dried on the cell side. The negative stain was composed of a mixture of sodium silicotungstate (2%; Agar Scientific) and aurothioglucose (1%; Wako Chemicals), pH 7.0. Cells were observed and imaged immediately in the electron microscope (FEI Morgagni).

Cells, constructs and transfection. B16-F1 mouse melanoma cells were maintained as described previously[2] and transiently transfected using Fugene 6 (Roche), according to the manufacturer's instructions. Cells were transfected with pEGFP–β-actin (BD Biosciences); actin fused to Ruby, a monomeric RFP variant[3]; a mixture of pEGFP–actin and mCherry–VASP; or a mixture of mCherry–actin and PA–GFP–actin. mCherry–VASP was generated by exchanging EGFP in EGFP–VASP[4,5], an improved version of mRFP, kindly provided by Roger Tsien (University of California, San Diego, CA). PA–GFP–actin was made by exchanging EGFP in pEGFP–β-actin (Clontech) for PA–GFP, kindly provided by George Patterson and Jennifer Lippincott-Schwartz (National Institutes of Health, Bethesda, MD). mCherry–actin was kindly provided by Malgorzata Szczodrak (Helmholz Centre for Infection Research, Braunschweig, Germany). The myosin light chain GFP construct and Ruby construct were kindly provided by Rex Chisholm (Nothwestern University, Chicago IL) and Annette Muller-Taubenberger (Ludwig Maximillian University, Munich, Germany), respectively. Carcinoma MTLn3 cells were kindly provided by Jeff Segall (Albert Einstein College of Medicine, New York, NY) and Bob van de Water (Amsterdam Center for Drug Research, Leiden, The Netherlands) and maintained in α-MEM containing ribonucleosides and deoxyribonucleosides, 5% fetal bovine serum (Sigma) and penicillin/streptomycin.

Live-cell imaging and fixation. For light microscopy, the film-coverslip combination carrying the cells was mounted in a home made plexiglass flow-through chamber that fitted on a temperature-controlled heating platform (Harvard Instruments). The chamber (40 × 20 × 8 mm) featured two syringe needles glued into each end that connected to a central channel (0.5 mm deep) between the filmed coverslip on the base and an upper, round coverslip glued to a central depression in the chamber.

Imaging was performed on a Zeiss Axiovert 200M inverted microscope equipped with a rear-illuminated, cooled CCD camera (Micromax or Cascade, Roper), together with a filter wheel and shutters controlled with Metamorph software. Halogen lamps were used for imaging in both the phase contrast and fluorescence channels. Images were collected in one or two fluorescent channels and in phase contrast, with 8–15 s between frames (see legends).

Cells were fixed at the end of a selected video sequence by sucking the fixative/detergent mixture through the chamber. For B16 cells, the composition of the mixture was: 0.5% Triton, 0.25% glutaraldehyde in CB, with phalloidin (1 µg ml⁻¹) added. For MTLn3 cells, the procedure was the same but with 0.25% Triton and 1% glutaraldehyde. An initial fixation of 2 min in this mixture was followed by a post-fixation in 2% glutaraldehyde (in CB containing 1 µg ml⁻¹ phalloidin) for 5–10 min. Final fluorescence images of the selected cell were recorded during the initial fixation period. The coverslip was removed from the chamber and stored in CB containing 2% glutaraldehyde and 10 µg ml⁻¹ phalloidin at 4 °C until processing for electron microscopy.

For acquisition of the images displayed in Supplementary Information, Fig. S5a–d and Movie 3, cells were maintained in an open heating chamber (Warner Instruments) at 37 °C, on an inverted microscope (Axiovert 100TV, Zeiss) equipped with a rear-illuminated CCD camera (TE/CCD-1000 TKB, Princeton Instruments) driven by IPLab software (Scanalytics). Images were collected with a time between frames of 12.5 s (Supplementary Information, Fig. S3a) or 18 s (Supplementary Information, Fig. S3b–d).

Experiments with photoactivation of fluorescence were performed on cells co-transfected with PA–GFP–actin and mCherry–actin, using a Zeiss LSM510 laser scanning confocal microscope equipped with argon and helium-neon lasers for fluorescence observation and a diode-UV laser for photoactivation.

Image analysis and processing. Electron micrographs were processed in ImageJ using a bandpass filter to equalize the staining density and enhance filament contrast. For filament counts and angle measurements, a line of 1 µm (B16 cells) or 0.5 µm (MTLn3 cells) was drawn parallel to the cell edge using Adobe Photoshop; filaments crossing this line were overlaid with short lines and the angles between these lines and the cell edge measured in Photoshop.

Fluorescence intensities were measured with the linescan tool of Metamorph (Molecular Devices). For velocity measurements, sequential GFP–actin images were processed with the 'detect edges' filter in Metamorph. The position of the peak value of a line scan across the lamellipodium was used to define the position of the cell edge and the velocity was calculated from one frame to the next. Regression curves were drawn with Microsoft Excel.

Note: Supplementary Information is available on the Nature Cell Biology website.

1. Abercrombie, M., Heaysman, J. E. & Pegrum, S. M. The locomotion of fibroblasts in culture. II. 'Ruffling'. *Exp. Cell Res.* **60,** 437–444 (1970).
2. Ponti, A., Machacek, M. S., Gupton, L., Waterman-Storer, C. M. & Danuser, G. Two distinct actin networks drive the protrusion of migrating cells. *Science* **305,** 1782–1786 (2004).
3. Svitkina, T. M. & Borisy, G. G. Arp2/3 complex and actin depolymerizing factor/cofilin in dendritic organization and treadmilling of actin filament array in lamellipodia. *J. Cell Biol.* **145,** 1009–1026 (1999).
4. Small, J. V., Stradal, T., Vignal, E. & Rottner, K. The lamellipodium: where motility begins. *Trends Cell Biol.* **12,** 112–20 (2002).
5. Small, J. V., Isenberg, G. & Celis, J. E. Polarity of actin at the leading edge of cultured cells. *Nature* **272,** 638–639 (1978).
6. Small, J. V., Herzog, M. & Anderson, K. Actin filament organization in the fish keratocyte lamellipodium. *J. Cell Biol.* **129,** 1275–1286 (1995).
7. Pollard, T. D. & Borisy, G. Cellular motility driven by assembly and disassembly of actin filaments. *Cell* **112,** 453–465 (2003).
8. Pollard, T. D. Regulation of actin filament assembly by arp2/3 complex and formins. *Annu. Rev. Biophys. Biomol. Struct.* **36,** 451–477 (2007).
9. Heath, J. P. & Holifield, B. F. On the mechanisms of cortical actin flow and its role in cytoskeletal organisation of fibroblasts. *Symp. Soc. Exp. Biol.* **47,** 35–56 (1993).
10. Rottner, K., Behrendt, B., Small, J. V. & Wehland, J. VASP dynamics during lamellipodia protrusion. *Nature Cell Biol.* **1,** 321–322 (1999).
11. Condeelis, J. & Segall, J. E. Intravital imaging of cell movement in tumours. *Nature Rev. Cancer* **3,** 921–930 (2003).
12. Small, J. V. & Resch, G. P. The comings and goings of actin: coupling protrusion and retraction in cell motility. *Curr. Opin. Cell Biol.* **17,** 517–523 (2005).

36

13. Medeiros, N. A., Burnette, D. T. & Forscher, P. Myosin II functions in actin-bundle turnover in neuronal growth cones. *Nature Cell Biol.* **8,** 215–226 (2006).

14. Small, J. V. The actin cytoskeleton. *Electron Microsc. Rev.* **1,** 155–174 (1988).

15. Abraham, V. C., Krishnamurthi, V., Taylor, D. L. & Lanni, F. The actin-based nanomachine at the leading edge of migrating cells. *Biophys. J.* **77,** 1721–1732 (1999).

16. Kozlov, M. M. & Bershadsky, A. D. Processive capping by formin suggests a force-driven mechanism of actin polymerization. *J. Cell Biol.* **167,** 1011–1017 (2004).

17. Carlier, M. F. & Pantaloni, D. Control of actin assembly dynamics in cell motility. *J. Biol. Chem.* **282,** 23005–23009 (2007).

18. Mogilner, A. On the edge: modeling protrusion. *Curr. Opin. Cell Biol.* **18,** 32–39 (2006).

19. Fisher, G. W., Conrad, P. A., DeBiasio, R. L. & Taylor, D. L. Centripetal transport of cytoplasm, actin, and the cell surface in lamellipodia of fibroblasts. *Cell Motil. Cytoskeleton* **11,** 235–247 (1988).

20. Vallotton, P., Danuser, G., Bohnet, S., Meister, J. J. & Verkhovsky, A. B. Tracking retrograde flow in keratocytes: news from the front. *Mol. Biol. Cell* **16,** 1223–1231 (2005).

21. Hotulainen, P. & Lappalainen, P. Stress fibers are generated by two distinct actin assembly mechanisms in motile cells. *J. Cell Biol.* **173,** 383–394 (2006).

22. Blanchoin, L., Pollard, T. D. & Hitchcock-DeGregori, S. E. Inhibition of the Arp2/3 complex-nucleated actin polymerization and branch formation by tropomyosin. *Curr. Biol.* **11,** 1300–1304 (2001).

23. Pollard, T. D., Blanchoin, L. & Mullins, R. D. Actin dynamics. *J. Cell Sci.* **114,** 3–4 (2001).

24. Amann, K. J. & Pollard, T. D. Direct real-time observation of actin filament branching mediated by Arp2/3 complex using total internal reflection fluorescence microscopy. *Proc. Natl Acad. Sci. USA.* **98,** 15009–15013 (2001).

25. Mullins, R. D., Heuser, J. A. & Pollard, T. D. The interaction of Arp2/3 complex with actin: nucleation, high affinity pointed end capping, and formation of branching networks of filaments. *Proc. Natl Acad. Sci. USA.* **95,** 6181–6186 (1998).

26. Resch, G. P., Goldie, K. N., Hoenger, A., & Small, J. V. Pure F-actin networks are distorted and branched by steps in the critical-point drying method. *J. Struct. Biol.* **137,** 305–312 (2002).

27. Medalia, O., Weber, I., Frangakis, A. S., Nicastro, D., Gerisch, G. & Baumeister, W. Macromolecular architecture in eukaryotic cells visualized by cryoelectron tomography. *Science.* **298,** 1209–1213 (2002).

28. Gupton, S. L. *et al.* Cell migration without a lamellipodium: translation of actin dynamics into cell movement mediated by tropomyosin. *J. Cell Biol.* **168,** 619–631 (2005).

29. Giannone, G. *et al.* Lamellipodial actin mechanically links myosin activity with adhesion-site formation. *Cell* **128,** 561–575 (2007).

30. Hebert, B., Costantino, S. & Wiseman, P. W. Spatiotemporal image correlation spectroscopy (STICS) theory, verification, and application to protein velocity mapping in living CHO cells. *Biophys. J.* **88,** 3601–3614 (2005).
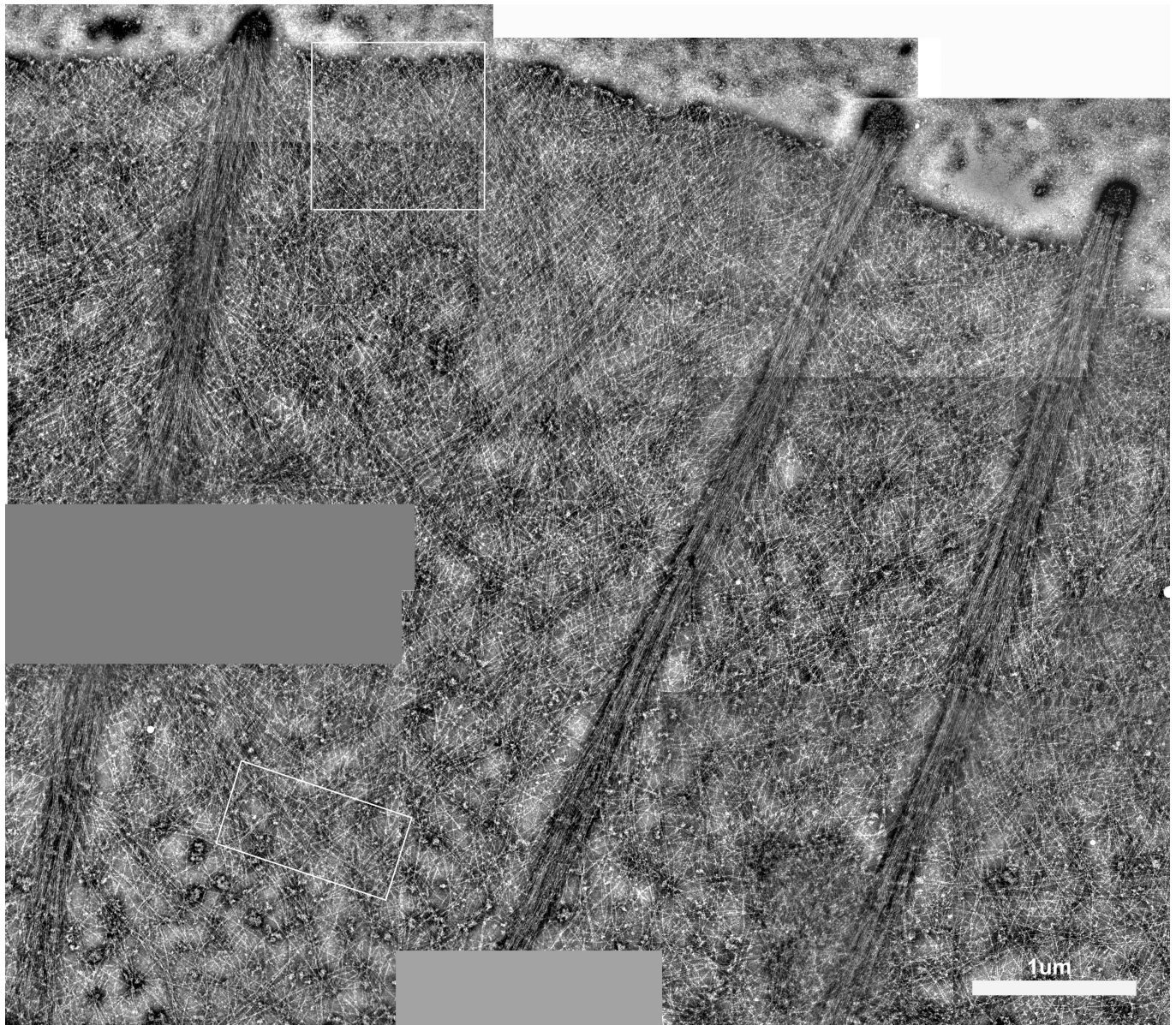
Figure S1 Electron micrograph overview of the region corresponding to Fig. 1c, with the positions of Figs. 2a and b boxed.
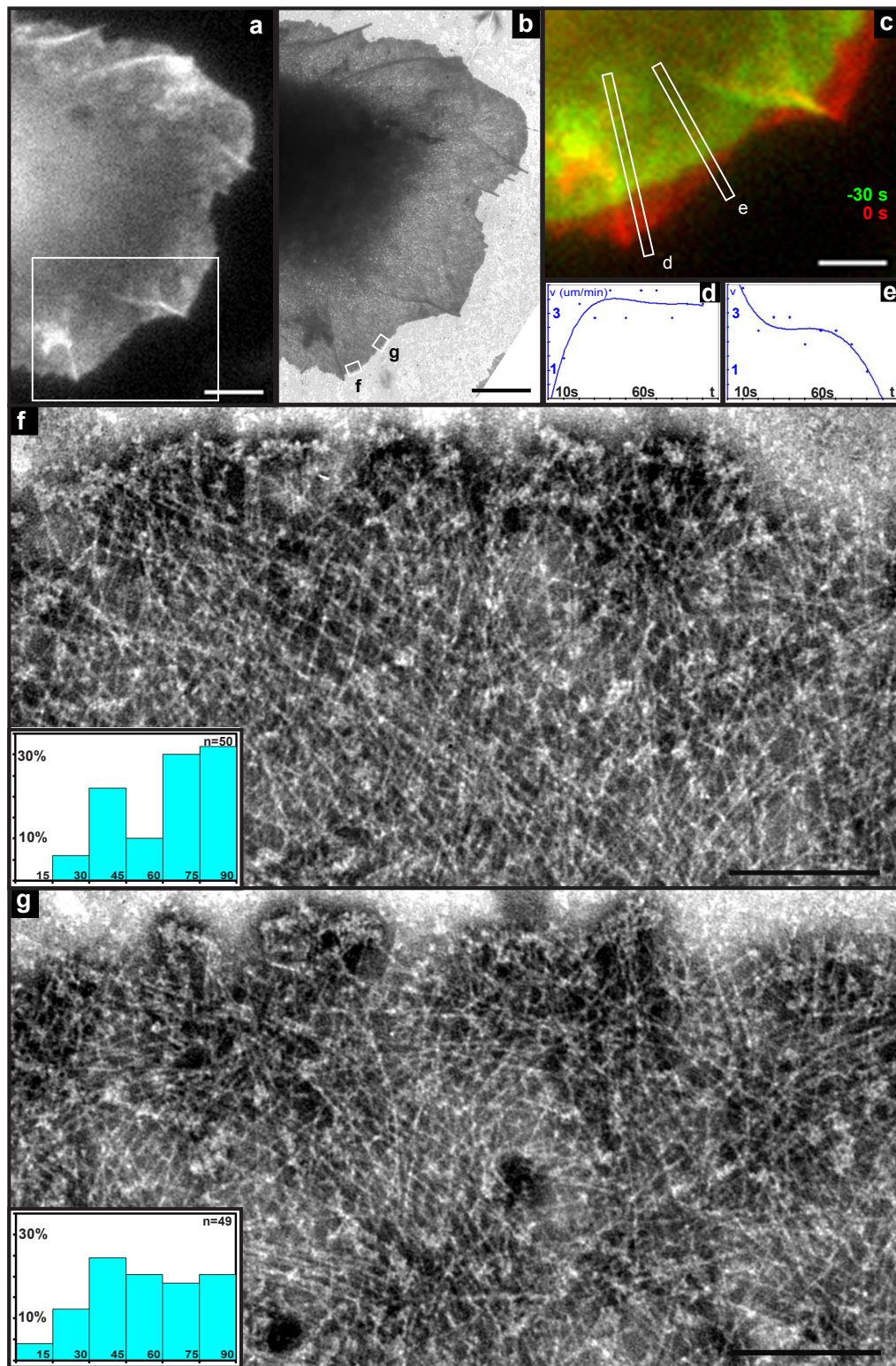
Figure S2 Transition from protrusion to pause in MTLn3 cell lamellipodia. a, video frame, prior to fixation, of an MTLn3 cell transfected with EGFP-actin. b, overview of the fixed and stained cell in the electron microscope. c, region of the cell boxed in a, with the last video frame before fixation (red) overlayed with the frame 30 seconds before (green) to show the relative degrees of protrusion along the lamellipodium segment. d and e show the velocity traces of the cell edge for the corresponding positions marked in "c" by the white rectangles. f and g, electron micrographs of the positions shown in the overview b and corresponding to the cell edge positions d and e in c. Histograms in f and g show the angular distribution of filaments measured at 200 nm from the cell edge. Counts were made along 0.5 μm lines drawn parallel to the cell edge, to avoid overlap with adjacent zones. Bars, a,b, 5 μm; c, 3 μm; f, g, 200 nm.
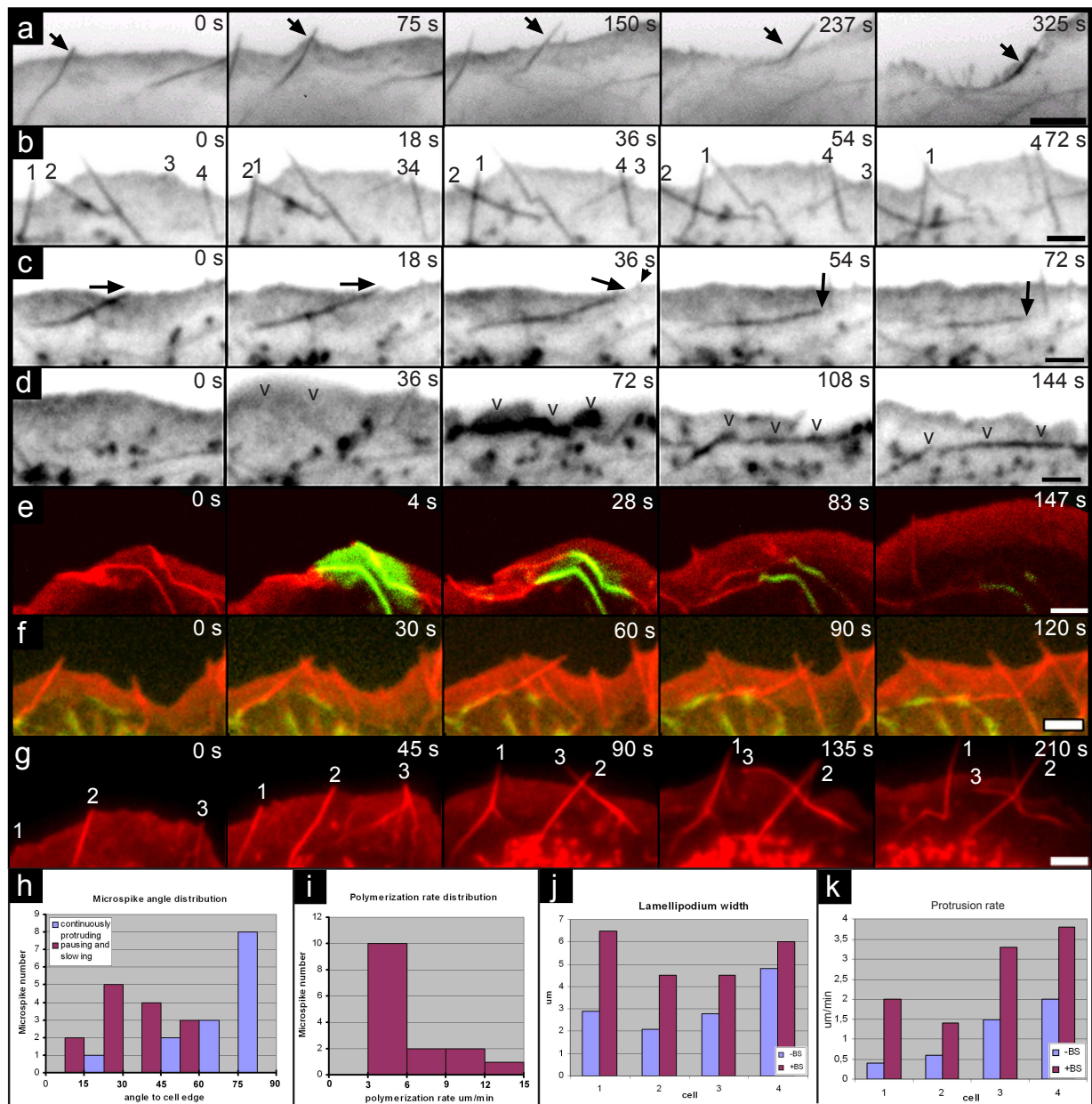
39

Figure S3 Bi-lateral flow of microspike bundles along the lamellipodium results in the contribution of bipolar arrays of actin filaments to the lamella. a. Video sequence of a lamellipodium segment of a B16 melanoma cell transfected with actin-GFP showing contribution of a laterally translating microspike to the construction of a retracting edge that forms in the last frame (arrow). This and the following sequences (b-d) are shown in negative contrast. All times are in seconds. Bar, 4 µm. b-d, selected frames of video sequences of the same region of a B16 melanoma cell expressing Ruby-actin. b shows two pairs of microspike bundles (numbered 1-4) crossing during the sequence (at 18 and 36 s). c, the tip of a laterally translating, long microspike (arrow) is stopped by a small radial microspike at 36 s (arrowhead), leading to dissociation of the long microspike from the lamellipodium tip and retrograde flow of the remaining bundle to the base. d, generation of an actin bundle parallel to the base of the lamellipodium (144 s) from a ruffle (v) that folds rearwards from the front (36-108 s), without a microspike. Bars, 2 µm. e. Lamellipodium segment of a B16 melanoma cell transfected with mCherry-actin and photoactivatable GFP-actin. The PA-GFP was photoactivated at 4 s. Note contribution of microspike bundles to the lamella as well as the continued turnover of actin. The time between frames after photoactivation was 8 s. Bar, 3 µm. f. Engagement of

myosin at base of lamellipodium. Selected video frames of B16 melanoma cell expressing mCherry-actin and GFP-myosin regulatory light chain. Note again bi-lateral translation of microspike bundles and their contribution to bundles at the base of the lamellipodium, where myosin is recruited. Bar, 3 µm. g. Myosin is not required for the lateral translation of microspikes. Frames of a video sequence of a B16 melanoma cell expressing mCherry-actin that was treated with 50 µM blebbistatin. Numbers indicate translating microspikes; time in seconds; bar, 3µm. h, i. Angular distribution and growth rate of microspikes in B16 melanoma cells. h, comparison of microspike angles (to the cell edge) in pausing or slowing cells (purple bars) as compared to fast moving cells (blue bars). 14 microspikes each measured in 5 slow cells and 3 fast cells. i, distribution of actin polymerization rates in microspikes measured using photoactivatable GFP-actin in cells co-transfected with mCherry-actin (as for e). The rate was determined from the extension of microspikes from the point of photoactivation. j, k. Data from 4 cells on the effect of 50-100 µM blebbistatin (BS) on lamellipodium width and protrusion rate in B16 melanoma cells. Within 2-10 minutes of blebbistatin treatment, the extended width of the lamellipodium increased by 15-100% (j) and the protrusion rate by at least two fold (k)

SUPPLEMENTARY INFORMATION

Supplementary movie legends

Movie S1 Video Fig.1, including actin-GFP image after fixation. Time between frames was 8s.

Movie S2 Video Fig.3. Time between frames was 8s.

Movie S3 Video Fig. S5.

Movie S4 Simulation of slowing, pause and retraction in a lamellipodium. During slowing to pause, filaments show a varied reduction in polymersation rate (red and yellow plus ends), resulting in the faster filaments (red) adopting curved trajectories, culminating in a subpopulation of filaments parallel to the cell edge. Slower polymerising filaments (yellow to green) act as tethers and restrain protrusion. Shorter filaments at high angles depolymerise first, leaving longer filaments in antiparallel arrays to recruit myosin (orange bars) for retraction. Microspike bundles also contribute filaments to retracting edges (not depicted).

Supplementary references

1. Auinger, S., and J.V. Small. 2007. Correlated light and electron microscopy of the actin cytoskeleton. *Methods in Cell Biology*. in press.
2. Rottner, K., B. Behrendt, J.V. Small, and J. Wehland. 1999. VASP dynamics during lamellipodia protrusion. *Nat Cell Biol*. 1:321-2.
3. Muller-Taubenberger, A., M.J. Vos, A. Bottger, M. Lasi, F.P. Lai, M. Fischer, and   K. Rottner. 2006. Monomeric red fluorescent protein variants used for imaging studies in different species. *Eur J Cell Biol*. 85:1119-29.
4. Carl, U.D., Pollmann, M, Orr, E., Gertler, F.B., Chakraborty, T and Wehland, J. 1999. Aromatic and basic residues within the EVH1 domain of VASP specify its interaction with proline-rich ligands. Curr. Biol. 9:715-8.
5. Shaner, N.C., Campbell, R.E., Steinbach, P.A., Giepmans, B.N.G., Palmer, A.E. and Tsien, R.Y. 2004. Improved monomeric red, orange and yellow fluorescent proteins derived from *Discosoma* sp. red fluorescent protein. Nature Biotechnology 22:1567-72.

Discussion

First I want to briefly introduce my view of the regulation of lamellipodial structure and dynamics, including some new suggestions, and will then discuss some points in more detail, also in relation to the current dendritic nucleation model. As a basis for discussion, I present in Fig. 3 a hypothetical scheme of events leading to the generation of the actin network.
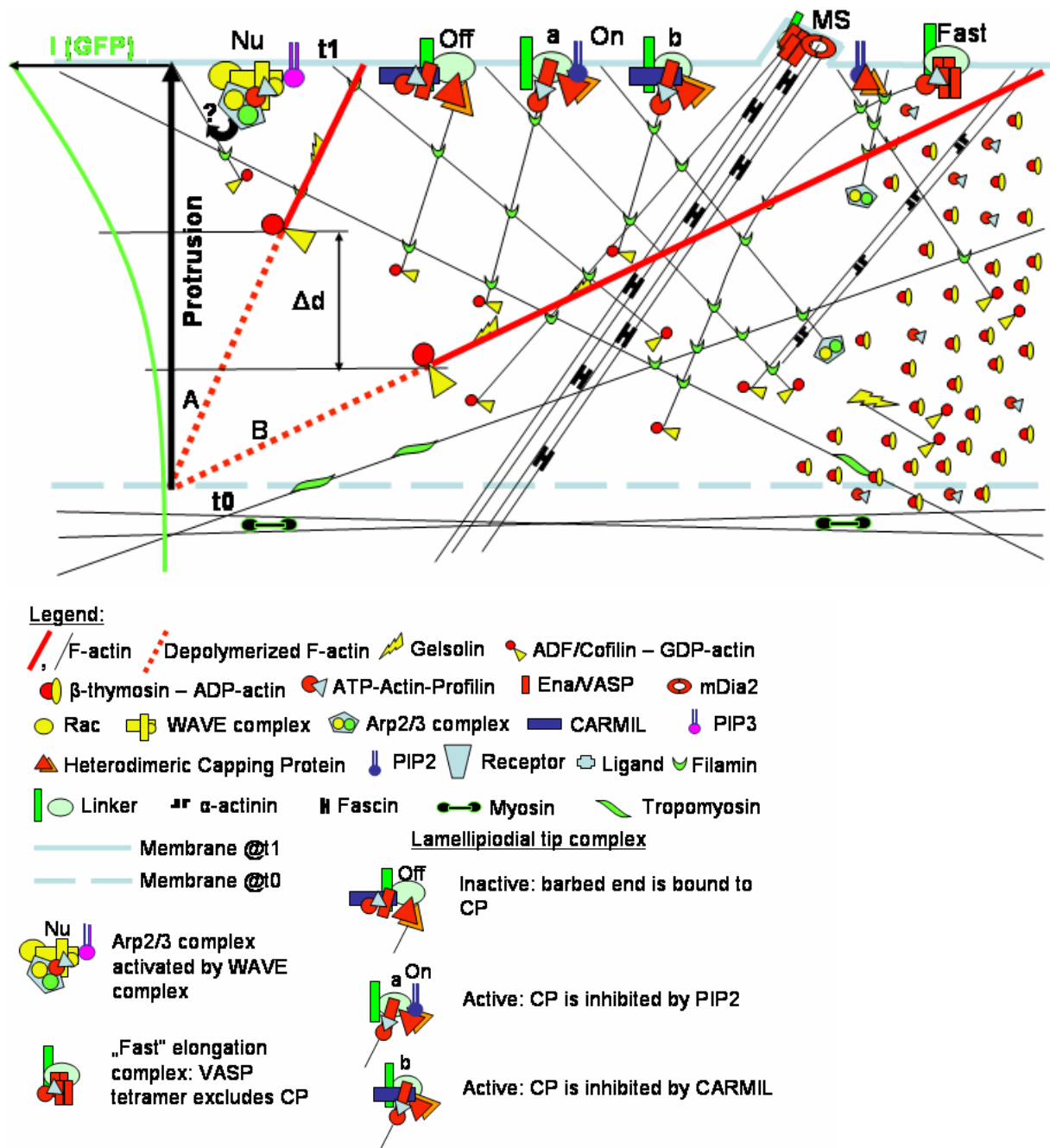

Figure 3: Hypothetical scheme of lamellipodia structure and dynamics. Not drawn to scale. For details, see text.

Coordinating birth, life and death of a filament.

According to the scheme, new filaments are initiated by the WAVE complex which activates the Arp2/3 complex and recruits the first actin monomer, thereby speeding up the rate-limiting step (nucleation- Nu). Whether or not this occurs on the side of an existing filament is a matter of debate (hence the "?" – see below). In any case the Arp2/3 complex may serve as a pointed-end capping protein, protecting the filaments from depolymerization. With this model I suggest, that elongation of a filament takes place at a lamellipodial elongation complex consisting of elongation promoting and inhibiting factors. The promoting factor could be Ena/VASP, the inhibiting factor heterodimeric capping protein (CP). CP binds barbed ends to inhibit elongation (Off) and is displaced by binding to PIP2 (On, a) or CARMIL (On, b). The proximity of components in the complex enables fast binding-unbinding and facilitates control. Tetramerization of Ena/VASP leads to exclusion of CP and to fast processive polymerization (Fast; (Breitsprecher et al.), which can lead to curved filament trajectories in regions held back by more slowly growing filaments. Tetramerization of VASP and filament clustering can lead to the formation of microspikes and filopodia either by recruitment of lamellipodial filaments or possibly in a cooperative fashion together with nucleation and elongation by mDia2. The lamellipodial network is stabilized by cross-linkers like filamin and alpha-actinin and microspike/filopodia bundles with e.g. fascin. Depolymerization by ADF/Cofilin from the pointed end takes place after severing, which may also be performed by gelsolin, which also caps the barbed end of the severed fragment to block polymerization. ADF/cofilin competes with β-thymosin and profilin for ADP-actin. Profilin exchanges ADP with ATP on G-actin and provides the lamellipodial elongation complex, Ena/VASP and mDia2 with ATP-actin to feed polymerization. The dashed lines of filaments A and B indicate the depolymerized filament length during a random time interval (assuming equivalent rates) and d the difference in the net distance depolymerized towards the edge. Long, low angled filaments may survive, aided by binding of tropomyosin, and contribute to the generation of contractile arrays of antiparallel actin filaments with myosin in the lamella (see also below).

How much nucleation occurs after a lamellipodium is formed? In principal it would be enough to nucleate a fixed number of filaments and elongate them to drive protrusion

without significant de-novo assembly (Brieher et al., 2006). New filaments only have to be generated to replace those that are lost by lateral flow or by depolymerization. Arp2/3 complex is indeed incorporated at the leading edge with a similar rate as actin suggesting constant nucleation (Lai et al., 2008). But the relative contributions of elongation and nucleation in an established, constantly protruding lamellipodium remain to be shown. Experimental protocols devised to specifically block Arp2/3 or formin activity during imaging of protrusion events are required to answer this question.

Dendritic array or crosslinked filaments?

Is nucleation of new filaments by the Arp2/3 complex linked to branching? The direct observation of branches growing off single filaments under the microscope in-vitro suggests that branching can take place. The argument, that by branching the new filament is directly incorporated into the network and can thereby immediately take part in exerting its force onto the membrane is intuitively attractive. Recent structural analysis combined with modelling could fit the Arp2/3 complex into a branch, even though the mother filament had to be twisted in an unfavourable way. But how close are in-vitro studies to the actual process inside the cell? The advantage that the number of proteins that take part in the reaction in vitro is well defined goes hand in hand with the drawback that many components of the in vivo machinery are lacking. In addition, the in vitro concentrations are completely different from those inside the lamellipodium. The nucleation, polymerization and probably also the capping reactions take place close to the membrane of the cell – a situation not yet mimicked in vitro. One complication with the in vitro assays is the use of phalloidin as an actin marker. Recent experiments by a strong proponent of the branching idea have shown that actin branching by Arp2/3 is potentiated by phalloidin, which binds Arp subunits in addition to F-actin (Mahaffy and Pollard, 2008).

The evidence for branches in the lamellipodium is also questionable, since the primary evidence comes from electron micrographs of cells that were prepared with the critical point drying method, which has been shown to introduce branches into samples of pure F-actin (Resch et al., 2002). Despite the weak evidence for branched actin filaments in cells (Small et al., 2008) the "dendritic branching" model

has become dogma, so much so that it is cited in all reviews on cell motility and has entered current textbooks.

What are the implications of the dendritic nucleation model? According to this model new filaments are nucleated on the side of existing ones in a 70° angle at a spacing of 20 – 50 nm along the actin filament (Svitkina and Borisy, 1999). Nucleation is suggested to occur in bursts of ¼ of a second (Pollard et al., 2000), until a filament incorporating around 200 monomers (about 600 nm long) is capped by heterodimeric capping protein, (Pollard et al., 2000). We did not find any evidence however for a major contribution of filaments in this length range at the front. A further discrepancy between the dendritic nucleation model and the experimental data is also given by the localization of heterodimeric capping protein (CP): In the dendritic nucleation model elongation is terminated by binding of CP to the barbed ends away from the front of the lamellipodium. From this it would be expected to find CP all over the lamellipodium. Instead, its localization is restricted to the lamellipodium tip (Lai et al., 2008).

In paper 2 we show, that the lamellipodium consists of filaments of varying lengths and, more importantly, in practically all angles, without any obvious branches. We also provide a model for the rearrangement of filaments during slowing, pause and retraction. One consequence of these rearrangements is the production of antiparallel filaments which can form contractile bundles with myosin II after translocation into the lamella. The structural model emerging from our studies is inconsistent with a highly branched network.

As Pollard himself states "… false or questionable conclusions have become beliefs through repetition in print rather than confirmation in the laboratory" (Pollard, 2007).

-                    -   -

Regulating actin turnover

How are elongation rates modulated in the lamellipodium and what is the role of capping protein, which is found concentrated at the lamellipodium tip (Lai et al., 2008;

Mejillano et al., 2004). In the absence of any control of polymerisation, the high endogenous concentration of G-actin in lamellipodia (paper 1) would lead to very high polymerization rates, calculated as 1000 monomers or 3 µm per second (at 100 µM) based on the rate constants derived for actin in vitro (Pollard et al., 2000). A tight regulation of protrusion rates must therefore operate in lamellipodia, presumably involving both elongation promoting and inhibiting factors. Several observations point towards the existance of a "lamellipodial elongation complex": In electron micrographs unidentified material is found at the barbed ends of all filaments under weak extraction conditions (own observations). Several factors, including Ena/VASP, WAVE complex components and Capping Protein (CP) are localized at the tip of the lamellipodium (Hahne et al., 2001; Lai et al., 2008; Mejillano et al., 2004; Rottner et al., 1999; Stradal et al., 2001), and Arp2/3 is incorporated at the same site(Lai et al., 2008). It has also been shown that the lamellipodium tip poses a lipid diffusion barrier in the membrane indicating an accumulation of protein complexes, most likely anchored to actin filaments (Weisswange et al., 2005). According to the dendritic nucleation model the function of CP is the termination of short bursts of elongation. Additionally it was suggested, that the function of CP is also to quickly cap filaments that branch in unproductive directions (backwards; (Schaus et al., 2007). The disadvantage of regulating elongation by capping protein alone is that it would lead to intermittent bursts of polymerisation, which seems unlikely. In this scenario, some kind of capping clutch would be required to give a smooth variation in protrusion rate. Here I suggest a variation in the function of capping protein: the elongation rate could be modulated by a transient binding of capping protein to barbed ends (Figure: Off), with dissociation promoted by binding to PIP2 (On a) or CARMIL (On b) (Huang et al., 2006; Kim et al., 2007; Wear et al., 2003). Candidates for positive regulation of elongation are Ena/VASP proteins. VASP binds actin filaments, recruits profilin-actin and has been shown to increase the protrusion rate of actin-based mimetic models in vitro. In lamellipodia, the amount of GFP-VASP at the tip increases proportionally with protrusion rate (Rottner et al., 1999). When attached to beads, VASP enhances the polymerization rate of actin and at high surface concentrations protects barbed ends from capping (Breitsprecher et al.). Filaments protected from capping in this way could be those that continue to elongate fast during slowing and therefore have to reorient towards lower angles (see curved "Fast" filament in Figure,). The different filament angles in lamellipodia imply a varying elongation rate, which could involve

additional regulation by orientation dependent feedback mechanisms: The lower the filament angle the less force is exerted onto the membrane by insertion of a monomer, thereby enabling VASP a higher insertion rate, and on the other hand giving CP more space to wobble and rendering it more likely to be displaced from the barbed end by antagonists like CARMIL (Uruno et al., 2006).

Reorganising the web.

Filaments in the lamellipodium are oriented in a wide range of angles towards the membrane. The mean angle between the filaments and the membrane is about 55° in continuously protruding lamellipodia (paper 2). Since early protrusions show a wide range of filament angles (Figure 4) the convergence towards a mean is probably established by self-organization in order to optimize network stability and the transduction of filament elongation into protrusion. Approximately the same angle, which corresponds to 70° between filaments pointing equally towards the membrane, is also derived for filaments in a mathematical model for lamellipodia in a self organizing system (Mogilner and Oster 1996; (Mogilner and Oster, 1996; Schaus et al., 2007). The stability of the network is probably established by cross-linking proteins, like filamin, which has a flexible spacer region and can link filaments with varying angles to each other.
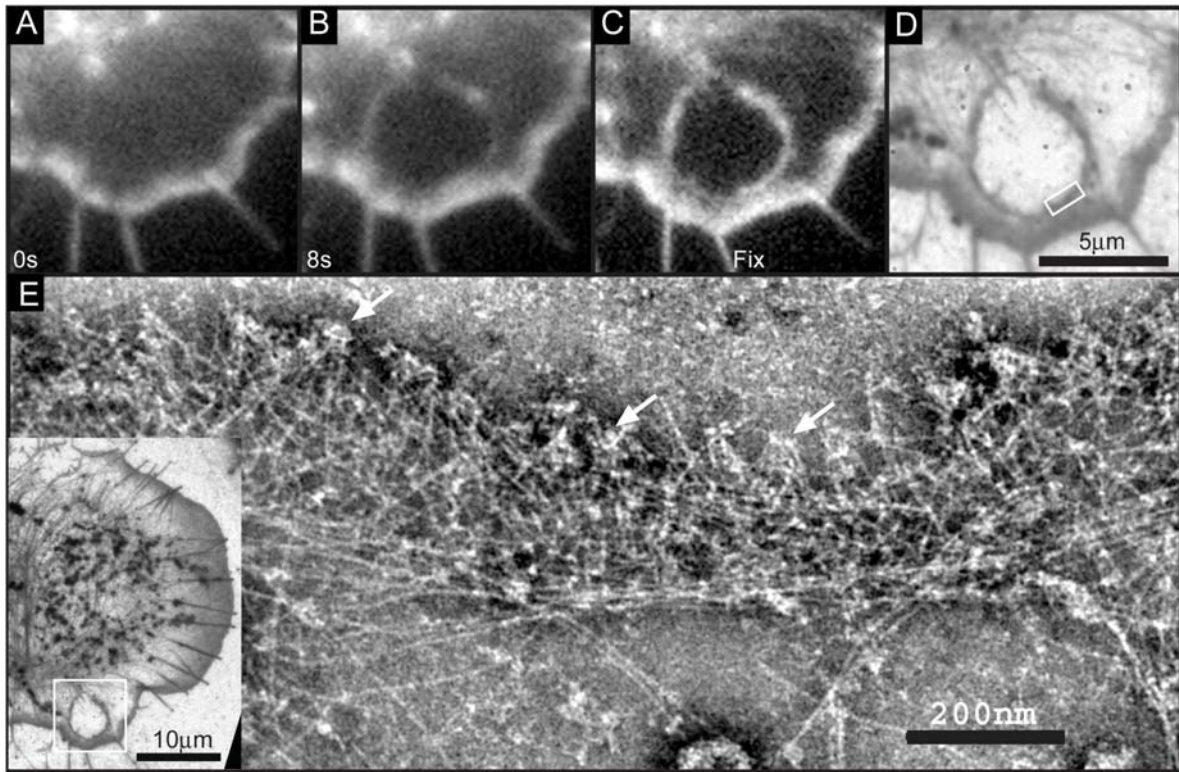
Figure 4: An early protrusion displays a wide range of filament angles. A hole appeared and a lamellipodium started to form at its edge about 5 to 10 s before fixation. A – C: GFP-actin, D: electron micrograph, boxed region of overview in E. E: high magnification of boxed region in D. Note also the tripod-like structures with proteins at the tip, corresponding presumably to sites of polymerization. Inset: overview. A region from the cell in paper 2 figure 1 is shown.

How do elongation/depolymerization and angle distribution influence lamellipodium dynamics?

From paper 2 we conclude that the elongation rate varies with the angle that the filaments make with the membrane, namely that a steep angle corresponds to a low elongation rate and vice-versa (In the Figure, compare lengths of filaments indicated as thick red lines, that polymerize for the same time (t0 till t1p)). But what happens at the pointed end? From the equal distribution and recovery after photobleaching of cofilin across the lamellipodium (Lai et al., 2008), it can be assumed that the depoylmerization rate is equal all over the lamellipodium. This leads to the following consequences:

The filaments depolymerize at the pointed ends during the same time frame by equal lengths (dashed lines). Therefore the pointed end of the filament in the steeper angle (A) is closer to the membrane than the pointed end of the filament in a shallower angle (B) (pointed ends are indicated by ADF/cofilin). And this in turn leads to a gradient of filament lengths from the lamellipodium tip to the base, with an increase in the number of filaments at lower angles towards the lamellipodium base. We indeed observe these consequences, by GFP-actin expression and electron microscopy, respectively. When the lamellipodium slows down filaments at steeper angles will be the first ones to be completely depolymerized, since their elongation rate falls earlier below the depolymerization rate. This leads to a shift of the angle distribution towards shallower angles and fewer filaments as protrusion ceases as reported in paper 2.

From a known protrusion rate, together with filament angle distribution and depolymerization rate, it should be possible to estimate the proportional contribution of filaments to the lamella. This could be compared with the filament density change at the lamellipodia/lamella boundary in the electron microscope.

The lamellipodium: pusher or passenger?

From experiments in which cells were injected with tropomyosin it was recently suggested that cells can advance without a lamellipodium (Gupton et al., 2005). Analysis of results from actin speckle microscopy (Ponti et al., 2004) lead the same group to propose that where lamellipodia exist, they surf on top of a lamella beneath. In fluorescent speckle microscopy cells are doped with a small amount of a fluorescently tagged protein of interest, in this case actin. It is assumed that speckles correspond to the polymerized form and that appearance of a speckle indicates polymerization and disappearance depolymerization. Also, the speckles can be tracked. In these studies the lamellipodium was defined by fast-moving short-lived, and the lamella by slowly-moving long-lived speckles. Amazingly enough, slowly-moving long-lived speckles were also found at the front, in the lamellipodium region. Hence the idea that the lamella extends to the front driving protrusion. In paper 2 we already show that the architecture of the lamellipodium leads to a wide range of filament lengths, consistent with a distribution of speckle lifetimes. However, as we must assume from FRAP and pseudo-FLIP experiments, that the network moves

backwards as one with the retrograde flow, we did not have an explanation for the different rates of speckle movement. This was given recently by Vallotton and Small (Vallotton and Small, 2008), who showed by careful comparison with manual tracking that the automatic tracking of Ponti et al (Ponti et al., 2004) erroneously assigned speckles with different velocities. This reassessment of the actin speckle data shows that there is one species of speckles in lamellipodia, arguing against any overlap with the lamella. Our own structural data from electron microscopy is also inconsistent with the lamellipodium surfing on the lamella. The lamella contains antiparallel arrays of actin and myosin filaments and such arrays would be visible as a separate filament network under the lamellipodium meshwork, if they exist. We found no evidence for a second network in our electron microscope images. In the same context, we observed recruitment of myosin II only at the base of the lamellipodium, at the boundary with the lamella. Further, lamellipodia protrusion rates increased transiently on inhibition of myosin II with blebbistatin (Koestler et al., 2008) confirming that myosin II is dispensable for protrusion, as first shown in Dictyostelium (De Lozanne and Spudich, 1987). The proposal (Ponti et al., 2004) that the lamellipodium surfs on a lamella pushing the cell forwards from underneath is not supported by our data.

Prospects

Along with new insights into lamellipodia structure come new questions about the roles of the different molecular players.

What are the components of the lamellipodial tip complexes that are responsible for the initiation and elongation of actin filaments and what is their role in modulating the structure and dynamics of the lamellipodium?

How do the different cross-linking proteins affect the structure of the lamellipodium?

How are the lamellipodial actin filaments incorporated into the lamella network?

What is the relevance of nucleation relative to elongation and what is its actual rate in the lamellipodium of a moving cell?

Does nucleation take place by branching?

What is the role of capping protein?

How is actin filament depolymerisation regulated?

How is the lamellipodium width regulated?

How are early protrusions formed and how is the organization into a highly regular network of a constantly protruding lamellipodium achieved?

What is the function of ruffles and what is the mechanism of their formation?

How is the interplay of all the players coordinated?

Altogether, there are lots of unanswered questions and controversial opinions making this area an exciting field of future research and I am looking excitedly forward to new answers and new questions.

References

Abercrombie, M., J.E. Heaysman, and S.M. Pegrum. 1970a. The locomotion of fibroblasts in culture. 3. Movements of particles on the dorsal surface of the leading lamella. *Exp Cell Res*. 62:389-98.

Abercrombie, M., J.E. Heaysman, and S.M. Pegrum. 1970b. The locomotion of fibroblasts in culture. I. Movements of the leading edge. *Exp Cell Res*. 59:393-8.

Abercrombie, M., J.E. Heaysman, and S.M. Pegrum. 1970c. The locomotion of fibroblasts in culture. II. "RRuffling". *Exp Cell Res*. 60:437-44.

Abraham, V.C., V. Krishnamurthi, D.L. Taylor, and F. Lanni. 1999. The actin-based nanomachine at the leading edge of migrating cells. *Biophys J*. 77:1721-32.

Aizawa, H., Y. Fukui, and I. Yahara. 1997. Live dynamics of Dictyostelium cofilin suggests a role in remodeling actin latticework into bundles. *J Cell Sci*. 110 (Pt 19):2333-44.

Alberts, A.S. 2001. Identification of a carboxyl-terminal diaphanous-related formin homology protein autoregulatory domain. *J Biol Chem*. 276:2824-30.

Aspenstrom, P., A. Fransson, and J. Saras. 2004. Rho GTPases have diverse effects on the organization of the actin filament system. *Biochem J*. 377:327-37.

Axelrod, D., D.E. Koppel, J. Schlessinger, E. Elson, and W.W. Webb. 1976. Mobility measurement by analysis of fluorescence photobleaching recovery kinetics. *Biophys J*. 16:1055-69.

Blikstad, I., F. Markey, L. Carlsson, T. Persson, and U. Lindberg. 1978. Selective assay of monomeric and filamentous actin in cell extracts, using inhibition of deoxyribonuclease I. *Cell*. 15:935-43.

Bray, D. 1992. Cell Movements. Garland Publishing, Inc., New York & London.

Bray, D., and C. Thomas. 1976. Unpolymerized actin in fibroblasts and brain. *J Mol Biol*. 105:527-44.

Breitsprecher, D., A.K. Kiesewetter, C. Urbanke, G.P. Resch, J.V. Small, and J. Faix. Clustering of VASP Actively Drives Processive, WH2 Domain-Mediated Actin Filament Elongation.

Brieher, W.M., H.Y. Kueh, B.A. Ballif, and T.J. Mitchison. 2006. Rapid actin monomer-insensitive depolymerization of Listeria actin comet tails by cofilin, coronin, and Aip1. *J Cell Biol*. 175:315-24.

Carlier, M.F., V. Laurent, J. Santolini, R. Melki, D. Didry, G.X. Xia, Y. Hong, N.H. Chua, and D. Pantaloni. 1997. Actin depolymerizing factor (ADF/cofilin) enhances the rate of filament turnover: implication in actin-based motility. *J Cell Biol*. 136:1307-22.

Chen, W.T. 1981. Mechanism of retraction of the trailing edge during fibroblast movement. *J Cell Biol*. 90:187-200.

Chhabra, E.S., and H.N. Higgs. 2007. The many faces of actin: matching assembly factors with cellular structures. *Nat Cell Biol*. 9:1110-21.

Cole, N.B., C.L. Smith, N. Sciaky, M. Terasaki, M. Edidin, and J. Lippincott-Schwartz. 1996. Diffusional mobility of Golgi proteins in membranes of living cells. *Science*. 273:797-801.

Condeelis, J. 2001. How is actin polymerization nucleated in vivo? *Trends Cell Biol*. 11:288-93.

Curtis, A.S. 1964. The Mechanism of Adhesion of Cells to Glass. a Study by Interference Reflection Microscopy. *J Cell Biol*. 20:199-215.

De Lozanne, A., and J.A. Spudich. 1987. Disruption of the Dictyostelium myosin heavy chain gene by homologous recombination. *Science*. 236:1086-91.

Dedova, I.V., O.P. Nikolaeva, D. Safer, E.M. De La Cruz, and C.G. dos Remedios. 2006. Thymosin beta4 induces a conformational change in actin monomers. *Biophys J*. 90:985-92.

DesMarais, V., M. Ghosh, R. Eddy, and J. Condeelis. 2005. Cofilin takes the lead. *J Cell Sci*. 118:19-26.

Drees, F., and F.B. Gertler. 2008. Ena/VASP: proteins at the tip of the nervous system. *Curr Opin Neurobiol*. 18:53-9.

Dunn, G.A. 1980. Cell Adhesion and Motility. Cambridge University Press Cambridge.

Dunn, G.A., I.M. Dobbie, J. Monypenny, M.R. Holt, and D. Zicha. 2002. Fluorescence localization after photobleaching (FLAP): a new method for studying protein dynamics in living cells. *J Microsc*. 205:109-12.

Dunn, G.A., and G.E. Jones. 2004. Cell motility under the microscope: Vorsprung durch Technik. *Nat Rev Mol Cell Biol*. 5:667-72.

Faix, J., and R. Grosse. 2006. Staying in shape with formins. *Dev Cell*. 10:693-706.

Faix, J., and K. Rottner. 2006. The making of filopodia. *Curr Opin Cell Biol*. 18:18-25.

Fattoum, A., J.H. Hartwig, and T.P. Stossel. 1983. Isolation and some structural and functional properties of macrophage tropomyosin. *Biochemistry*. 22:1187-93.

Fechheimer, M., and S.H. Zigmond. 1983. Changes in cytoskeletal proteins of polymorphonuclear leukocytes induced by chemotactic peptides. *Cell Motil*. 3:349-61.

Gerisch, G. 1982. Chemotaxis in Dictyostelium. *Annu Rev Physiol*. 44:535-52.

Ghosh, M., X. Song, G. Mouneimne, M. Sidani, D.S. Lawrence, and J.S. Condeelis. 2004. Cofilin promotes actin polymerization and defines the direction of cell motility. *Science*. 304:743-6.

Giannone, G., B.J. Dubin-Thaler, O. Rossier, Y. Cai, O. Chaga, G. Jiang, W. Beaver, H.G. Dobereiner, Y. Freund, G. Borisy, and M.P. Sheetz. 2007. Lamellipodial actin mechanically links myosin activity with adhesion-site formation. *Cell*. 128:561-75.

Goldschmidt-Clermont, P.J., M.I. Furman, D. Wachsstock, D. Safer, V.T. Nachmias, and T.D. Pollard. 1992. The control of actin nucleotide exchange by thymosin beta 4 and profilin. A potential regulatory mechanism for actin polymerization in cells. *Mol Biol Cell*. 3:1015-24.

Goode, B.L., and M.J. Eck. 2007. Mechanism and function of formins in the control of actin assembly. *Annu Rev Biochem*. 76:593-627.

Gouin, E., M.D. Welch, and P. Cossart. 2005. Actin-based motility of intracellular pathogens. *Curr Opin Microbiol*. 8:35-45.

Gupton, S.L., K.L. Anderson, T.P. Kole, R.S. Fischer, A. Ponti, S.E. Hitchcock-DeGregori, G. Danuser, V.M. Fowler, D. Wirtz, D. Hanein, and C.M. Waterman-Storer. 2005. Cell migration without a lamellipodium: translation of actin dynamics into cell movement mediated by tropomyosin. *J Cell Biol*. 168:619-31.

Gupton, S.L., and F.B. Gertler. 2007. Filopodia: the fingers that do the walking. *Sci STKE*. 2007:re5.

Gustafsson, M.G. 2008. Super-resolution light microscopy goes live. *Nat Methods*. 5:385-7.

Hahne, P., A. Sechi, S. Benesch, and J.V. Small. 2001. Scar/WAVE is localised at the tips of protruding lamellipodia in living cells. *FEBS Lett*. 492:215-20.

Hall, A. 1998. Rho GTPases and the actin cytoskeleton. *Science*. 279:509-14.

Hartwig, J.H., and P. Shevlin. 1986. The architecture of actin filaments and the ultrastructural location of actin-binding protein in the periphery of lung macrophages. *J Cell Biol*. 103:1007-20.

Heacock, C.S., K.E. Eidsvoog, and J.R. Bamburg. 1984. The influence of contact-inhibited growth and of agents which alter cell morphology on the levels of G- and F-actin in cultured cells. *Exp Cell Res*. 153:402-12.

Heuser, J. 2002. Whatever happened to the 'microtrabecular concept'? *Biol Cell*. 94:561-96.

Hoglund, A.S., R. Karlsson, E. Arro, B.A. Fredriksson, and U. Lindberg. 1980. Visualization of the peripheral weave of microfilaments in glia cells. *J Muscle Res Cell Motil*. 1:127-46.

Hotulainen, P., and P. Lappalainen. 2006. Stress fibers are generated by two distinct actin assembly mechanisms in motile cells. *J Cell Biol*. 173:383-94.

Hotulainen, P., E. Paunola, M.K. Vartiainen, and P. Lappalainen. 2005. Actin-depolymerizing factor and cofilin-1 play overlapping roles in promoting rapid F-actin depolymerization in mammalian nonmuscle cells. *Mol Biol Cell*. 16:649-64.

Huang, S., L. Gao, L. Blanchoin, and C.J. Staiger. 2006. Heterodimeric capping protein from Arabidopsis is regulated by phosphatidic acid. *Mol Biol Cell*. 17:1946-58.

Inoue. 1986. Video Microscopy. Plenum Press, New York and London. 584 pp.

Isenberg, G., U. Aebi, and T.D. Pollard. 1980. An actin-binding protein from Acanthamoeba regulates actin filament polymerization and interactions. *Nature*. 288:455-9.

Jacinto, A., and L. Wolpert. 2001. Filopodia. *Curr Biol*. 11:R634.

Kaverina, I., O. Krylyshkina, and J.V. Small. 2002. Regulation of substrate adhesion dynamics during cell motility. *Int J Biochem Cell Biol*. 34:746-61.

Kerkhoff, E. 2006. Cellular functions of the Spir actin-nucleation factors. *Trends Cell Biol*. 16:477-83.

Kim, A.S., L.T. Kakalis, N. Abdul-Manan, G.A. Liu, and M.K. Rosen. 2000. Autoinhibition and activation mechanisms of the Wiskott-Aldrich syndrome protein. *Nature*. 404:151-8.

Kim, K., M.E. McCully, N. Bhattacharya, B. Butler, D. Sept, and J.A. Cooper. 2007. Structure/function analysis of the interaction of phosphatidylinositol 4,5-bisphosphate with actin-capping protein: implications for how capping protein binds the actin filament. *J Biol Chem*. 282:5871-9.

Koestler, S.A., S. Auinger, M. Vinzenz, K. Rottner, and J.V. Small. 2008. Differentially oriented populations of actin filaments generated in lamellipodia collaborate in pushing and pausing at the cell front. *Nat Cell Biol*. 10:306-13.

Kovar, D.R. 2006. Molecular details of formin-mediated actin assembly. *Curr Opin Cell Biol*. 18:11-7.

Kovar, D.R., J.R. Kuhn, A.L. Tichy, and T.D. Pollard. 2003. The fission yeast cytokinesis formin Cdc12p is a barbed end actin filament capping protein gated by profilin. *J Cell Biol*. 161:875-87.

Ladwein, M., and K. Rottner. 2008. On the Rho'd: the regulation of membrane protrusions by Rho-GTPases. *FEBS Lett*. 582:2066-74.

Laham, L.E., M. Way, H.L. Yin, and P.A. Janmey. 1995. Identification of two sites in gelsolin with different sensitivities to adenine nucleotides. *Eur J Biochem*. 234:1-7.

Lai, F.P., M. Szczodrak, J. Block, J. Faix, D. Breitsprecher, H.G. Mannherz, T.E. Stradal, G.A. Dunn, J.V. Small, and K. Rottner. 2008. Arp2/3 complex interactions and actin network turnover in lamellipodia. *Embo J*. 27:982-92.

Lanni, F., A.S. Waggoner, and D.L. Taylor. 1985. Structural organization of interphase 3T3 fibroblasts studied by total internal reflection fluorescence microscopy. *J Cell Biol*. 100:1091-102.

Laurent, V., T.P. Loisel, B. Harbeck, A. Wehman, L. Grobe, B.M. Jockusch, J. Wehland, F.B. Gertler, and M.F. Carlier. 1999. Role of proteins of the Ena/VASP family in actin-based motility of Listeria monocytogenes. *J Cell Biol*. 144:1245-58.

Le Clainche, C., and M.F. Carlier. 2007. Regulation of Actin Assembly Associated With Protrusion
and Adhesion in Cell Migration. *Physiol Rev : , 2008;*
doi:10.1152/physrev.00021.2007. 88:489-513.

Li, F., and H.N. Higgs. 2003. The mouse Formin mDia1 is a potent actin nucleation factor regulated by autoinhibition. *Curr Biol*. 13:1335-40.

Loisel, T.P., R. Boujemaa, D. Pantaloni, and M.F. Carlier. 1999. Reconstitution of actin-based motility of Listeria and Shigella using pure proteins. *Nature*. 401:613-6.

Machesky, L.M., and R.H. Insall. 1999. Signaling to actin dynamics. *J Cell Biol*. 146:267-72.

Mahaffy, R.E., and T.D. Pollard. 2008. Influence of phalloidin on the formation of actin filament branches by Arp2/3 complex. *Biochemistry*. 47:6460-7.

Mejillano, M.R., S. Kojima, D.A. Applewhite, F.B. Gertler, T.M. Svitkina, and G.G. Borisy. 2004. Lamellipodial versus filopodial mode of the actin nanomachinery: pivotal role of the filament barbed end. *Cell*. 118:363-73.

Miki, M., J.A. Barden, and C.G. dos Remedios. 1986. Fluorescence resonance energy transfer between the nucleotide binding site and Cys-10 in G-actin and F-actin. *Biochim Biophys Acta*. 872:76-82.

Mogilner, A., and G. Oster. 1996. Cell motility driven by actin polymerization. *Biophys J*. 71:3030-45.

Mose-Larsen, P., R. Bravo, S.J. Fey, J.V. Small, and J.E. Celis. 1982. Putative association of mitochondria with a subpopulation of intermediate-sized filaments in cultured human skin fibroblasts. *Cell*. 31:681-92.

Mullins, R.D., J.A. Heuser, and T.D. Pollard. 1998. The interaction of Arp2/3 complex with actin: nucleation, high affinity pointed end capping, and formation of branching networks of filaments. *Proc Natl Acad Sci U S A*. 95:6181-6.

Nemethova, M., S. Auinger, and J.V. Small. 2008. Building the actin cytoskeleton: filopodia contribute to the construction of contractile bundles in the lamella. *J Cell Biol*. 180:1233-44.

Novak, I.L., B.M. Slepchenko, and A. Mogilner. 2008. Quantitative analysis of G-actin transport in motile cells. *Biophys J*. 95:1627-38.

Ono, S. 2007. Mechanism of depolymerization and severing of actin filaments and its significance in cytoskeletal dynamics. *Int Rev Cytol*. 258:1-82.

Pantaloni, D., and M.F. Carlier. 1993. How profilin promotes actin filament assembly in the presence of thymosin beta 4. *Cell*. 75:1007-14.

Pantaloni, D., C. Le Clainche, and M.F. Carlier. 2001. Mechanism of actin-based motility. *Science*. 292:1502-6.

Patterson, G.H., and J. Lippincott-Schwartz. 2002. A photoactivatable GFP for selective photolabeling of proteins and cells. *Science*. 297:1873-7.

Peckham, M., C. Wells, P. Taylor-Harris, D. Coles, D. Zicha, and G.A. Dunn. 1999. Using molecular genetics as a tool in understanding crawling cell locomotion in myoblasts. *Biochem Soc Symp*. 65:281-99.

Pellegrin, S., and H. Mellor. 2005. The Rho family GTPase Rif induces filopodia through mDia2. *Curr Biol*. 15:129-33.

Pollard, T.D. 2007. Regulation of actin filament assembly by Arp2/3 complex and formins. *Annu Rev Biophys Biomol Struct*. 36:451-77.

Pollard, T.D., L. Blanchoin, and R.D. Mullins. 2000. Molecular mechanisms controlling actin filament dynamics in nonmuscle cells. *Annu Rev Biophys Biomol Struct*. 29:545-76.

Pollard, T.D., and G.G. Borisy. 2003. Cellular motility driven by assembly and disassembly of actin filaments. *Cell*. 112:453-65.

Pollard, T.D., and J.A. Cooper. 1984. Quantitative analysis of the effect of Acanthamoeba profilin on actin filament nucleation and elongation. *Biochemistry*. 23:6631-41.

Ponti, A., M. Machacek, S.L. Gupton, C.M. Waterman-Storer, and G. Danuser. 2004. Two distinct actin networks drive the protrusion of migrating cells. *Science*. 305:1782-6.

Posern, G., and R. Treisman. 2006. Actin' together: serum response factor, its cofactors and the link to signal transduction. *Trends Cell Biol*. 16:588-96.

Prehoda, K.E., J.A. Scott, R.D. Mullins, and W.A. Lim. 2000. Integration of multiple signals through cooperative regulation of the N-WASP-Arp2/3 complex. *Science*. 290:801-6.

Price, L.S., J. Leng, M.A. Schwartz, and G.M. Bokoch. 1998. Activation of Rac and Cdc42 by integrins mediates cell spreading. *Mol Biol Cell*. 9:1863-71.

Pring, M., A. Weber, and M.R. Bubb. 1992. Profilin-actin complexes directly elongate actin filaments at the barbed end. *Biochemistry*. 31:1827-36.

Pruyne, D., M. Evangelista, C. Yang, E. Bi, S. Zigmond, A. Bretscher, and C. Boone. 2002. Role of formins in actin assembly: nucleation and barbed-end association. *Science*. 297:612-5.

Reinhard, M., M. Halbrugge, U. Scheer, C. Wiegand, B.M. Jockusch, and U. Walter. 1992. The 46/50 kDa phosphoprotein VASP purified from human platelets is a novel protein associated with actin filaments and focal contacts. *Embo J*. 11:2063-70.

Reisler, E., and E.H. Egelman. 2007. Actin structure and function: what we still do not understand. *J Biol Chem*. 282:36133-7.

Resch, G.P., K.N. Goldie, A. Hoenger, and J.V. Small. 2002. Pure F-actin networks are distorted and branched by steps in the critical-point drying method. *J Struct Biol*. 137:305-12.

Ridley, A.J. 2001. Rho GTPases and cell migration. *J Cell Sci*. 114:2713-22.

Ridley, A.J. 2006. Rho GTPases and actin dynamics in membrane protrusions and vesicle trafficking. *Trends Cell Biol*. 16:522-9.

Rinnerthaler, G., B. Geiger, and J.V. Small. 1988. Contact formation during fibroblast locomotion: involvement of membrane ruffles and microtubules. *J Cell Biol*. 106:747-60.

Rottner, K., B. Behrendt, J.V. Small, and J. Wehland. 1999. VASP dynamics during lamellipodia protrusion. *Nat Cell Biol*. 1:321-2.

Schaus, T.E., E.W. Taylor, and G.G. Borisy. 2007. Self-organization of actin filament orientation in the dendritic-nucleation/array-treadmilling model. *Proc Natl Acad Sci U S A*. 104:7086-91.

Scita, G., P. Tenca, E. Frittoli, A. Tocchetti, M. Innocenti, G. Giardina, and P.P. Di Fiore. 2000. Signaling from Ras to Rac and beyond: not just a matter of GEFs. *Embo J*. 19:2393-8.

Shaner, N.C., P.A. Steinbach, and R.Y. Tsien. 2005. A guide to choosing fluorescent proteins. *Nat Methods*. 2:905-9.

Shroff, H., C.G. Galbraith, J.A. Galbraith, and E. Betzig. 2008. Live-cell photoactivated localization microscopy of nanoscale adhesion dynamics. *Nat Methods*. 5:417-23.

Small, J.V. 1988. The actin cytoskeleton. *Electron Microsc Rev*. 1:155-74.

Small, J.V., S. Auinger, M. Nemethova, S. Koestler, K.N. Goldie, A. Hoenger, and G.P. Resch. 2008. Unravelling the structure of the lamellipodium. *J Microsc*. 231:479-85.

Small, J.V., G. Isenberg, and J.E. Celis. 1978. Polarity of actin at the leading edge of cultured cells. *Nature*. 272:638-9.

Small, J.V., and G.P. Resch. 2005. The comings and goings of actin: coupling protrusion and retraction in cell motility. *Curr Opin Cell Biol*. 17:517-23.

Steffen, A., J. Faix, G.P. Resch, J. Linkner, J. Wehland, J.V. Small, K. Rottner, and T.E. Stradal. 2006. Filopodia formation in the absence of functional WAVE- and Arp2/3-complexes. *Mol Biol Cell*. 17:2581-91.

Stradal, T., K.D. Courtney, K. Rottner, P. Hahne, J.V. Small, and A.M. Pendergast. 2001. The Abl interactor proteins localize to sites of actin polymerization at the tips of lamellipodia and filopodia. *Curr Biol*. 11:891-5.

Stradal, T.E., K. Rottner, A. Disanza, S. Confalonieri, M. Innocenti, and G. Scita. 2004. Regulation of actin dynamics by WASP and WAVE family proteins. *Trends Cell Biol*. 14:303-11.

Svitkina, T.M., and G.G. Borisy. 1999. Arp2/3 complex and actin depolymerizing factor/cofilin in dendritic organization and treadmilling of actin filament array in lamellipodia. *J Cell Biol*. 145:1009-26.

Svitkina, T.M., E.A. Bulanova, O.Y. Chaga, D.M. Vignjevic, S. Kojima, J.M. Vasiliev, and G.G. Borisy. 2003. Mechanism of filopodia initiation by reorganization of a dendritic network. *J Cell Biol*. 160:409-21.

Swanson, J.A., and S.C. Baer. 1995. Phagocytosis by zippers and triggers. *Trends Cell Biol*. 5:89-93.

Takai, Y., T. Sasaki, and T. Matozaki. 2001. Small GTP-binding proteins. *Physiol Rev*. 81:153-208.

Takenawa, T., and H. Miki. 2001. WASP and WAVE family proteins: key molecules for rapid rearrangement of cortical actin filaments and cell movement. *J Cell Sci*. 114:1801-9.

Takenawa, T., and S. Suetsugu. 2007. The WASP-WAVE protein network: connecting the membrane to the cytoskeleton. *Nat Rev Mol Cell Biol*. 8:37-48.

Theriot, J.A., and T.J. Mitchison. 1991. Actin microfilament dynamics in locomoting cells. *Nature*. 352:126-31.

Tilney, L.G., E.M. Bonder, L.M. Coluccio, and M.S. Mooseker. 1983. Actin from Thyone sperm assembles on only one end of an actin filament: a behavior regulated by profilin. *J Cell Biol*. 97:112-24.

Trinkaus, J.P. 1984. Cells Into Organs

Uruno, T., K. Remmert, and J.A. Hammer, 3rd. 2006. CARMIL is a potent capping protein antagonist: identification of a conserved CARMIL domain that inhibits the activity of capping protein and uncaps capped actin filaments. *J Biol Chem*. 281:10635-50.

Vallotton, P., and J.V. Small. 2008. Two Actin Networks at the Leading Edge of Migrating Cells? - Not So Fast!

Vidali, L., F. Chen, G. Cicchetti, Y. Ohta, and D.J. Kwiatkowski. 2006. Rac1-null mouse embryonic fibroblasts are motile and respond to platelet-derived growth factor. *Mol Biol Cell*. 17:2377-90.

Wang, Y.L. 1985. Exchange of actin subunits at the leading edge of living fibroblasts: possible role of treadmilling. *J Cell Biol*. 101:597-602.

Watanabe, N., T. Kato, A. Fujita, T. Ishizaki, and S. Narumiya. 1999. Cooperation between mDia1 and ROCK in Rho-induced actin reorganization. *Nat Cell Biol*. 1:136-43.

Waterman-Storer, C.M., A. Desai, J.C. Bulinski, and E.D. Salmon. 1998. Fluorescent speckle microscopy, a method to visualize the dynamics of protein assemblies in living cells. *Curr Biol*. 8:1227-30.

Waterman-Storer, C.M., and E.D. Salmon. 1997. Actomyosin-based retrograde flow of microtubules in the lamella of migrating epithelial cells influences microtubule dynamic instability and turnover and is associated with microtubule breakage and treadmilling. *J Cell Biol*. 139:417-34.

Wear, M.A., A. Yamashita, K. Kim, Y. Maeda, and J.A. Cooper. 2003. How capping protein binds the barbed end of the actin filament. *Curr Biol*. 13:1531-7.

Wegner, A. 1976. Head to tail polymerization of actin. *J Mol Biol*. 108:139-50.

Weisswange, I., T. Bretschneider, and K.I. Anderson. 2005. The leading edge is a lipid diffusion barrier. *J Cell Sci*. 118:4375-80.

Welch, M.D., A.H. DePace, S. Verma, A. Iwamatsu, and T.J. Mitchison. 1997. The human Arp2/3 complex is composed of evolutionarily conserved subunits and is localized to cellular regions of dynamic actin filament assembly. *J Cell Biol*. 138:375-84.

Wood, W., and P. Martin. 2002. Structures in focus--filopodia. *Int J Biochem Cell Biol*. 34:726-30.

Wu, J.Q., and T.D. Pollard. 2005. Counting cytokinesis proteins globally and locally in fission yeast. *Science*. 310:310-4.

Zicha, D., I.M. Dobbie, M.R. Holt, J. Monypenny, D.Y. Soong, C. Gray, and G.A. Dunn. 2003. Rapid actin transport during cell protrusion. *Science*. 300:142-5.

Zigmond, S.H., M. Evangelista, C. Boone, C. Yang, A.C. Dar, F. Sicheri, J. Forkey, and M. Pring. 2003. Formin leaky cap allows elongation in the presence of tight capping proteins. *Curr Biol*. 13:1820-3.

Appendix

Summary

Eukaryotic cells move in phases of extension and retraction of a leaf-like structure, the lamellipodium, at the cell front. Protrusion occurs by the polymerization of monomeric (G) into polymeric (F) actin filaments at the tip of the lamellipodium, thereby pushing the membrane forward. Actin filaments are depolymerized towards the rear of the lamellipodium in a treadmilling process, thereby supplementing a G-actin pool for a new round of polymerization. During my thesis I used correlative light cell imaging and negative stain electron microscopy on B16 mouse melanoma cells transfected with GFP-actin and other constructs encoding cell motility proteins to determine the correlation between the protrusive activity and the ultra-structure of the lamellipodium. I show that during a shift from protrusion to retraction lamellipodial filaments rearrange to generate, together with myosin, contractile arrays of antiparallel filaments behind the lamellipodium. The results challenge current models of how actin filaments are used to drive protrusion.

Moreover, I developed a technique to determine the F- and G-actin concentrations in lamellipodia of living cells. The strategy was to first determine the F- to G-actin ratio by exploiting the light microscopy technique FRAP (fluorescence recovery after photobleaching) to spatially segregate the F- and G-actin components of the total fluorescence intensity and specifically extract the G-actin component by cell lysis. The F-actin concentration was determined from electron micrographs. The concentration parameters can be incorporated into mathematical models and have implications on the way protrusion is regulated. In conclusion these studies have provided new information about the dynamics of actin filament turn-over during cell migration.

Zusammenfassung

Eukaryotische Zellen bewegen sich in Phasen des Schiebens und Ziehens einer flachen Struktur an der Zell-Vorderseite, dem Lamellipodium. Die Vorwärtsbewegung entsteht durch die Polymerisation von Aktin-Monomeren (G-Aktin) in Aktin-Filamente (F-Aktin) am vorderen Rand des Lamellipodiums, wodurch die Membran nach vorne geschoben wird. Aktin-Filamente werden in Richtung zum hinteren Ende des Lamellipodiums abgebaut wodurch ein Vorrat an Aktin-Monomeren aufrecht erhalten wird. Im Laufe meiner Doktorarbeit habe ich mittels korrelativer Licht- und Negativ-Färbungs-Elektronenmikroskopie anhand von B16 Maus Melanomzellen, die mit GFP-Aktin und anderen Konstrukten, die Zellbewegungsproteine kodieren, den Zusammenhang zwischen den unterschiedlichen Aktivitäten des Lamellipodiums und seiner Ultrastruktur untersucht. Ich konnte zeigen, dass sich die Aktinfilamente während des Übergangs vom Schieben zum Ziehen neu anordnen um zusammen mit Myosin hinter dem Lamellipodium kontraktile Einheiten aus antiparallen Filamenten zu bilden. Die Ergebnisse stellen derzeitige Modelle für die Zellbewegung mittels Aktin infrage.

Außerdem haben wir eine Methode entwickelt um die F- und G-Aktin-Konzentrationen im Lamellipodium von sich bewegenden Zellen zu bestimmen. Die Strategie war zunächst das Verhältnis von F- zu G-Aktin zu ermitteln. Dazu haben wir die Möglichkeiten von FRAP (Fluorescence Recovery After Photobleaching - das Wiedererlangen der Fluoreszenz nach Bleichen mit starkem Licht.) genutzt um die F- und G-Aktin-Komponenten der gesamten Fluoreszenzintensität räumlich zu trennen um dann die G-actin-Komponente durch Zell-Lyse zu erhalten. Die F-actin Konzentration wurde von Elektronenmikroskopiebildern ermittelt. Die Konzentrationsparameter können in mathematische Modelle inkorporiert werden und haben Auswirkungen auf die Art, wie Zellbewegung reguliert wird. Zusammenfassend haben die Studien neue Erkenntnisse über die Dynamik der Aktin-Filamente während der Zellbewegung geliefert.

Co-author papers

Unravelling the structure of the lamellipodium

J.V. SMALL*, S. AUINGER*, M. NEMETHOVA*,
S. KOESTLER*, K.N. GOLDIE‡§, A. HOENGER§**
& G.P. RESCH*†

*Institute of Molecular Biotechnology, Austrian Academy of Sciences (IMBA),
1030 Vienna, Austria*

†*Research Institute of Molecular Pathology (IMP)/IMBA Electron Microscopy Service,
Dr. Bohr-Gasse 3, 1030 Vienna, Austria*

‡*Bio21 Molecular Science and Biotechnology Institute, University of Melbourne, Parkville,
VIC 3010, Australia*

§*European Molecular Biology Laboratory Heidelberg, Meyerhofstrasse 1, 69117 Heidelberg,
Germany*

***The Boulder Laboratory for 3D Electron Microscopy of Cells, University of Colorado,
MCD-Biology, Boulder, CO 80309, U.S.A.*

Summary

Pushing at the cell front is the business of lamellipodia and
understanding how lamellipodia function requires knowledge
of their structural organization. Analysis of extracted, critical-
point-dried cells by electron microscopy has led to a current
dogma that the lamellipodium pushes as a branched array of
actin filaments, with a branching angle of 70°, defined by the
Arp2/3 complex. Comparison of different preparative methods
indicates that the critical-point-drying-replica technique
introduces distortions into actin networks, such that crossing
filaments may appear branched. After negative staining and
from preliminary studies by cryo-electron tomography, no
clear evidence could be found for actin filament branching
in lamellipodia. From recent observations of a sub-class
of actin speckles in lamellipodia that exhibit a dynamic
behaviour similar to speckles in the lamella region behind,
it has been proposed that the lamellipodium surfs on top of
the lamella. Negative stain electron microscopy and cryo-
electron microscopy of fixed cells, which reveal the entire
complement of filaments in lamellipodia show, however, that
there is no separate, second array of filaments beneath the
lamellipodium network. From present data, we conclude that
the lamellipodium is a distinct protrusive entity composed
of a network of primarily unbranched actin filaments. Cryo-
electron tomography of snap-frozen intact cells will be required
to finally clarify the three-dimensional arrangement of actin
filaments in lamellipodia *in vivo*.

Correspondence to: J. V. Small. Tel: 0043 1 79044 4600; fax: 0043 1 79044 4600;
e-mail: vic.small@imba.oeaw.ac.at

Introduction

The morphological features of crawling fibroblasts, visualized
by phase-contrast microscopy, were described in the seminal
papers of Abercrombie and co-workers around 1970. The
sheet-like protrusions at the cell front were termed *lamellipodia*
by analogy with rod-like filopodia (Abercrombie *et al.*, 1970a,
b). Lamellipodia were shown to lift away from the substrate, or
to protrude vertically and move rearwards as ruffles (Ingram,
1969; Abercrombie *et al.*, 1970b; Harris, 1973). Electron
microscopy of embedded cells showed that lamellipodia that
extended parallel to or folded away from the substrate
exhibited a more or less constant thickness, ranging from 110
to 160 nm (Abercrombie *et al.*, 1971). Other studies at about
the same time described the movements of filopodia, especially
on neuronal growth cones where they are particularly
prevalent (Bray, 1970; Wessels, 1973). The dual involvement
of lamellipodia and filopodia in protrusion and retraction was
described, the retrograde flow of particles on the surface of
lamellipodia and filopodia (Bray, 1970; Harris, 1973) as well
as the rearward folding of both structures into the region
behind the lamellipodium, that has been referred to as the
lamella (Harris, 1973; Heath & Holifield, 1991).

Subsequent studies showed that the core of both
lamellipodia and filopodia are composed of meshworks and
bundles of actin filaments (Small, 1988) and that actin
polymerization is the pushing force behind protrusion. The
different parts of the actin cytoskeleton of a migrating fibroblast
transfected with EGFP-actin are illustrated in Fig. 1. Just how
actin filaments are organized in lamellipodia to exert force is,
however, a matter of debate. In a currently popular model,
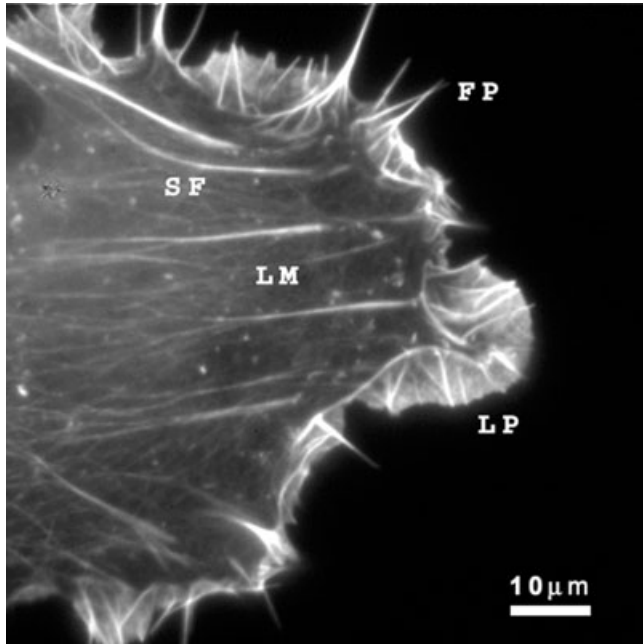actin filaments in lamellipodia form branched arrays with an

Fig. 1. Sub-compartments of the actin cytoskeleton. Image of living fish fibroblast expressing EGFP-actin. LP, lamellipodium; FP, filopodium; SF, stress fibre bundle; LM, lamella region behind lamellipodium–filopodium boundary, containing stress fibres and inter-linked actin network. Bar, 10 μm.

angle of 70° between filaments and the Arp2/3 complex at the branch points (Svitkina & Borisy, 1999; Pollard, 2007). This model is based on two principle lines of evidence: (1) the activated Arp2/3 complex induces the branching of actin filaments *in vitro*, as seen by fluorescence microscopy (Amann and Pollard, 2001) and electron microscopy (Mullins *et al.*, 1998); and (2) branching of actin filaments has been described in electron microscope images of lamellipodia prepared by the critical-point-drying platinum replica technique (Svitkina & Borisy, 1999). We will here review previous and more recent findings by electron microscopy of lamellipodia, using different approaches, which are inconsistent with the currently favoured 'dendritic model' of lamellipodia protrusion.

Preserving actin networks for electron microscopy

Over the last decade, there has been a surge of publications dealing with different aspects of lamellipodium ultra-structure using the critical-point-drying platinum replica procedure developed by Svitkina for electron microscopy of cytoskeletons (Svitkina *et al.*, 1995). Appealing images of lamellipodia in fish epidermal keratocytes obtained by this method showed a filament network within which actin filaments appeared to be branched (Svitkina & Borisy, 1999). Results obtained from applying the same method to other cells have been interpreted to show the generality of the branching phenomenon (Bear *et al.*, 2002; Svitkina *et al.*, 2003; Biyasheva *et al.*, 2004;

Mejillano *et al.*, 2004; Vignjevic *et al.*, 2006; Applewhite *et al.*, 2007; Mongiu *et al.*, 2007) and have led to the propagation of the dendritic branching model (Pollard & Borisy, 2003; Pollard, 2007). But why were such branches not observed in previous studies of lamellipodia networks (Small, 1988) including those of the epidermal keratocyte (Small *et al.*, 1995)? Do actin branches actually exist *in vivo*, or are we dealing with a subtle preparation artefact of electron microscopy?

In discussing this issue, it is worth reflecting on the early difficulties encountered in identifying actin networks in lamellipodia. After traditional plastic embedding and thin sectioning of cultured cells, lamellipodia appeared devoid of structure (Abercrombie *et al.*, 1971) or exhibited a 'fuzzy' material, interpreted to be filamentous (Wessels, 1973). Because of their inherent thinness, it was found that lamellipodia could be readily observed whole by electron microscopy of cells grown on electron microscope support films. The first direct evidence for a network of actin filaments in lamellipodia then came from observations of such whole mounts that were detergent extracted, aldehyde fixed and negatively stained with uranyl acetate (Fig. 2) (Small & Celis, 1978; Small *et al.*, 1978; Small *et al.*, 1980). A
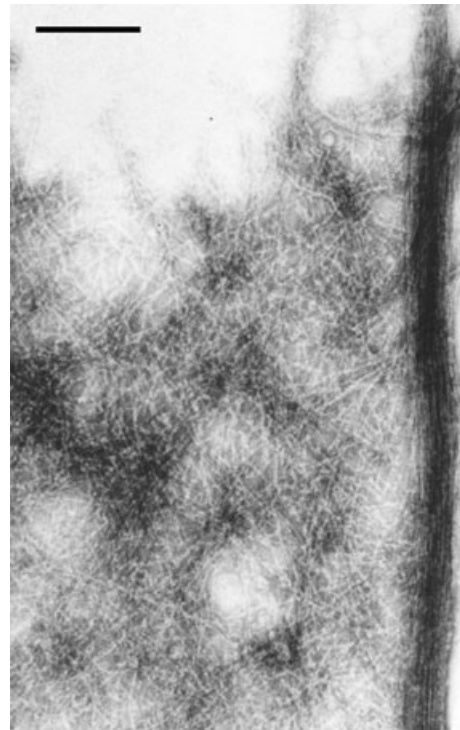

Fig. 2. Lamellipodium network and associated filopodium in a human skin fibroblast that was extracted with Triton X-100, fixed in glutaraldehyde and negatively stained in aqueous uranyl acetate (modified from Small & Celis, 1978). For these first images, phalloidin was not used to stabilize the actin and the filaments in the lamellipodium were disordered. Bar, 0.2 μm.

remarkable improvement in order was subsequently achieved using combined aldehyde–detergent extraction and neutral negative stains (Hoglund *et al.*, 1980; Small, 1981, 1988; Small *et al.*, 1982). At the same time, it was shown that osmium tetroxide and dehydration, both commonly used for plastic embedding, caused a marked deterioration in order of actin filaments in lamellipodia (Small, 1981) and in the organization of the cytoskeleton as a whole (Heuser & Kirschner, 1980). These findings signalled the demise of the 'microtrabecular lattice' (Wolosewick & Porter, 1979) that had been put forward as the framework of the cytoplasm on the basis of images obtained from cells first fixed and dehydrated as for embedding, but then subjected to critical point drying and viewed in a high-voltage electron microscope. Hans Ris attributed the artefacts obtained by the critical-point-drying procedure to the use of improperly dehydrated carbon dioxide, but even then the regular network of actin filaments in lamellipodia, identified by negative staining, was absent in the critical-point-dried preparations (Ris, 1985).

Evidently, actin meshworks require special treatment to be visualized intact in the electron microscope (Small *et al.*, 1999). Alternative attempts to apply the quick-freeze deep-etch method (Heuser, 1983) to lamellipodia were disappointing. A comparison of results obtained using the quick-freeze deep-etch method and negative staining on the lamellipodium of the fish keratocyte is shown in Figs 3(a) and (b) (Small *et al.*, 1994). A disordered reticular network was generally observed in the freeze-etched preparations (Heuser & Kirschner, 1980; Hartwig & Shevlin, 1986; Small *et al.*, 1994) which, in retrospect can be attributed to the lack of a direct control

of the freezing step, leading to a high probability of ice crystal damage on the nanometre scale.

Unheeded by earlier reservations about the critical-point-drying procedure, as applied to actin networks, Svitkina introduced additional steps and modifications that lead to a marked improvement in preservation of cytoskeletons as compared to earlier applications of this method (Svitkina *et al.*, 1995). Following gluraraldehyde fixation, tannic acid and uranyl acetate were included to 'stabilize' the actin filaments and the cytoskeletons were rotary-shadowed with platinum to provide contrast. Nevertheless, potentially damaging dehydration effects by organic solvents (Small, 1981) could not be avoided and tannic acid had been shown to cause distortions in lamellipodia networks that were subsequently processed by negative staining (Small, 1985). We are left with the concern that despite improvements of the critical-point-drying procedure (Svitkina *et al.*, 1995), minor distortions of the lamellipodia actin network could lead to the generation of apparently branched arrays from a network of un-branched filaments. This concern was heightened by the finding that pure actin filaments prepared by the critical-point-drying procedure, in the absence of the Arp2/3 complex, also showed branched arrays (Resch *et al.*, 2002a). In addition, actin filaments in preparations of lamellipodia contrasted by neutral negative stains such as sodium silicotungstate were essentially linear (Hoglund *et al.*, 1980; Small, 1981, 1988; Small *et al.*, 1982), but were not so in the critical-point-dried preparations. In Figs 4(a) and (b), images are shown of the cell edge of fish fibroblasts (CAR cell line), fixed identically in glutaraldehyde-Triton mixtures, but then
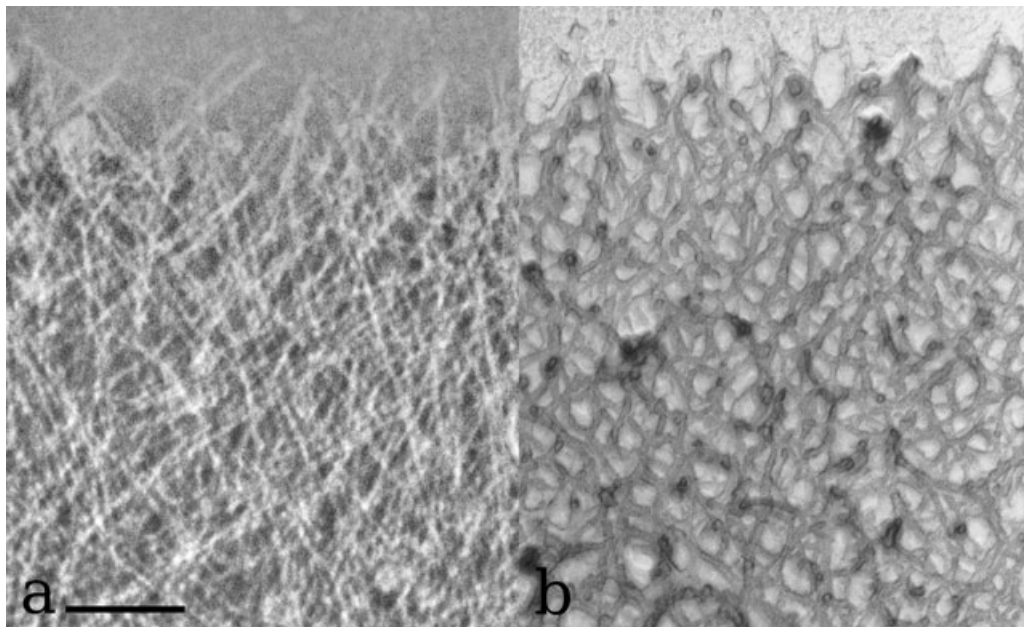

Fig. 3. Electron micrographs of equivalent regions in the lamellipodium of fish keratocytes prepared by negative staining (a) or quick freezing, deep etching and platinum coating. (b) After quick-freeze-deep-etching, the linearity of filaments is lost. Modified from Small *et al.* (1994). Bar, 0.2 μm.
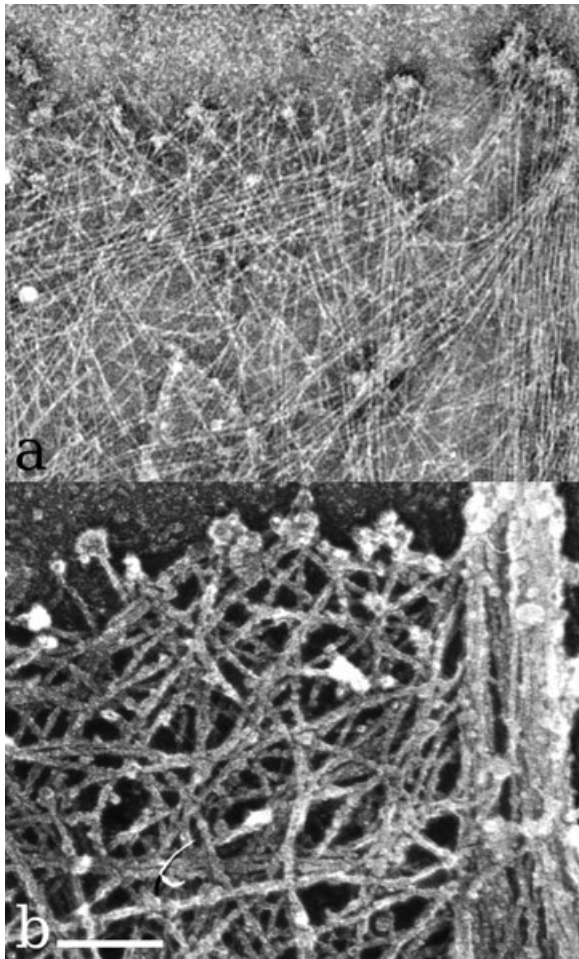
Fig. 4. Electron micrographs of equivalent regions in the lamellipodia of fish fibroblasts (CAR line) fixed identically in a glutaraldehyde–Triton mixture and stabilized with phalloidin. (a) Processed by negative staining in sodium silicotungstate/aurothioglucose; (b) Processed by the critical-point-drying platinum replica procedure, according to Svitkina (Svitkina *et al.*, 1995).

processed through the multi-step critical-point-drying replica procedure described by Svitkina & Borisy (1998) (Fig. 4(b)) or negatively stained in a mixture of aurothioglucose and sodium silicotungstate (Auinger & Small, 2007; Fig. 4(a)). In the negatively stained preparations, individual filaments can be traced from the cell edge through the whole micrograph and branched junctions are not observed (Fig. 4(a)). After the critical-point-drying protocol, the filament net is less ordered and short filament stubs occur that could be interpreted as branches. However, from comparison of the two figures, it is evident that apparent junction points in Fig. 4(b) are more readily explained as the result of minor distortions in the actin network introduced during processing.

Immunolocalization of proteins in lamellipodia meshworks involves several additional labelling and washing steps and introduces additional distortions, particularly notable after weak fixation (J.V.S., unpublished observations). This situation poses an additional challenge to defining the interactions of actin-associated proteins and actin cross-linkers in the lamellipodium meshwork.

Moving towards three-dimensional imaging of lamellipodia

Recent advances in cryo-electron tomography (cryo-ET; Steven & Aebi, 2003; Baumeister, 2005; McIntosh *et al.*, 2005) have opened the way to a minimally invasive approach for specimen preparation of whole cells for electron microscopy. They now allow access to the three-dimensional organization of the cytoskeleton in frozen, un-extracted cells, obviating the need to prepare cytoskeletons by detergent extraction. In a study of *Dictyostelium amoebae*, Medalia *et al.* (2002) provided the first reconstructions of actin networks in a cell frozen live and then imaged by cryo-ET. However, information about the motile activity of the re-constructed cell edge was not available. Nevertheless, the clarity of the processed images indicated that the three-dimensional geometry of actin networks could be resolved in intact, frozen cells. At about the same time, we could show that lamellipodia networks were readily visualized in cytoskeletons embedded in vitreous ice (Resch *et al.*, 2002b).

The challenge that remains is to combine live cell imaging with cryo-ET to correlate local motile events with ultra-structure. Suitable methodologies to transfer living samples from the light microscope to the cryo-EM are now being developed (Sartori *et al.*, 2007; Schwartz *et al.*, 2007). As far as lamellipodia are concerned, we have currently two alternatives; to use cells that have a constant morphology and motile activity, or to accept a single chemical fixation step that would allow correlated live cell imaging (Auinger & Small, 2007). As a first step in this direction, we have performed cryo-ET on Drosophila S2 cells that spread as uniform discs on concanavalin A–coated substrates and show retrograde flow of lamellipodia around their entire periphery (Rogers *et al.*, 2003; Fig. 5). In a series of attempts, we found that blotting the grids carrying S2 cells to remove excess liquid before plunge freezing, caused cell disruption, making it impossible to observe intact cell edges. However, tilt series could be obtained from S2 cells that were first fixed in glutaraldehyde and then frozen. Z-sections from a tomogram of the periphery of an S2 cell in ice are shown in Fig. 6. Note the linearity of the individual filaments, as seen in the negatively stained preparations. Single filaments were also tracked through the tomograms to assess the possible existence of branches within the network (Resch, 2005). From this preliminary data (Resch *et al.*, in preparation), we could not detect an organization consistent with the dendritic branching model. Further work, currently in progress, is aimed at imaging lamellipodia networks in cells fixed exclusively by physical means (freezing) to shed further light on their three-dimensional architecture.
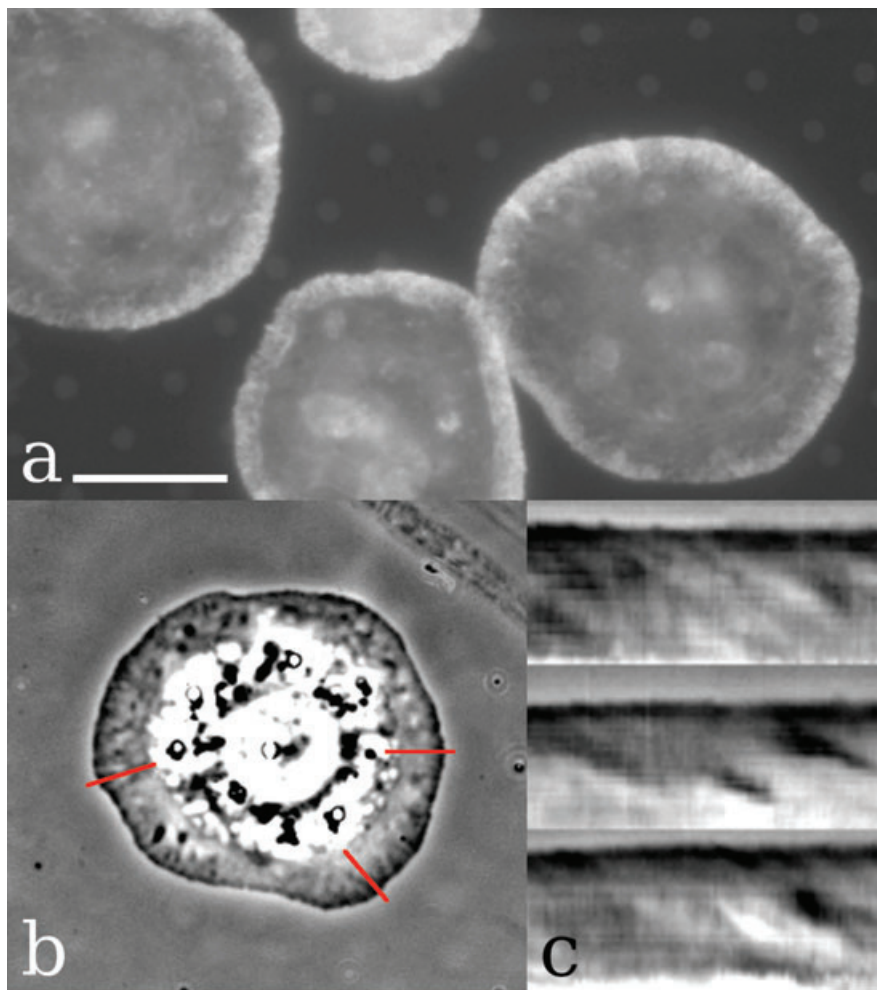
Fig. 5. Morphology and retrograde flow in S2 cells on concanavalin A–coated substrates. (a) Cells spread on Quantifoil perforated carbon films (as used for cryo-ET) and stained with fluorescently labelled phalloidin. The dense zone of actin at the periphery corresponds to the lamellipodium. The structure of the underlying carbon film was visualized by weak transmitted light illumination. (b) Contrast-enhanced frame from a phase-contrast movie of an S2 cell spread on glass. Kymographs were acquired along the red lines and (c) shows the rearward flow of material, driven by actin polymerization. Bar a, b, 10 μm; c, 97 s × 4.5 μm per kymograph.

Concluding remarks

The order of actin filament networks in lamellipodia is easily disrupted by conventional procedures employed in electron microscopy that involve multiple processing steps and in particular, dehydration in organic solvents. Because of the high density of filaments in lamellipodia, minor distortions suffice to transform an ordered network of linear filaments into one where filaments appear branched. Our results indicate that the branching of filaments described in critical-point-dried preparations of cytoskeletons is mostly an artefact of the preparation technique, at least for lamellipodia. This raises new questions about the exact role of the Arp2/3 complex, which has been shown to be an essential component of the lamellipodium polymerization machinery (Pollard, 2007). In

the current scheme, the Arp2/3 complex engages with the WAVE complex at the membrane to nucleate actin filament growth (Stradal & Scita, 2006). But how much nucleation is required in the steady-state situation? If new filaments are nucleated continuously at the lamellipodium tip, we would expect to see many short filaments at the front of the lamellipodium, which is not the case. We are lead to the conclusion that once a saturated filament density has been reached, there is no need for further nucleation. In this case, the Arp2/3 complex could be seen as a necessary partner of the WAVE complex in both nucleation and in maintaining the plus end addition of actin monomers until the polymerization machinery at the plus end is turned off. To explain the distribution of Arp2/3 throughout the lamellipodium, we

Fig. 6. Four-nanometre-thick z-sections from the leading edge of chemically fixed and immersion frozen Drosophila S2 cells obtained by cryo-electron tomography; the section shown in (b) is at a distance of 30 nm towards the substrate from the more ventral section shown in (a). A dense meshwork of long, linear actin filaments is clearly visible, with the filaments appearing shorter than they actually are due to computational sectioning. Other prominent features include the plasma membrane at the cell front and a microtubule in (b). Bar, 200 nm.

assume its association with the WAVE complex at the tip is most likely transient. Whatever the case, our results already call for a re-evaluation of the branching model as envisioned in the popular scheme (Pollard, 2007). At the same time, we cannot exclude the possibility of branching in processes involving activation of the Arp2/3 complex by N-WASP, in pathogen or vesicle propulsion. Structural studies by cryo-ET (Medalia et al., 2002) will be necessary to resolve this issue as well as the three-dimensional arrangement of actin filaments in lamellipodia of vitrified cells.

Acknowledgements

References

Abercrombie, M., Heaysman, J.E. & Pegrum, S.M. (1970a) The locomotion of fibroblasts in culture. I. Movements of the leading edge. *Exp. Cell Res.* **59**, 393–398.

Abercrombie, M., Heaysman, J.E. & Pegrum, S.M. (1970b) The locomotion of fibroblasts in culture. II. "Ruffling". *Exp. Cell Res.* **60**, 437–444.

Abercrombie, M., Heaysman, J.E. & Pegrum, S.M. (1971) The locomotion of fibroblasts in culture. IV. Electron microscopy of the leading lamella. *Exp. Cell Res.* **67**, 359–367.

Amann, K.J. & Pollard, T.D. (2001) Direct real-time observation of actin filament branching mediated by Arp2/3 complex using total internal reflection fluorescence microscopy. *Proc. Natl. Acad. Sci. U.S.A.* **98**, 15009–15013.

Applewhite, D.A., Barzik, M., Kojima, S.I., Svitkina, T.M., Gertler, F.B. & Borisy, G.G. (2007) Ena/VASP Proteins Have an Anti-Capping Independent Function in Filopodia Formation. *Mol. Biol. Cell* **18**, 2579–2591.

Auinger, S. & Small, J.V. (2008) Correlated light and electron microscopy of the cytoskeleton. *Methods in Cell Biology, Basic Biological Electron Microscopy* (ed. by T.D. Allen). Academic Press. In press.

Baumeister, W. (2005) From proteomic inventory to architecture. *FEBS Lett.* **579**, 933–937.

Bear, J.E., Svitkina, T.M., Krause, M., *et al.* (2002) Antagonism between Ena/VASP proteins and actin filament capping regulates fibroblast motility. *Cell* **109**, 509–521.

Biyasheva, A., Svitkina, T., Kunda, P., Baum, B. & Borisy, G. (2004) Cascade pathway of filopodia formation downstream of SCAR. *J. Cell Sci.* **117**, 837–848.

Bray, D. (1970) Surface movements during the growth of single explanted neurons. *Proc. Natl. Acad. Sci. U.S.A.* **65**, 905–910.

Harris, A.K. (1973) Cell surface movements related to cell locomotion. *Ciba Foundation Symposium*, Vol. 14, pp. 3–26. Elsevier, London.

Hartwig, J.H. & Shevlin, P. (1986) The architecture of actin filaments and the ultrastructural location of actin-binding protein in the periphery of lung macrophages. *J. Cell Biol.* **103**, 1007–1020.

Heath, J.P. & Holifield, B.F. (1991) Cell locomotion: new research tests old ideas on membrane and cytoskeletal flow. *Cell Motil. Cytoskeleton* **18**, 245–257.

Heuser, J.E. (1983) Procedure for freeze-drying molecules adsorbed to mica flakes. *J. Mol. Biol.* **169**, 155–195.

Heuser, J.E. & Kirschner, M.W. (1980) Filament organization revealed in platinum replicas of freeze-dried cytoskeletons. *J. Cell Biol.* **86**, 212–234.

Hoglund, A.S., Karlsson, R., Arro, E., Fredriksson, B.A. & Lindberg, U. (1980) Visualization of the peripheral weave of microfilaments in glia cells. *J. Muscle. Res. Cell Motil.* **1**, 127–146.

Ingram, V.M. (1969) A side view of moving fibroblasts. *Nature* **222**, 641–644.

McIntosh, R., Nicastro, D. & Mastronarde, D. (2005) New views of cells in 3D: an introduction to electron tomography. *Trends Cell Biol.* **15**, 43–51.

Medalia, O., Weber, I., Frangakis, A.S., Nicastro, D., Gerisch, G. & Baumeister, W. (2002) Macromolecular architecture in eukaryotic cells visualized by cryoelectron tomography. *Science* **298**, 1209–1213.

Mejillano, M.R., Kojima, S., Applewhite, D.A., Gertler, F.B., Svitkina, T.M. & Borisy, G.G. (2004) Lamellipodial versus filopodial mode of the actin nanomachinery: pivotal role of the filament barbed end. *Cell* **118**, 363–373.

Mongiu, A.K., Weitzke, E.L., Chaga, O.Y. & Borisy, G.G. (2007) Kinetic-structural analysis of neuronal growth cone veil motility. *J. Cell Sci.* **120**, 1113–1125.

Mullins, R.D., Heuser, J.A. & Pollard, T.D. (1998) The interaction of Arp2/3 complex with actin: nucleation, high affinity pointed end capping, and formation of branching networks of filaments. *Proc. Natl. Acad. Sci. U.S.A.* **95**, 6181–6186.

Pollard, T.D. (2007) Regulation of actin filament assembly by arp2/3 complex and formins. *Annu. Rev. Biophys. Biomol. Struct.* **36**, 451–477.

Pollard, T.D. & Borisy, G.G. (2003) Cellular motility driven by assembly and disassembly of actin filaments. *Cell* **112**, 453–465.

Resch, G.P. (2005) Correlating nanostructure and function in the actin cytoskeleton. PhD Thesis, University of Salzburg.

Resch, G.P., Goldie, K.N., Hoenger, A. & Small, J.V. (2002a) Pure F-actin networks are distorted and branched by steps in the critical-point drying method. *J. Struct. Biol.* **137**, 305–312.

Resch, G.P., Goldie, K.N., Krebs, A., Hoenger, A. & Small, J.V. (2002b) Visualisation of the actin cytoskeleton by cryo-electron microscopy. *J. Cell Sci.* **115**, 1877–1882.

Ris, H. (1985) The cytoplasmic filament system in critical point-dried whole mounts and plastic-embedded sections. *J. Cell Biol.* **100**, 1474–1487.

Rogers, S.L., Wiedemann, U., Stuurman, N. & Vale, R.D. (2003) Molecular requirements for actin-based lamella formation in Drosophila S2 cells. *J. Cell Biol.* **162**, 1079–1088.

Sartori, A., Gatz, R., Beck, F., Rigort, A., Baumeister, W. & Plitzko, J.M. (2007) Correlative microscopy: bridging the gap between fluorescent light and cryo-electron tomography. *J. Struct. Biol.* **160**, 135–145.

Schwartz, C.L., Sarbash, V.I., Ataullakhanov, F.I., McIntosh, J.R. & Nicastro, D. (2007) Cryo-fluorescence microscopy facilitates correlations between light and cryo-electron microscopy and reduces the rate of photobleaching. *J. Microsc.* **227**, 98–109.

Small, J., Rottner, K., Hahne, P. & Anderson, K.I. (1999) Visualising the actin cytoskeleton. *Microsc. Res. Tech.* **47**, 3–17.

Small, J.V. (1981) Organization of actin in the leading edge of cultured cells: influence of osmium tetroxide and dehydration on the ultrastructure of actin meshworks. *J. Cell Biol.* **91**, 695–705.

Small, J.V. (1985) Factors affecting the integrity of actin meshworks in cultured cells. *Yamada Conference on Cell Motility*, Vol. II (ed. by H.H. Ishikawa, S. Hatano and Sato, H.), pp. 493–506. Univ. Tokyo Press, Tokyo.

Small, J.V. (1988) The actin cytoskeleton. *Electron. Microsc. Rev.* **1**, 155–574.

Small, J.V. & Celis, J.E. (1978) Filament arrangements in negatively stained cultured cells: the organization of actin. *Cytobiologie* **16**, 308–325.

Small, J.V., Celis, J.E. & Isenberg, G. (1980) Aspects of cell architecture and locomotion. *Transfer of Cell Constituents into Eukaryotic Cells* (ed. by J.E.Celis, A. Graessmann & A. Loyter), pp. 75–111. Plenum Press, Sintra-Estoril, Portugal.

Small, J.V., Herzog, M. & Anderson, K. (1995) Actin filament organization in the fish keratocyte lamellipodium. *J. Cell Biol.* **129**, 1275–1286.

Small, J.V., Herzog, M., Haner, M. & Abei, U. (1994) Visualization of actin filaments in keratocyte lamellipodia: negative staining compared with freeze-drying. *J. Struct. Biol.* **113**, 135–141.

Small, J.V., Isenberg, G. & Celis, J.E. (1978) Polarity of actin at the leading edge of cultured cells. *Nature* **272**, 638–639.

Small, J.V., Rinnerthaler, G. & Hinssen, H. (1982) Organization of actin meshworks in cultured cells: the leading edge. *Cold. Spring. Harb. Symp. Quant. Biol.* 46(Pt **2**), 599–611.

Steven, A.C. & Aebi, U. (2003) The next ice age: cryo-electron tomography of intact cells. *Trends Cell. Biol.* **13**, 107–110.

Stradal, T.E. & Scita, G. (2006) Protein complexes regulating Arp2/3-mediated actin assembly. *Curr. Opin. Cell Biol.* **18**, 4–10.

Svitkina, T.M. & Borisy, G.G. (1999) Arp2/3 complex and actin depolymerizing factor/cofilin in dendritic organization and treadmilling of actin filament array in lamellipodia. *J. Cell Biol.* **145**, 1009–1026.

Svitkina, T.M., Bulanova, E.A., Chaga, O.Y., Vignjevic, D.M., Kojima, S., Vasiliev, J.M. & Borisy, G.G. (2003) Mechanism of filopodia initiation by reorganization of a dendritic network. *J. Cell Biol.* **160**, 409–421.

Svitkina, T.M., Verkhovsky, A.B. & Borisy, G.G. (1995) Improved procedures for electron microscopic visualization of the cytoskeleton of cultured cells. *J. Struct. Biol.* **115**, 290–303.

Vignjevic, D., Kojima, S., Aratyn, Y., Danciu, O., Svitkina, T. & Borisy, G.G. (2006) Role of fascin in filopodial protrusion. *J. Cell Biol.* **174**, 863–875.

Wessels, N. K., Spooner, B.S., Luduena, M.A. (1973) Surface movements, microfilaments and cell locomotion. *Ciba Foundation Symposium*, Vol. 14, pp. 53–82. Elsevier, London.

Wolosewick, J.J. & Porter, K.R. (1979) Microtrabecular lattice of the cytoplasmic ground substance. Artifact or reality. *J. Cell Biol.* **82**, 114–139.

Filopodia formation induced by active mDia2/Drf3

J. BLOCK*, T.E.B. STRADAL†, J. HÄNISCH†, R. GEFFERS‡,
S.A. KÖSTLER§, E. URBAN§, J.V. SMALL§, K. ROTTNER*
& J. FAIX**

**Cytoskeleton Dynamics Group, Helmholtz Centre for Infection Research (HZI), Inhoffen Strasse 7, D-38124 Braunschweig, Germany*

†*Signalling and Motility Group, Helmholtz Centre for Infection Research (HZI), Inhoffen Strasse 7, D-38124 Braunschweig, Germany*

‡*Mucosal Immunity Group, Helmholtz Centre for Infection Research (HZI), Inhoffen Strasse 7, D-38124 Braunschweig, Germany*

§*Institute of Molecular Biotechnology, Austrian Academy of Sciences, Dr. Bohr Gasse 3, A-1030 Vienna, Austria*

***Institute for Biophysical Chemistry, Hannover Medical School, Carl-Neubergstr. 1, D-30623 Hannover, Germany*

Summary

Filopodia are rod-shaped cell surface protrusions composed of a parallel bundle of actin filaments. Since filopodia frequently emanate from lamellipodia, it has been proposed that they form exclusively by the convergence and elongation of actin filaments generated in lamellipodia networks. However, filopodia form without Arp2/3-complex, which is essential for lamellipodia formation, indicating that actin filaments in filopodia may be generated by other nucleators. Here we analyzed the effects of ectopic expression of GFP-tagged full length or a constitutively active variant of the human formin mDia2/Drf3. By contrast to the full-length molecule, which did not affect cell behaviour and was entirely cytosolic, active Drf3 lacking the C-terminal regulatory region (Drf3ΔDAD) induced the formation of filopodia and accumulated at their tips. Low expression of Drf3ΔDAD induced rod-shaped or tapered filopodia, whereas over-expression resulted in multiple, club-shaped filopodia. The clubs were filled with densely bundled actin filaments, whose number but not packing density decreased further away from the tip. Interestingly, clubs frequently increased in width after protrusion beyond the cell periphery, which correlated with increased amounts of Drf3ΔDAD at their tips. These data suggest Drf3-induced filopodia form and extend by *de novo* nucleation of actin filaments instead of convergent elongation. Finally, Drf3ΔDAD also induced the

formation of unusual, lamellipodia-like structures, which contained both lamellipodial markers and the prominent filopodial protein fascin. Microarray analyses revealed highly variable Drf3 expression levels in different commonly used cell lines, reflecting the need for more detailed analyses of the functions of distinct formins in actin cytoskeleton turnover and different cell types.

Introduction

Non-muscle cells contain a large pool of globular monomeric actin, which upon appropriate stimuli can reversibly polymerize into filaments to alter cell shape and morphology. These processes involve Rho-family GTPases, which drive cell locomotion by regulating adhesion and protrusion at the front and de-adhesion/retraction at the rear (Hall, 1998; Small *et al.*, 1996). The two most prominent and best-characterized protrusive organelles are lamellipodia and filopodia (Small *et al.*, 2002; Pollard & Borisy, 2003). According to our current knowledge, actin filaments in cells are nucleated by two major machineries, Arp2/3-complex and formins (Pollard, 2007). After activation by so-called nucleation promoting factors such as N-WASP or Scar/WAVE-complex proteins (Stradal & Scita, 2006), Arp2/3-complex is thought to amplify the generation of barbed, fast-growing actin filament ends through the formation of branches, the fate and dwell-time of which in live cells is still under debate (Resch *et al.*, 2002; Goley & Welch, 2006).

Formins nucleate actin filaments by a mechanism different from Arp2/3 complex (Faix & Grosse, 2006; Goode & Eck,

Correspondence to: Jan Faix. Tel: +49 511 532 2928; fax: +49 511 532 5966; e-mail: faix@bpc.mh-hannover.de; Klemens Rottner. Tel: +49 531 6181 3070; fax: +49 531 6181 3099; e-mail: klemens.rottner@helmholtz-hzi.de

2007; Pollard, 2007). These dimeric multi-domain proteins recruit profilin-actin complexes by virtue of their proline-rich formin homology (FH) 1 – domains and *de novo* assemble linear actin filaments by their adjacent FH2 domains (Pruyne *et al.*, 2002). As processive motors, formins remain tightly bound to the fast-growing barbed end of the actin filament adding monomers for elongation (Kovar & Pollard, 2004; Romero *et al.*, 2004). Diaphanous-related formins (Drfs) constitute a conserved sub-family that act as effectors of Rho-family GTPases (Watanabe *et al.*, 1997). The core FH1 and FH2 domains are flanked by a large N-terminal regulatory region containing the Diaphanous-inhibitory domain (DID) and an adjacent GTPase binding domain (GBD). In addition, they harbour a small C-terminal Diaphanous-auto-regulatory domain (DAD). Binding of an activated Rho-GTPase to GBD releases an inhibitory intra-molecular interaction between DID and DAD, leading to an activated state (Watanabe *et al.*, 1999; Alberts, 2001). In addition, this release of auto-inhibition appears to enable proper cellular localization (Seth *et al.*, 2006). Collectively, these observations suggest that specific cellular F-actin nucleators are employed to fulfill different cellular functions.

By contrast to lamellipodia, which are composed of a dense criss-cross meshwork of actin filaments generated by the Arp2/3 complex (Small *et al.*, 2002; Pollard & Borisy, 2003; Steffen *et al.*, 2006), filopodia are rod-shaped cell surface protrusions built of parallel actin filaments that are cross-linked into compact bundles that elongate by actin incorporation at their tips (Mallavarapu & Mitchison, 1999; Faix & Rottner, 2006; Applewhite *et al.*, 2007). Filopodia typically extend a few micrometres beyond the cell periphery and are found in a wide range of evolutionary distant organisms such as mammalian cells and *Dictyostelium amoebae* (Small, 1988; Mitchison & Cramer, 1996; Schirenbeck *et al.*, 2005). However, despite the large number of proteins implicated in filopodia formation our knowledge about the precise molecular mechanisms underlying their formation is still preliminary (Faix & Rottner, 2006; Gupton & Gertler, 2007). They can be formed downstream of Rho GTPases such as Cdc42 and Rif, but their relative relevance and the downstream signalling cascades are less well defined (Hall, 1998; Pellegrin & Mellor, 2005). For instance, although Cdc42 can efficiently induce filopodium formation, it is not essential for this process (Czuchra *et al.*, 2005). Similarly, N-WASP, which was originally believed to bridge Cdc42 signalling to Arp2/3-complex-mediated filopodia formation, is dispensable for this process (Lommel *et al.*, 2001; Snapper *et al.*, 2001). Finally, since filopodia frequently emerge from lamellipodial structures (Small *et al.*, 1999), it has been hypothesized that lamellipodia serve as precursors for filopodia (Biyasheva *et al.*, 2004; Mejillano *et al.*, 2004). In the model coined 'the convergent elongation model of filopodia formation', filopodial actin filaments arise from the dendritic network of Arp2/3-nucleated filaments by selective elongation, coalescence and bundling by proteins of the filopodium tip complex (Svitkina *et al.*, 2003; Korobova & Svitkina, 2008). However, recent loss of function studies of Arp2/3-complex or its activators using RNAi in B16-F1 mouse melanoma and human T cells indicated that filopodium formation can still occur normally in the absence of lamellipodia (Steffen *et al.*, 2006; Gomez *et al.*, 2007). Consistently, ablation of WAVE-complex components by gene disruption in *Dictyostelium* also showed no effects on filopodia formation (Steffen *et al.*, 2006). Collectively, these data imply that filopodial actin filaments may exclusively be formed through nucleators other than the Arp2/3-complex. In line with this finding, in *Dictyostelium* cells, the Diaphanous-related formin dDia2 was shown to be critical for filopodium formation (Schirenbeck *et al.*, 2005). Most notably, GFP-tagged dDia2 was shown to surf on distal tips of filopodia as they elongated (Schirenbeck *et al.*, 2005). From the large number of formin isoforms in mammalian cells, so far only two Drfs, namely, mDia1/Drf1 and mDia2/Drf3, have been implicated in the assembly of filopodial actin filaments (Faix & Grosse, 2006). An active, N-terminally truncated form of mDia1 was reported to accumulate at the tips of filopodia-like structures in *Xenopus* fibroblasts (Higashida *et al.*, 2004), although this has not been confirmed by other studies. More strikingly, the Cdc42- and Rif-effector mDia2/Drf3 was linked to filopodia assembly and localized to their tips after co-over-expression with the active forms of these GTPases (Peng *et al.*, 2003; Pellegrin & Mellor, 2005; Wallar *et al.*, 2006). Finally, RNAi-mediated knockdown of mDia2/Drf3 was recently reported to impair not only filopodia but also lamellipodia protrusion in B16-F1 cells. It was accordingly proposed that mDia2/Drf3 is recruited to the lamellipodium by direct interaction with the WAVE-complex component Abi-1, and drives the formation as well as the convergence of lamellipodia into filopodia (Yang *et al.*, 2007).

Here, we have characterized a novel, constitutively active version of human Drf3 as compared to the full-length formin by light and electron microscopy methods. Evidence is provided that the exaggerated filopodia assembly induced by active Drf3 is mediated through *de novo* actin nucleation, not convergent elongation, and occurs in the virtual absence of functional WAVE-complex. Finally, expression patterns of this and related Drfs in a number of frequently used cell types were determined.

Materials and methods

Expression constructs

Sequences coding for N- and C-terminal fragments of human Drf3 were amplified from the cDNA clones BX649186 and BC048963, respectively, which were obtained from the Resource Centre of the German Human Genome Project (RZPD, Berlin). PCR fragments were combined using the
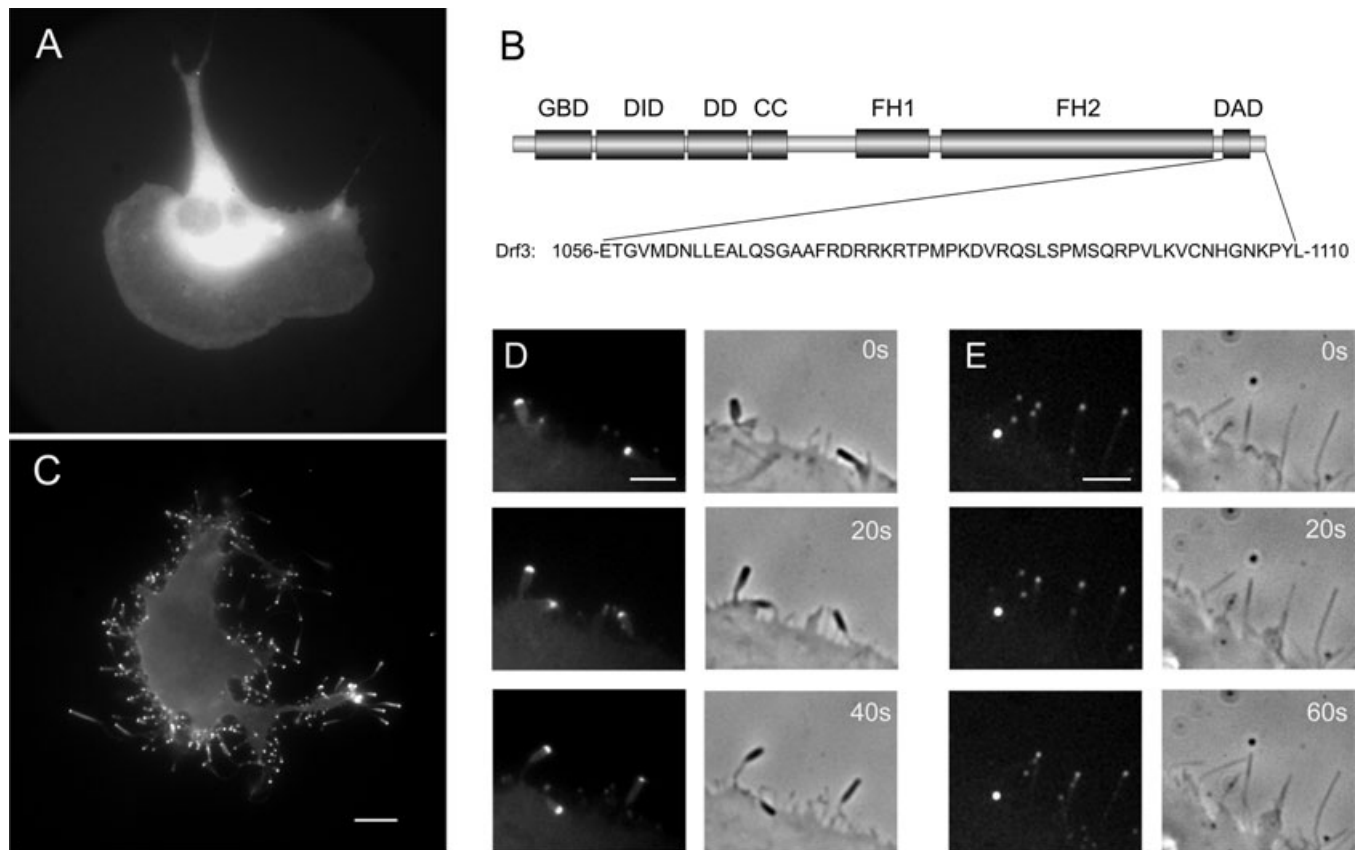
Fig. 1. Expression of active Drf3ΔDAD induces the formation of filopodia. (a) EGFP-tagged full-length Drf3 is entirely cytoplasmic. (b) Schematic illustration of the used Drf3ΔDAD constructs lacking amino acid residues 1056–1110. GBD, GTPase-binding domain; DID, Diaphanous-inhibitory domain; DD, Dimerization domain; CC, Coiled coil; FH, Formin-homology domain; DAD, Diaphanous-auto-inhibitory domain. (c) Drf3ΔDAD expressing cell displaying numerous filopodia. (d) and (e) Filopodial protrusions formed in high and low Drf3ΔDAD expressors, respectively. Scale bar in (c) is 10 μm and valid for (a) and (c). Scale bars in (d) and (e) are 5 μm.

internal BstXI restriction site and fused into the BglII and EcoRI sites of pEGFP-C1 (Clontech, Palo Alto). Primers were as follows: DRF3 fwd GAGAGGATCCAAGATGGAACGGCACCA-GCC, Drf3 rev GAGGAATTCTTAATACGGTTTATTAC, Drf3 internal fwd GAGAGATCTATGGAGGAGAGGAGC, Drf3 internal rev GAGAAGATCCACGGCTTTGGCCAATAAGGAA.

The C-terminally deleted active Drf3 (Drf3ΔDAD) was generated by replacement of a PCR-amplified ClaI/SalI fragment (primers: Drf3mut fwd GAGGAAGATATTGAAGA-AAGAAATCGATTAAGA and Drf3mut rev CGCGTCGACTT-ATTAATCACCCTCAGTCTTCATTTCTAATAAACG) lacking residues 1056–1110.

Cells and transfections

B16-F1 mouse melanoma cells (ATTC CRL-6323) and VA-13 human lung fibroblasts (ATCC CCL-75.1) were grown in DMEM high glucose (Gibco) supplemented with 10% FCS (EU, PAA, Austria), 2 mM glutamine and penicillin/streptomycin, and transfected over night using Superfect (Quiagen GmbH,

Hilden, Germany) and FuGene (Roche, Basel, Switzerland) according to manufacturers' instructions, respectively. B16-F1 cells were subsequently seeded onto acid-washed glass cover slips, coated with 25 μg ml^{-1} laminin, allowed to spread for approximately 2–3 h, and subjected to video microscopy or fixed as detailed later. Control and stable Nap1 knockdown VA-13 cell lines were maintained as described (Steffen *et al.*, 2004), plated on acid-washed glass cover slips coated with fibronectin (25 μg ml^{-1}) and subjected to video microscopy 12–16 h later.

Light microscopy

For fluorescence microscopy, cells expressing EGFP-tagged Drf3 were fixed with 4% formaldehyde (PFA) in phosphate-buffered saline (PBS) for 20 min, extracted with 0.1% Triton X-100 for 1 min and stained with Alexa594-coupled phalloidin (Invitrogen, Karlsruhe, Germany) or monoclonal antibodies directed against p16/ArpC5 (Olazabal *et al.*, 2002), cortactin (clone 289H10) or Abi-1, kindly provided by Giorgio Scita
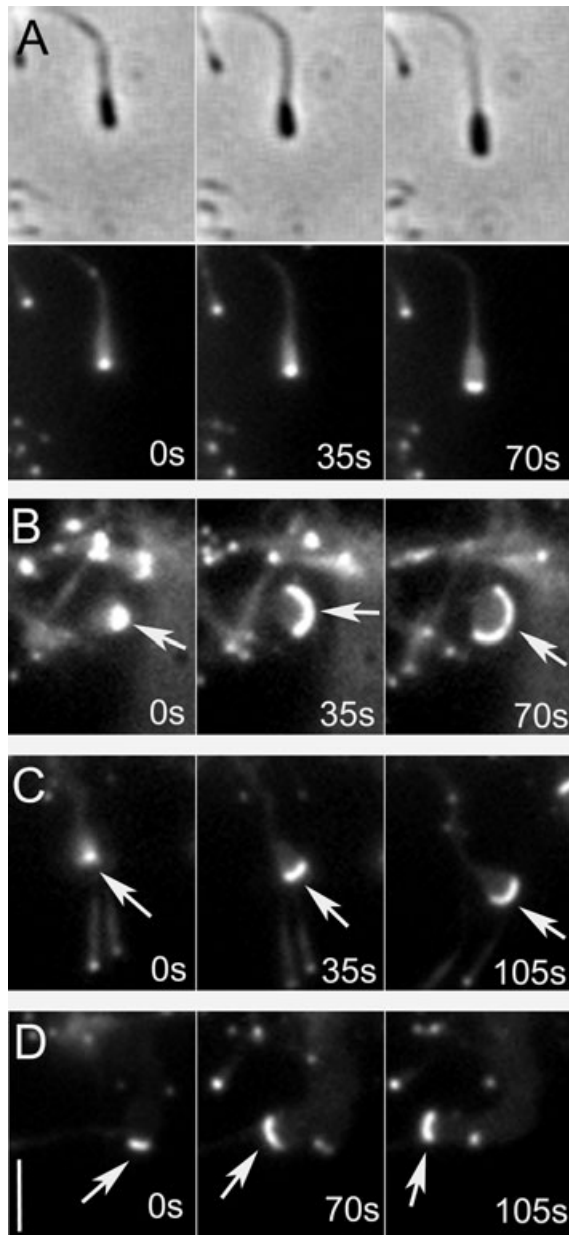
Fig. 2. Spontaneous thickening of Drf3ΔDAD-induced filopodia. Panels of time-lapse sequences of parts of Drf3ΔDAD-over-expressers showing filopodia after having separated from the cell periphery. Note thickening of filopodia tips and concomitant increase in intensity (a) or widening of the fluorescence signal (arrows in (b–d)). Bar in (d) is valid for all panels and corresponds to 2 μm.

(Innocenti *et al.*, 2004). For fascin staining using monoclonal antibody 55K2 (Santa Cruz Biotechnology Inc, Santa Cruz, CA, USA), cells were fixed with methanol. Alexa594-coupled secondary antibodies were from Invitrogen (Karlsruhe). The generation of monoclonal anti-cortactin antibodies will be described elsewhere (Lai *et al.*, unpublished data).

Live cells were observed in an open heated chamber (Warner Instruments, Hamden, CT, USA) at 37°C on an inverted

microscope (Axiovert 135TV, Zeiss, Jena, Germany) equipped for fluorescence and phase-contrast microscopy, and with shutters (Optilas, Puchheim, Germany) in the transmitted and epifluorescence light paths controlled by an home-made interface. Data were acquired with a back-illuminated, cooled charge-coupled device camera (TE-CCD 800PB; Princeton Scientific Instruments, Princeton, NJ) driven by IPLab software (Scanalytics, Fairfax, VA). Data were stored as 16-bit digital images and processed using IPLab, ImageJ and Adobe Photoshop CS software (Adobe Systems, Mountain View, CA).

Electron microscopy

For negative stain electron microscopy cells were grown on formvar films and processed essentially as described by Auinger & Small (2008). Briefly, cells were fixed for 2 min in a mixture of Triton X-100 and glutaraldehyde in a cytoskeleton buffer (CB: 10 mM MES, 150 mM NaCl, 5 mM EGTA, 5 mM glucose, 5 mM $MgCl_2$; pH 6.1), with added 1 μg ml^{-1} phalloidin and post-fixed in 2% glutaraldehyde in the same buffer, including 1 μg ml^{-1} phalloidin. They were then stained in a mixture of sodium silicotungstate (2%) and aurothioglucose (1%) and examined in an FEI morgagni electron microscope operating at 80 kV.

DNA microarray hybridization and analysis

Cell lines used in this experiment were HeLaS3 (human cervix carcinoma CCL-2.2), A431 (human epidermoid carcinoma CRL-1555), VA-13 (human fibroblast SV40-transformed CCL-75.1), Caco-2 (colon carcinoma HTB-37), B16-F1 (mouse melanoma CRL-6323), NIH3T3 (mouse embryo fibroblast CRL-1658) and Swiss 3T3 (mouse embryo fibroblast CCL-92) and grown essentially as recommended by ATCC. Total RNA of 2×10^6 cells of each cell line was isolated and processed as described (Czuchra *et al.*, 2005), except that the Gene Chips were MOE 430 2.0 for murine and HG U133 2.0 for human samples, respectively, and analyzed using Gene Chip Operating Software GCOS 1.4 (Affymetrix, Santa Clara, CA, USA). Data for haematopoietic samples (PBM = human peripheral blood monocytes; THP-1, human acute monocytic leukaemia, TIB202) were extracted from the NCBI GEO data set GSE3280 (Gebhard *et al.*, 2006).

Results and discussion

We have previously shown that the product of a Drf3 cDNA (IMAGE clone BC048963) fused to EGFP localized to filopodia tips (Faix & Rottner, 2006). Although this cDNA was erroneously annotated as full-length, it lacked a 5′-sequence encoding 263 N-terminal amino acid residues, including N-terminal regulatory regions implicated in auto-inhibition and potential surfaces of interaction with other
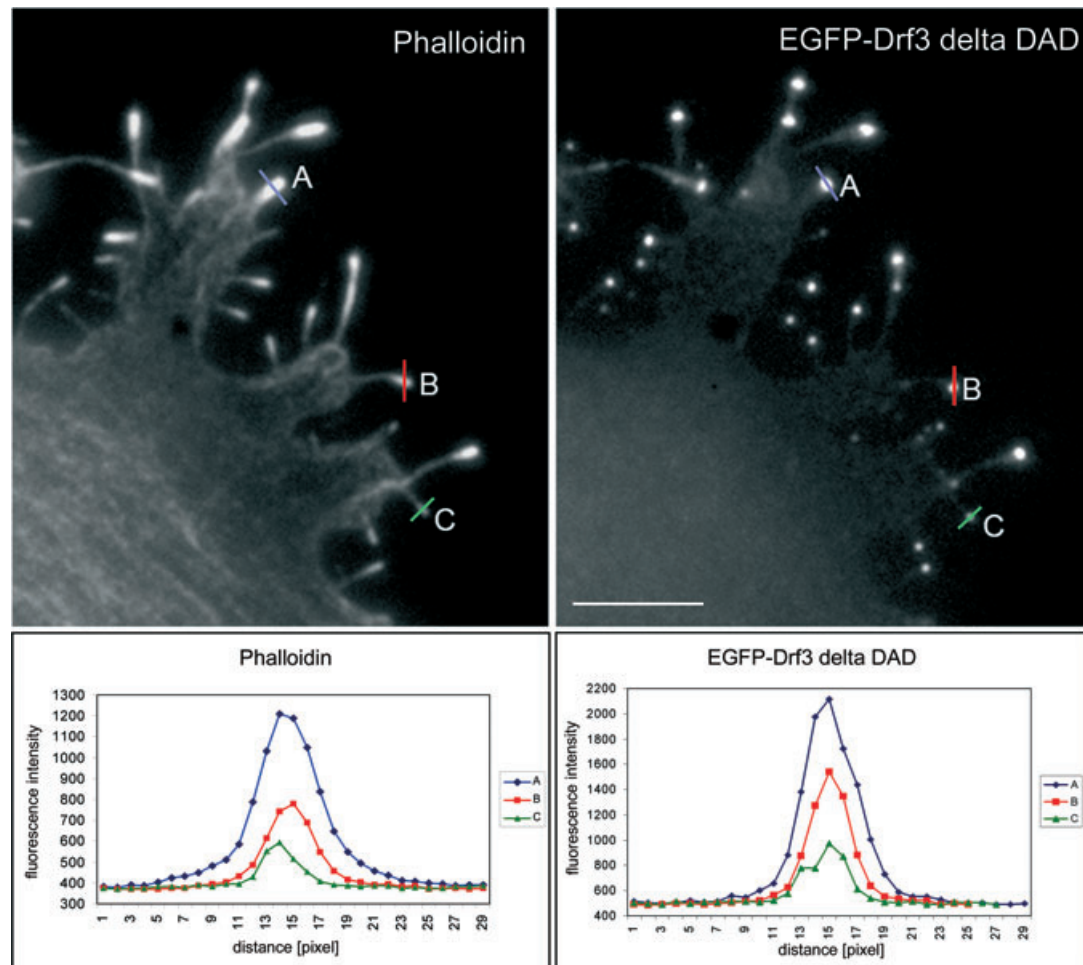
Fig. 3. B16-F1 cell over-expressing EGFP-tagged Drf3ΔDAD and counterstained for phalloidin. Line-scans show fluorescence intensities as measured for F-actin and Drf3ΔDAD in the tip regions of three distinct filopodia of variable prominence. Colour codes used in the curves at the bottom (curves A, B, C) highlight the different measurements as indicated in the images at the top. A robust correlation between Drf3ΔDAD and F-actin amounts is observed in these filopodia. Bar equals 3 μm.

cellular factors. Thus, we have now generated an EGFP-construct harbouring the full-length sequence (residues 1–1110). Similar to previous observations (Yang *et al.*, 2007), full-length Drf3, which could be readily detected in cell extracts at its expected molecular weight using anti-EGFP antibodies (not shown), was cytosolic and did not interfere with the motility of B16-F1 cells (Fig. 1(a), Supplementary Movie 1). This is consistent with data using myc-tagged murine Drf3 proteins (Pellegrin & Mellor, 2005; Wallar *et al.*, 2006), but not the EGFP-tagged filopodium formin dDia2 in *Dictyostelium* (Schirenbeck *et al.*, 2005).

It was reasonable to assume that the sub-cellular distribution of our ectopically expressed full length Drf3 was due to an intra-molecular interaction between its regulatory DID and DAD domains, as shown for instance for mDia1 (Seth *et al.*, 2006). To study the localization and dynamics of an active Drf3 protein, we removed a small C-terminal region encompassing the DAD-domain (Drf3ΔDAD),

as indicated in Fig. 1(b). Transient expression of this active Drf3 variant caused a dramatic induction of filopodia formation, with dozens of individual filopodia formed at a given time (Fig. 1(c), Supplementary Movie 2). In addition, the truncated formin strongly accumulated at the tip of each filopodium, suggesting actin polymerization to be powered at the tips of these structures by the ectopically expressed protein (Fig. 1(c), Supplementary Movie 2). Filopodia formation in most cells occurred at the expense of lamellipodia, indicative of a mutual antagonism between lamellipodia and filopodia formation in this motile cell type (Supplementary Movie 2 and not shown).

Depending on expression levels of the active formin, filopodia showed distinct morphologies. In strongly expressing cells, filopodia with club-shaped distal ends were observed (Fig. 1(d)), whereas in cells exhibiting moderate expression tapered filopodia, similar in morphology to constitutively formed filopodia, were seen (Fig. 1(e)). Similar clubs were recently described upon over-expression of an N-terminally
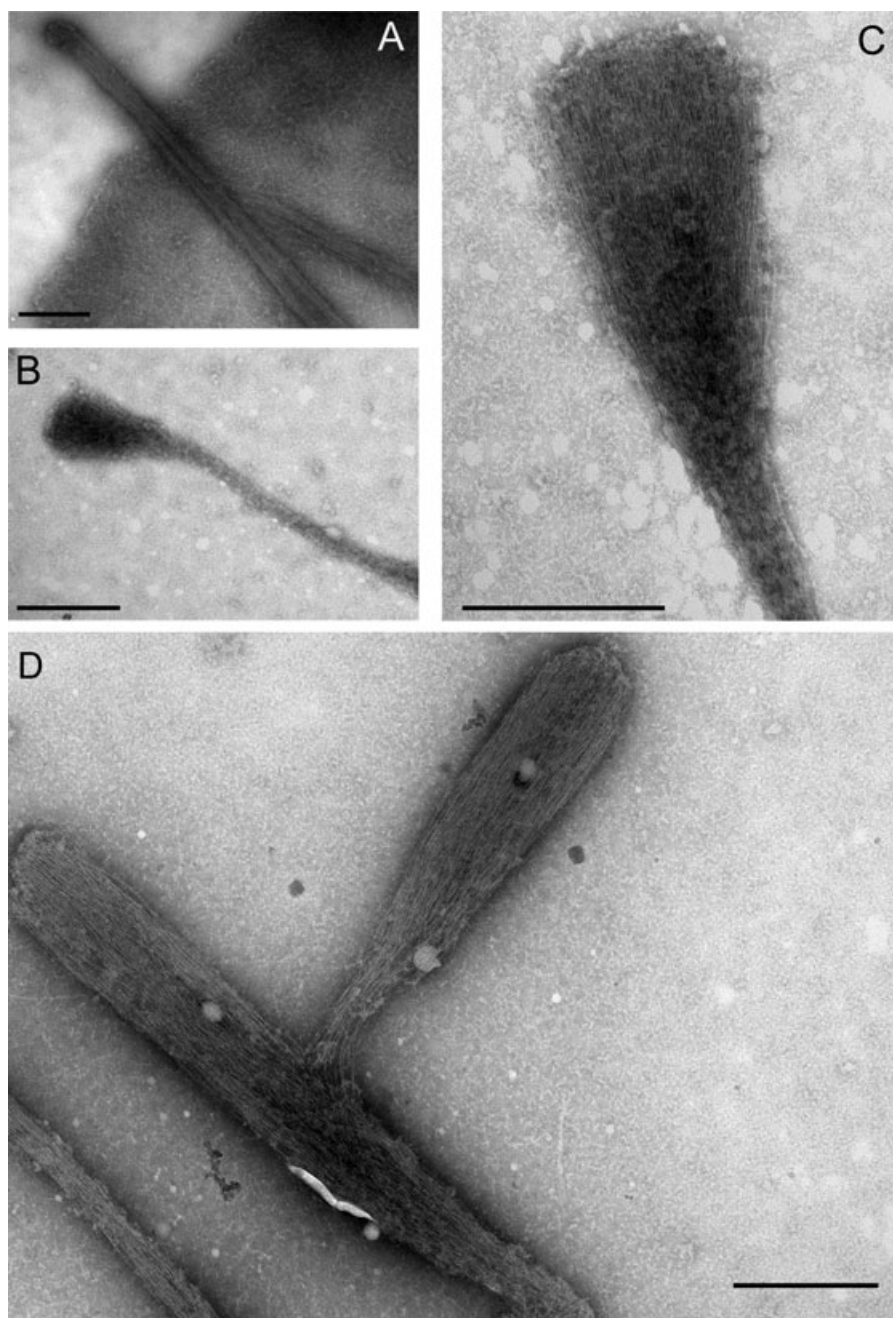
Fig. 4. Filopodia ultra-structure in control and Drf3ΔDAD over-expressing cells. Transmission electron micrographs of negatively stained whole mount cytoskeletons of B16-F1 control cell (a) or Drf3ΔDAD over-expressors (b–d). (a) Typical control filopodium formed in non-transfected B16-F1 cell, not displaying filopodial thickening in the tips frequently observed with Drf3ΔDAD-induced filopodia (b–d). Note prominent actin filament accumulation in filopodia clubs, and a low number of long, linear filaments along the shafts (b, c). (d) shows representative example of filopodial club, branching off another. Scale bars are 500 nm.

deleted mDia2 variant (Yang *et al.*, 2007). Club-shaped distal ends suggest the protrusion of these filopodia results from imbalanced biochemical activities between the active formin at the tip and other tip or shaft factors required for filament bundling and length regulation. The question is whether the formin at the tip generates filaments by continuous nucleation, or whether its activity is restricted to mere elongation of pre-existing filaments, as proposed by the convergent elongation model. Yang *et al.* (2007) concluded club-shaped filopodia to be formed by a combination of convergent elongation in the tip with increased depolymerization in the shaft. However, our observations argue against this hypothesis as
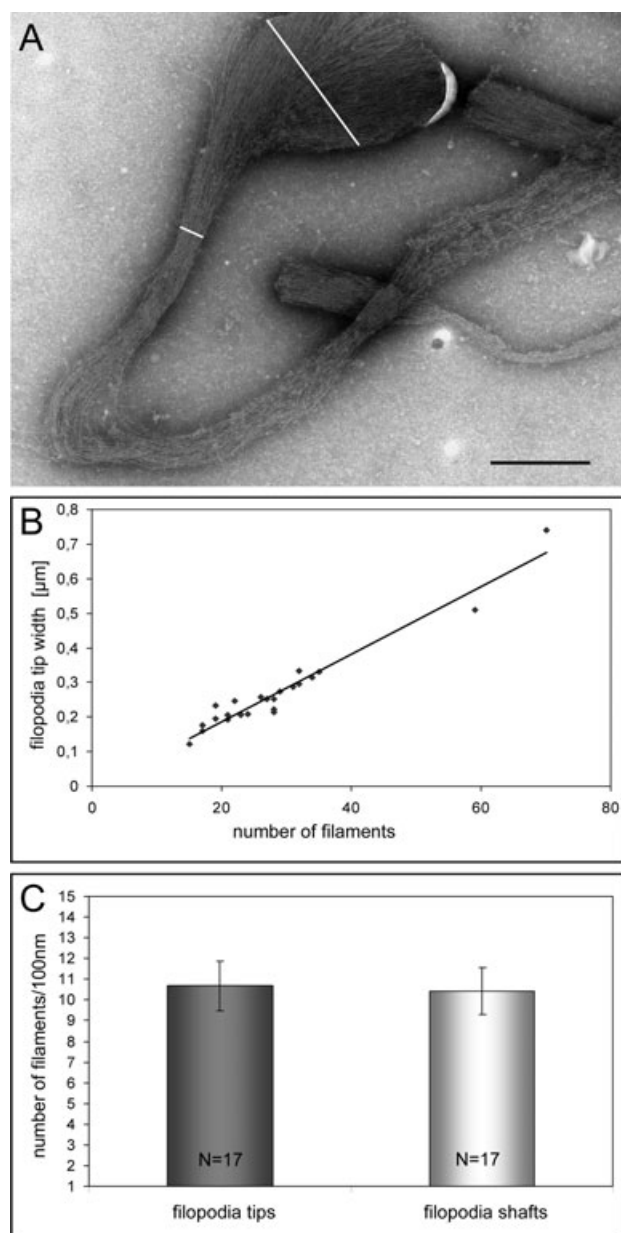
Fig. 5. Analysis of filament numbers in Drf3ΔDAD-induced filopodia. B16-F1 cells over-expressing EGFP-tagged Drf3ΔDAD were subjected to manual counting of filaments crossing white lines drawn across tip or shaft regions as indicated (a). Scale bar equals 500 nm. (b) Filament numbers as assessed from tips of filopodial clubs plotted versus tip widths ($N = 22$). (c) Comparison of filament numbers in tips and shafts of Drf3ΔDAD-induced filopodia as indicated, which corresponded on average to 10.68 ± 1.19 and 10.42 ± 1.13 filaments per 100 nm, respectively.

follows: First, filopodia induced at the cell periphery were frequently observed to thicken after they had separated from the surrounding cellular network (Fig. 2). Filopodia thickening frequently coincided with an increase of fluorescence intensity of the GFP-tagged formin in the tip (Fig. 2 and not shown), and comparison of mDia2 and phalloidin fluorescence revealed a

robust correlation between active mDia2 and filament mass in the filopodium (Fig. 3).

Electron microscopy of whole-mount specimens showed that the clubs contained bundles of closely packed actin filaments that decreased in number with distance from the tip (Figs 4(b) and (c)), giving rise to the tapered appearance. These structures were distinct from filopodia formed in non-transfected control B16-F1 cells (Fig. 4(a)) that showed an uniform diameter of 0.1–0.2 μm. In addition, the shafts of Drf3-induced filopodia consisted of a moderate number of long parallel filaments apparently protected from depolymerization (Fig. 4(b)). Counts of individual filaments in Drf3-induced tips as indicated in Fig. 5(a) revealed a linear correlation between tip width and filament number (Fig. 5(b)), with a constant packing density (Fig. 5(c)). These observations and those on phalloidin labelling showed that tip thickening as observed by video microscopy (Fig. 2) was not due to splicing of a constant number of filaments at their tips, but instead an increase in filament number, through additional nucleation events. Finally, the activity of the formin was apparently so strong that clubs branching off parent clubs could occasionally be observed (Fig. 4(d)); this evidently occurs in the absence of nucleation by Arp2/3-complex, which does not localize to filopodia (Svitkina & Borisy, 1999; Korobova & Svitkina, 2008).

Collectively, these data can only be explained by continuous nucleation activity at the filopodium tip, presumably mediated by the formin and concomitant depolymerization further behind. This mechanism is inconsistent with the 'convergent elongation' of a limited number of pre-existing lamellipodial into filopodial filaments, and is in line with other findings showing that filopodia can form in the absence of lamellipodia (Steffen et al., 2006; Gomez et al., 2007). Yang et al. (2007) recently described an inhibition of lamellipodia formation upon depletion of mDia2/Drf3 and an interaction between mDia2/Drf3 and the WAVE-complex sub-unit Abi-1. They concluded accordingly that this formin not only is essential for filopodia formation per se but drives them indirectly through elongating lamellipodial filaments and/or providing the mother filaments for Arp2/3-mediated generation of lamellipodia networks, in the absence of which filopodia formation would not occur. To test whether the active Drf3 variant (Drf3ΔDAD) used here required lamellipodial filaments as pre-cursers of filopodial filaments, we used VA-13 fibroblast cells stably suppressed for the WAVE-complex component Nap1, previously established to lack lamellipodia (Steffen et al., 2004). The same cells were already shown to form filopodia upon injection of constitutively active Cdc42 (Steffen et al., 2006), but formin functions such as that of Drf3 have not been explored in these cells. Mock siRNA-treated controls expressing Drf3ΔDAD formed filopodia tipped by the EGFP-tagged formin as expected, although the response was not as pronounced as observed in B16-F1 (Supplementary Movie 3). More important, Nap1 knockdown
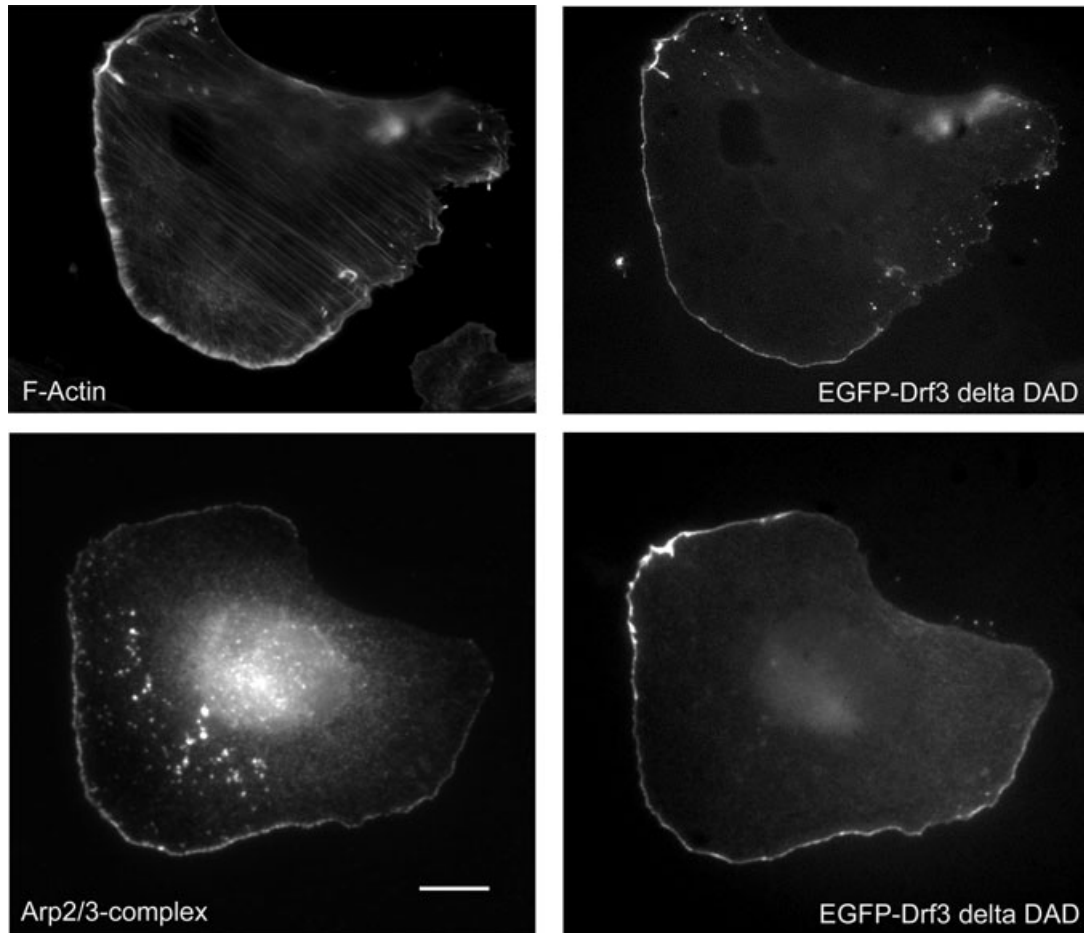
Fig. 6. Drf3∆DAD can target to the tip of a lamellipodium-like structure. EGFP-tagged Drf3∆DAD accumulation at the tips of lamellipodial actin filament networks, as stained by phalloidin (top), and harbouring Arp2/3-complex (bottom) as indicated. Bars are 10 µm.

cells, which displayed strongly reduced levels of all WAVE-complex sub-units, including Abi (Steffen *et al.*, 2006) formed numerous Drf3∆DAD-driven filopodia (Supplementary Movie 4), indicating not only that this response can occur in the absence of functional WAVE-complex but also that lamellipodial filaments are dispensable for the formation of Drf3-induced filopodia.

As mentioned earlier, most Drf3∆DAD over-expressors formed filopodia at the expense of lamellipodia, causing a virtually exclusive accumulation of the formin variant in the tips of finger-like plasma membrane extensions. However, in a small number of cells still capable of lamellipodia formation, active Drf3 also appeared enriched in the tip region of these protrusive sheet-like structures (see Supplementary Movie 5 and also Yang *et al.*, 2007). Notably, the dynamics of the active formin in the front region of these protrusions differed from canonical lamellipodial tip factors such as VASP (Rottner *et al.*, 1999) or WAVE-complex components (Stradal *et al.*, 2001; Steffen *et al.*, 2004). More specifically, the width of Drf3 enrichment was more variable than observed with

the former components, and active Drf3 appeared to display more rapid lateral movements (see Supplementary Movie 3), which may be linked to tight association of the formin with laterally polymerizing filaments (unpublished data). To test whether the structures accumulating Drf3∆DAD at their tips indeed constituted lamellipodia, Drf3 over-expressors were counterstained for the actin cytoskeleton with phalloidin or antibodies specific for the Arp2/3-complex sub-unit ArpC5 (p16). These data showed Drf3 enriched at the tip of actin filament networks reminiscent of lamellipodia (Fig. 6), that were labelled by Arp2/3-complex antibodies (Fig. 6), and by reagents specific for Arp2/3-complex activators, WAVE-complex (Abi) and cortactin (Fig. 7). These data confirmed that formins and the Arp2/3 complex machinery can in principle co-exist in the same sub-cellular location. Interestingly, however, the same structures were also prominently labelled with the filopodial actin bundling protein fascin (Fig. 7), that is normally enriched in micro-spikes and required for their formation in B16-F1 cells (Vignjevic *et al.*, 2006). These Drf3∆DAD-induced 'lamellipodia' may therefore represent
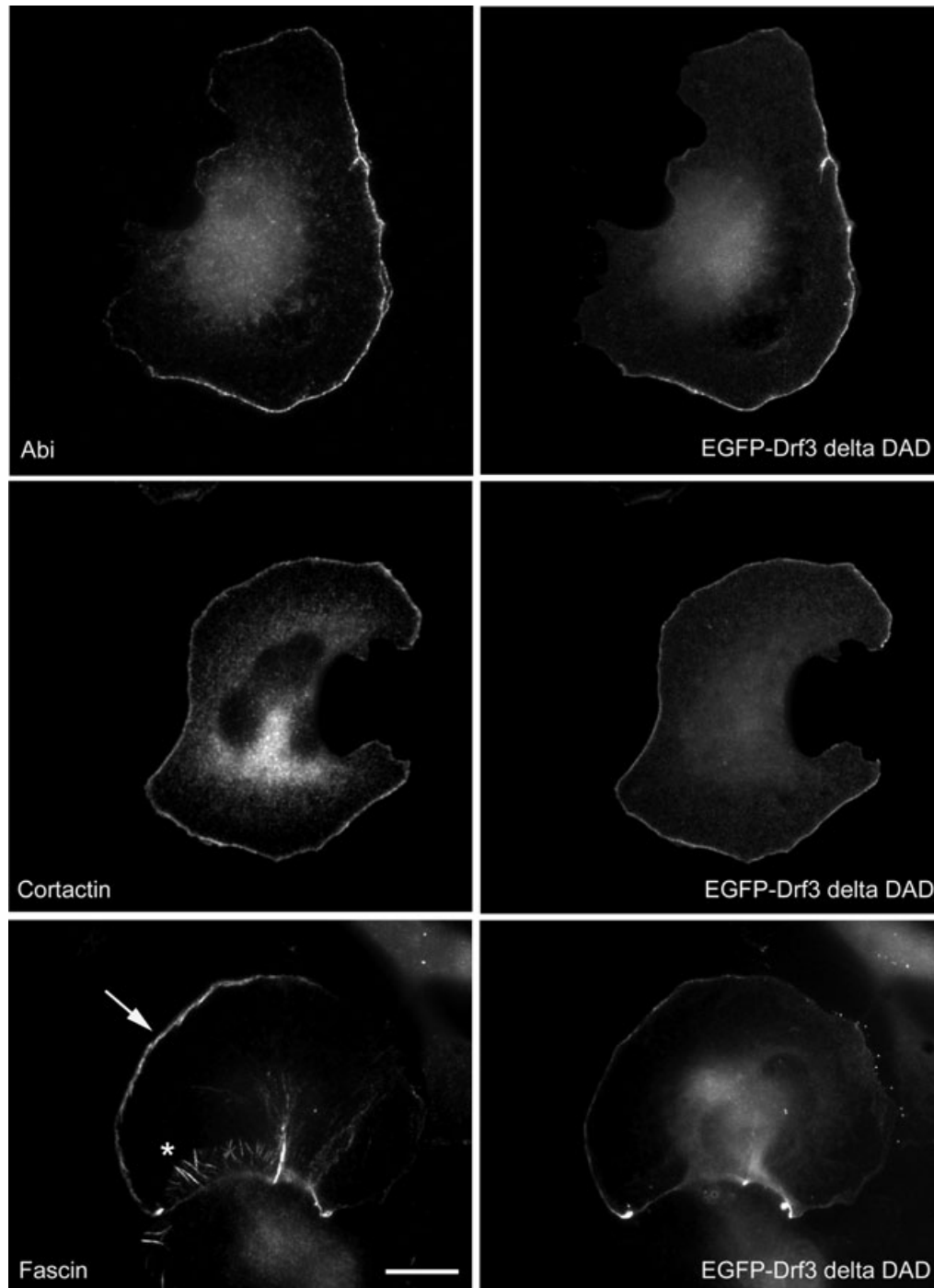
Fig. 7. Drf3ΔDAD-induced lamellipodia-like structures contain Arp2/3-complex activators and fascin. B16-F1 cells expressing EGFP-tagged Drf3ΔDAD were counterstained for the WAVE-complex component Abi, cortactin and fascin as indicated. Note prominent co-accumulation of Drf3ΔDAD with the respective component. Asterisk in fascin image highlights typical label on micro-spikes (Vignjevic *et al.*, 2006) embedded into the lamellipodium of a neighbouring, non-transfected cell. Scale bar equals 10 μm.

hybrids of lamellipodia and filopodia. Future studies will have to establish whether mDia2 and potentially other formins are components of genuine lamellipodia and whether they are indeed required for the nucleation of filaments in both lamellipodia and filopodia.

One important prerequisite for future analyses of formin function in mammalian cells and tissues is information about their relative expression in different cell types. Thus, we performed expression profiling of Drfs and other relevant actin regulators by microarray analyses of B16-F1 cells and two
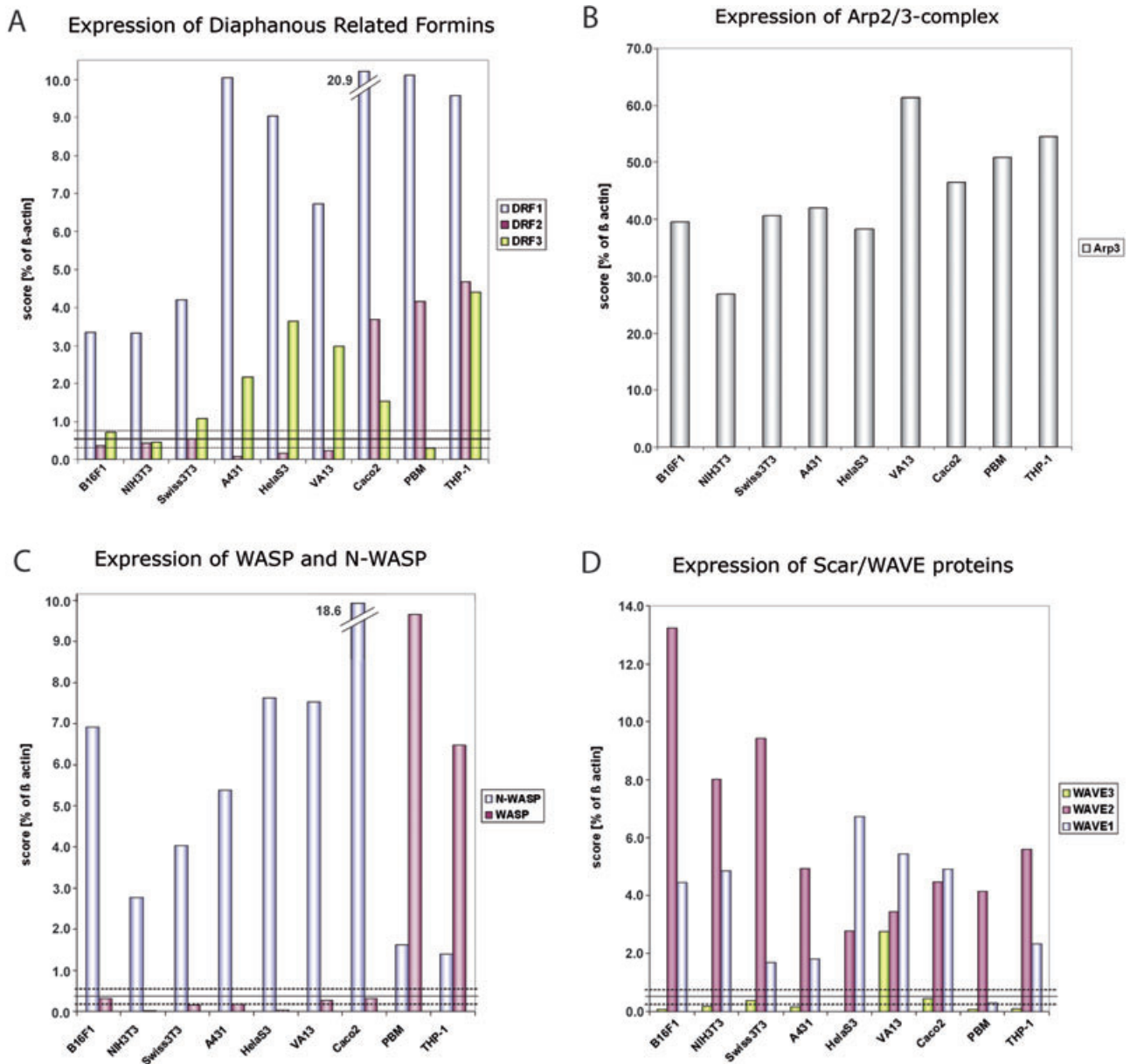
Fig. 8. Microarray analyses of cell lines as indicated. (a) Expression levels of Drf1−3 normalized to β-actin. Note most prominent Drf3 expression in HelaS3, VA-13 and THP-1. (b) Arp3, (c) N-WASP/WASP and (d) WAVE isoform expression as normalized to β-actin. Black solid and dashed lines in (a), (c) and (d) indicate average background levels ± standard deviation from all Gene Chips.

commonly used murine fibroblast cell lines (Swiss and NIH 3T3) as well as different human cell lines (Fig. 8). Interestingly, Drf1 (Dia1) was expressed in all studied lines, whereas Drf2 and Drf3 were much less abundant in most cell lines. Specifically, and quite surprisingly, Drf3 was almost absent in our murine lines, including B16-F1 used in a recent RNAi study (Yang *et al.*, 2007), and in NIH 3T3 fibroblasts, as previously reported (Tominaga *et al.*, 2000; Peng *et al.*, 2003). By contrast, expression was observed in the human fibroblast cell lines VA-13 and epithelial-like lines HeLaS3 and Caco-2 as well as the leukaemia line THP-1. Thus, these human cell lines

might be more appropriate for interference with endogenous Drf3 functions in future studies. Less surprisingly, the Arp2/3-complex, as monitored by the Arp3 sub-unit, was expressed at comparable levels in all lines, corroborating its key function in numerous actin-based processes (Goley & Welch, 2006). The expression levels of the Arp2/3-complex activators of the WASP and WAVE families, the latter known to be essential for lamellipodium protrusion (Stradal & Scita, 2006), were also consistent with previously published data. The expression pattern of haematopoietic WASP and ubiquitous N-WASP was mutually exclusive (Stradal *et al.*, 2004), and ubiquitous

WAVE2 was more abundant in our lines than the more neuronal isoform WAVE1, and most prominently expressed in the motile B16-F1 cells. Finally, mRNA encoding for WAVE3, known to be largely restricted to the nervous system (Stradal *et al.*, 2004), was exclusively detected in VA-13 cells, the significance of which remains unknown. However, these results await confirmation by Western Blotting using isoform-specific antibodies.

In conclusion, we have shown that the active Drf3 variant Drf3ΔDAD used here can prominently associate with both filopodia tips and lamellipodia-like structures. The strong filopodia induction observed upon Drf3ΔDAD over-expression correlated with generation of club-like structures containing numerous actin filaments formed by *de novo* nucleation. Future functional studies should address the relative relevance of Drf3 and potential additional formins in filopodia and perhaps lamellipodia formation in different cell types.

Acknowledgements

References

Alberts, A.S. (2001) Identification of a carboxyl-terminal diaphanous-related formin homology protein autoregulatory domain. *J. Biol. Chem.* **276**, 2824–2830.

Applewhite, D.A., Barzik, M., Kojima, S., Svitkina, T.M., Gertler, F.B. & Borisy, G.G. (2007) Ena/VASP proteins have an anti-capping independent function in filopodia formation. *Mol. Biol. Cell* **18**, 2579–2591.

Auinger, S. & Small, J.V. (2008) Correlated light and electron microscopy of the cytoskeleton. *Methods in Cell Biology, Basic Biological Electron Microscopy* (ed. by T.D. Allen). Academic Press. In press.

Biyasheva, A., Svitkina, T., Kunda, P., Baum, B. & Borisy, G. (2004) Cascade pathway of filopodia formation downstream of SCAR. *J. Cell Sci.* **117**, 837–848.

Czuchra, A., Wu, X., Meyer, H., *et al.* (2005) Cdc42 is not essential for filopodium formation, directed migration, cell polarization, and mitosis in fibroblastoid cells. *Mol. Biol. Cell* **16**, 4473–4484.

Faix, J. & Grosse, R. (2006) Staying in shape with formins. *Dev. Cell* **10**, 693–706.

Faix, J. & Rottner, K. (2006) The making of filopodia. *Curr. Opin. Cell Biol.* **18**, 18–25.

Gebhard, C., Schwarzfischer, L., Pham, T.H., Schilling, E., Klug, M., Andreesen, R. & Rehli, M. (2006) Genome-wide profiling of CpG methylation identifies novel targets of aberrant hypermethylation in myeloid leukemia. *Cancer Res.* **66**, 6118–6128.

Goley, E.D. & Welch, M.D. (2006) The ARP2/3 complex: an actin nucleator comes of age. *Nat. Rev. Mol. Cell Biol.* **7**, 713–726.

Gomez, T.S., Kumar, K., Medeiros, R.B., Shimizu, Y., Leibson, P.J. & Billadeau, D.D. (2007) Formins regulate the actin-related protein 2/3 complex-independent polarization of the centrosome to the immunological synapse. *Immunity* **26**, 177–190.

Goode, B.L. & Eck, M.J. (2007) Mechanism and function of formins in the control of actin assembly. *Annu. Rev. Biochem.* **76**, 593–627.

Gupton, S.L. & Gertler, F.B. (2007) Filopodia: the fingers that do the walking. *Sci. STKE* 2007, re5.

Hall, A. (1998) Rho GTPases and the actin cytoskeleton. *Science* **279**, 509–514.

Higashida, C., Miyoshi, T., Fujita, A., *et al.* (2004) Actin polymerization-driven molecular movement of mDia1 in living cells. *Science* **303**, 2007–2010.

Innocenti, M., Zucconi, A., Disanza, A., *et al.* (2004) Abi1 is essential for the formation and activation of a WAVE2 signalling complex. *Nat. Cell Biol.* **6**, 319–327.

Korobova, F. & Svitkina, T. (2008) Arp2/3 complex is important for filopodia formation, growth cone motility and neuritogenesis in neuronal cells. *Mol. Biol. Cell* **19**, 1561–1574.

Kovar, D.R. & Pollard, T.D. (2004) Insertional assembly of actin filament barbed ends in association with formins produces piconewton forces. *Proc. Natl. Acad. Sci. U.S.A.* **101**, 14725–14730.

Lommel, S., Benesch, S., Rottner, K., Franz, T., Wehland, J. & Kuhn, R. (2001) Actin pedestal formation by enteropathogenic *Escherichia coli* and intracellular motility of Shigella flexneri are abolished in N-WASP-defective cells. *EMBO Rep.* **2**, 850–857.

Mallavarapu, A. & Mitchison, T. (1999) Regulated actin cytoskeleton assembly at filopodium tips controls their extension and retraction. *J. Cell Biol.* **146**, 1097–1106.

Mejillano, M.R., Kojima, S., Applewhite, D.A., Gertler, F.B., Svitkina, T.M. & Borisy, G.G. (2004) Lamellipodial versus filopodial mode of the actin nanomachinery: pivotal role of the filament barbed end. *Cell* **118**, 363–373.

Mitchison, T.J. & Cramer, L.P. (1996) Actin-based cell motility and cell locomotion. *Cell* **84**, 371–379.

Olazabal, I.M., Caron, E., May, R.C., Schilling, K., Knecht, D.A. & Machesky, L.M. (2002) Rho-kinase and myosin-II control phagocytic cup formation during CR, but not FcgammaR, phagocytosis. *Curr. Biol.* **12**, 1413–1418.

Pellegrin, S. & Mellor, H. (2005) The Rho family GTPase Rif induces filopodia through mDia2. *Curr. Biol.* **15**, 129–133.

Peng, J., Wallar, B.J., Flanders, A., Swiatek, P.J. & Alberts, A.S. (2003) Disruption of the Diaphanous-related formin Drf1 gene encoding mDia1 reveals a role for Drf3 as an effector for Cdc42. *Curr. Biol.* **13**, 534–545.

Pollard, T.D. (2007) Regulation of actin filament assembly by Arp2/3 complex and formins. *Annu. Rev. Biophys. Biomol. Struct.* **36**, 451–477.

Pollard, T.D. & Borisy, G.G. (2003) Cellular motility driven by assembly and disassembly of actin filaments. *Cell* **112**, 453–465.

Pruyne, D., Evangelista, M., Yang, C., Bi, E., Zigmond, S., Bretscher, A. & Boone, C. (2002) Role of formins in actin assembly: nucleation and barbed-end association. *Science* **297**, 612–615.

Resch, G.P., Goldie, K.N., Krebs, A., Hoenger, A. & Small, J.V. (2002) Visualisation of the actin cytoskeleton by cryo-electron microscopy. *J. Cell Sci.* **115**, 1877–1882.

Romero, S., Le Clainche, C., Didry, D., Egile, C., Pantaloni, D. & Carlier, M.F. (2004) Formin is a processive motor that requires profilin to accelerate actin assembly and associated ATP hydrolysis. *Cell* **119**, 419–429.

Rottner, K., Behrendt, B., Small, J.V. & Wehland, J. (1999) VASP dynamics during lamellipodia protrusion. *Nat. Cell Biol.* **1**, 321–322.

Schirenbeck, A., Bretschneider, T., Arasada, R., Schleicher, M. & Faix, J. (2005) The Diaphanous-related formin dDia2 is required for the formation and maintenance of filopodia. *Nat. Cell Biol.* **7**, 619–625.

Seth, A., Otomo, C. & Rosen, M.K. (2006) Autoinhibition regulates cellular localization and actin assembly activity of the diaphanous-related formins FRLalpha and mDia1. *J. Cell Biol.* **174**, 701–713.

Small, J.V. (1988) The actin cytoskeleton. *Electron. Microsc. Rev.* **1**, 155–174.

Small, J.V., Anderson, K. & Rottner, K. (1996) Actin and the coordination of protrusion, attachment and retraction in cell crawling. *Biosci. Rep.* **16**, 351–368.

Small, J.V., Kaverina, I., Krylyshkina, O. & Rottner, K. (1999) Cytoskeleton cross-talk during cell motility. *FEBS Lett.* **452**, 96–99.

Small, J.V., Stradal, T., Vignal, E. & Rottner, K. (2002) The lamellipodium: where motility begins. *Trends Cell Biol.* **12**, 112–120.

Snapper, S.B., Takeshima, F., Anton, I., *et al.* (2001) N-WASP deficiency reveals distinct pathways for cell surface projections and microbial actin-based motility. *Nat. Cell Biol.* **3**, 897–904.

Steffen, A., Faix, J., Resch, G.P., *et al.* (2006) Filopodia formation in the absence of functional WAVE- and Arp2/3-complexes. *Mol. Biol. Cell* **17**, 2581–2591.

Steffen, A., Rottner, K., Ehinger, J., Innocenti, M., Scita, G., Wehland, J. & Stradal, T.E. (2004) Sra-1 and Nap1 link Rac to actin assembly driving lamellipodia formation. *EMBO J.* **23**, 749–759.

Stradal, T., Courtney, K.D., Rottner, K., Hahne, P., Small, J.V. & Pendergast, A.M. (2001) The Abl interactor proteins localize to sites of actin polymerization at the tips of lamellipodia and filopodia. *Curr. Biol.* **11**, 891–895.

Stradal, T.E., Rottner, K., Disanza, A., Confalonieri, S., Innocenti, M. & Scita, G. (2004) Regulation of actin dynamics by WASP and WAVE family proteins. *Trends Cell Biol.* **14**, 303–311.

Stradal, T.E. & Scita, G. (2006) Protein complexes regulating Arp2/3-mediated actin assembly. *Curr. Opin. Cell Biol.* **18**, 4–10.

Svitkina, T.M. & Borisy, G.G. (1999) Arp2/3 complex and actin depolymerizing factor/cofilin in dendritic organization and treadmilling of actin filament array in lamellipodia. *J. Cell Biol.* **145**, 1009–1026.

Svitkina, T.M., Bulanova, E.A., Chaga, O.Y., Vignjevic, D.M., Kojima, S., Vasiliev, J.M. & Borisy, G.G. (2003) Mechanism of filopodia initiation by reorganization of a dendritic network. *J. Cell Biol.* **160**, 409–421.

Tominaga, T., Sahai, E., Chardin, P., McCormick, F., Courtneidge, S.A. & Alberts, A.S. (2000) Diaphanous-related formins bridge Rho GTPase and Src tyrosine kinase signaling. *Mol. Cell* **5**, 13–25.

Vignjevic, D., Kojima, S., Aratyn, Y., Danciu, O., Svitkina, T. & Borisy, G.G. (2006) Role of fascin in filopodial protrusion. *J. Cell Biol.* **174**, 863–875.

Wallar, B.J., Stropich, B.N., Schoenherr, J.A., Holman, H.A., Kitchen, S.M. & Alberts, A.S. (2006) The basic region of the diaphanous-autoregulatory domain (DAD) is required for autoregulatory interactions with the diaphanous-related formin inhibitory domain. *J. Biol. Chem.* **281**, 4300–4307.

Watanabe, N., Kato, T., Fujita, A., Ishizaki, T. & Narumiya, S. (1999) Cooperation between mDia1 and ROCK in Rho-induced actin reorganization. *Nat. Cell Biol.* **1**, 136–143.

Watanabe, N., Madaule, P., Reid, T., *et al.* (1997) p140mDia, a mammalian homolog of Drosophila diaphanous, is a target protein for Rho small GTPase and is a ligand for profilin. *EMBO J.* **16**, 3044–3056.

Yang, C., Czech, L., Gerboth, S., Kojima, S., Scita, G. & Svitkina, T. (2007) Novel roles of formin mDia2 in lamellipodia and filopodia formation in motile cells. *PLoS Biol.* **5**, e317.

Supporting Information

Additional Supporting Information may be found in the online version of this article.

Movie 1. B16-F1 cell moving on laminin and expressing EGFP-tagged full-length human Drf3. Display rate is 330-fold. Bar is 10 μm.

Movie 2. B16-F1 cell over-expressing EGFP-tagged, active Drf3. Display rate is 330-fold. Bar is 10 μm.

Movie 3. Control siRNA-treated (Control RNAi) VA-13 fibroblast cell (Steffen *et al.*, 2006) transiently transfected with Drf3ΔDAD. Display rate is 330-fold. Bar is 10 μm.

Movie 4. Nap1 knockdown VA-13 fibroblast (Nap1 RNAi) transiently expressing Drf3ΔDAD. Note prominent formation of filopodia tipped by EGFP-tagged Drf3ΔDAD in spite of WAVE-complex loss of function and coincident lack of lamellipodia (Steffen *et al.*, 2004). Display rate is 330-fold. Bar is 10 μm.

Movie 5. B16-F1 cell moving on laminin and expressing EGFP-tagged, active Drf3. Note the accumulation of Drf3 at the tips of both filopodia and lamellipodia-like structures. Display rate is 330-fold. Bar is 10 μm.

Please note: Blackwell Publishing are not responsible for the content or functionality of any supporting materials supplied by the authors. Any queries (other than missing material) should be directed to the corresponding author for the article.

Curriculum Vitae

Name:	Stefan Andreas Köstler
Place and date of birth:	Salzburg, 23rd March 1977
Nationality:	Austrian

Education:

1983-1987	Volksschule Nonntal
1987-1995	Bundesrealgymnasium Salzburg, Akademiestrasse
1995	Matura
1995-1998	Studies of Biology at the University of Salzburg
1998-2004	Studies of Biology/Genetics at the University of Vienna
2001	Temporary employment at the Institute of Molecular Genetics in Montpellier/France
2002-2004	Diploma thesis in the Schweyen Lab at the Institutof Microbiology and Genetics, University of Vienna
since 4.2004	Ph.D. thesis in the Small lab at the Institute of Molecular Biotechnology Ges.m.b.H., Vienna, Austria

Publications:

Koestler, S.A., S. Auinger, M. Vinzenz, K. Rottner, and J.V. Small. 2008. Differentially oriented populations of actin filaments generated in lamellipodia collaborate in pushing and pausing at the cell front. *Nat Cell Biol.* 10:306-13.

Block, J., T.E. Stradal, J. Hanisch, R. Geffers, S.A. Kostler, E. Urban, J.V. Small, K. Rottner, and J. Faix. 2008. Filopodia formation induced by active mDia2/Drf3. *J Microsc.* 231:506-17.

Small, J.V., S. Auinger, M. Nemethova, S. Koestler, K.N. Goldie, A. Hoenger, and G.P. Resch. 2008. Unravelling the structure of the lamellipodium. *J Microsc.* 231:479-85.

Koestler, S., Auinger, S., and Small, J. V. 2007. Correlative Live Cell Imaging and Negative Stain Electron Microscopy of Migrating Cells. *Microscopy and Microanalysis* 13 (Suppl. 03):184-185

Koestler, S.A., Rottner, K., Lai, F., Block, J., Vinzenz, M., and Small, J.V. 2008. F- and G-actin concentrations in lamellipodia of moving cells. *Manuscript in preparation.*

Acknowledgements